Zeitschrift: Helvetica Physica Acta
Band: 67 (1994)
Heft: 5

Artikel: Field theory at finite temperature and phase transitions
Autor: Quirós, Mariano
DOI: https://doi.org/10.5169/seals-116659

Helv Phys Acta
Vol. 67 (1994)

0018-0238/94/050451-133$1.50+0.20/0

Field Theory at Finite Temperature and Phase Transitions[1]

By **Mariano Quirós**

Instituto de Estructura de la Materia (CSIC), Serrano 123
E–28006 Madrid, Spain

(9.VII.1994)

Abstract. We review different aspects of field theory at zero and finite temperature, related to the theory of phase transitions. We discuss different renormalization conditions for the effective potential at zero temperature, emphasizing in particular the $\overline{\rm MS}$ renormalization scheme. Finite temperature field theory is discussed in the real and imaginary time formalisms, showing their equivalence in simple examples. Bubble nucleation, by quantum and thermal tunnelling, and the subsequent development of the phase transition are described in some detail. Some attention is also devoted to the breakdown of the perturbative expansion and the infrared problem in the finite temperature field theory. We have discussed how to improve the theory by including plasma effects (Debye masses) using either a diagrammatic and a functional approach and showing explicitly their equivalence to a given order. Finally the application to baryogenesis at the electroweak phase transition is done in the Standard Model and several extensions thereof, as the case of the Minimal Supersymmetric Standard Model. In all cases we have translated the condition of not washing out any previously generated baryon asymmetry by upper bounds on the Higgs mass.

[1]Based on lectures given at the *Troisième Cycle de la Physique de la Suisse Romande*, Lausanne (Switzerland), June 1994.

TABLE OF CONTENTS

1 Introduction

Field theory at finite temperature is a *classic* (more than twenty-years old) subject, which has become *hot* during the last couple of years. In fact the possibility of generating the required baryon asymmetry of the universe at temperatures near the electroweak phase transition critical temperature ($\sim 100\ GeV$) has triggered a lot of activity related to investigating the nature of the phase transition in the Standard Model of strong and electroweak interactions -and minimal extensions thereof- as well as computing the amount of CP violation in these models. On the other hand *old* problems, as the failure of perturbative expansion of field theory at the phase transition critical temperature, needed to be resuscitated since the actual generation of baryon asymmetry depends to a large extent on the fine details of the theory. This degree of refinement has produced also a great deal of controversy inside the field.

Since the field is evolving very rapidly, any attempt to cover all the branching out of the different subjects, or present the ultimate version of them, is damned to failure. For the same reason, many results are open to controversy and it would be audacious to be so bold as to draw firm conclusions on them. As an example we can anticipate here the case of whether or not the Standard Model phase transition is strong enough first order for the baryon violating interactions (mediated by sphalerons) to go out of equilibrium at the bubble walls, thus preventing the erasure of any generated baryon asymmetry. The one-loop result is negative in the sense of imposing an upper bound which is below the present LEP bound. Introducing plasma effect to one-loop (leading order) the result is worsened since temperature effects screen part (one third) of the first order phase transition. On the other hand two-loop plasma effects seem to improve the previous result, and alleviate the

bound on the Higgs mass, while non-perturbative effects also seem to go along the same direction. However, to rely upon two-loop corrections to rescue our model can be in conflict (as everybody can understand) with the validity of our perturbative expansion (whatever this expansion could be), while our degree of mastery of non-perturbative effects in field theory would make it hard to draw any final conclusion on the basis of the latter. Finally it might be that one-loop corrections of fermionic fluctuations (in particular the top's ones) could be capable of suppressing the sphaleron transitions and increase the upper bound on the Higgs mass beyond its experimental limit, as it has been recently suggested. Again it would be premature and bold to draw a firm conclusion on this basis. For all those reasons I have preferred to present here the *tools* which should enable the reader to go through the technicalities of the different papers and raise his/her own judgement, which presumably will not coincide with that of this author.

These notes are based on a twelve-hour *Cours de Troisième Cycle de Physique de la Suisse Romande*, held at Lausanne in June 1994. The aim of them is to provide a pedagogical and self-contained description of the basic elements which are necessary to follow the most recent evolution of the field. Completeness has been sacrificed to pedagogy and detail and, as a consequence, many topics have not been touched upon. I have made what I have considered a primary choice of topics, which I have described in some detail, while I have ignored others. If my choice is not the most successful one I have to apologize in advance for that. However I have tried to provide enough material for the reader to be able to follow all untouched topics. The outline of these lecture notes is as follows:

Since the effective potential of a field theory inside a thermal bath contains, in particular, the usual effective potential at zero temperature, the latter is reviewed in **Section 2**. We describe the contribution of scalar, fermion and gauge fields to the one-loop, and higher-loop, effective potential. We discuss the regularization of the one-loop effective potential using a cut-off in integration momenta and also using dimensional regularization. As an example we present the case of the Standard Model using both, a cut-off regularization and renormalization conditions such that the location of the minimum of the potential and its second derivative (the Higgs mass) do not change with respect to their tree level values, and also using the most useful $\overline{\rm MS}$ renormalization scheme. Finally the relationship between the effective potential and the renormalization group, giving rise to the so-called improved effective potential, is described in some detail.

The general elements of field theory at finite temperature are described in **Section 3**. The different thermodynamical ensembles (microcanonical, canonical and grand canonical) are briefly presented, and the statistical average on the grand canonical ensemble is defined.

The generating functional for bosonic and fermionic fields are defined over an arbitrary path in complex time. Convergence of the two-point Green function is shown to constrain the possible paths along the complex time. We present explicit expressions for two-point Green functions of scalar and fermion fields, as well as periodicity properties of them, known as Kubo-Martin-Schwinger relations. Two particularly interesting paths are studied in some detail: they are known as imaginary and real time formalisms. In both cases we present the propagators and Feynman rules. For the case of the imaginary time formalism we summarize some standard tricks to perform infinite summations over all Matsubara frequencies in Feynman integrals, both for bosonic and fermionic fields.

In **Section 4** the contribution of scalar fields, fermion fields and gauge bosons to the one-loop effective potential at finite temperature is computed. In all cases, and for the imaginary time formalism, we use two different methods: the usual procedure of evaluating the diagrams contributing to the one-loop potential using the Feynman rules for the *unshifted* theory deduced in section 3, and a simpler procedure, which can be called *tadpole method*, which consists in computing the tadpole in the *shifted* theory, using the standard tricks of infinite summations over the thermal modes described in section 3, and integrating over the external leg. Both methods are explicitly shown to lead to the same results. In the real time formalism we have also computed the one-loop effective potential for scalar and fermion fields using the corresponding Feynman rules deduced in section 3 and the tadpole method, and shown to agree with that computed in the imaginary time formalism. Finally the Standard Model case is presented as an example.

Some essential elements of the theory of phase transitions at finite temperature are presented in **Section 5**. The phenomenon of *symmetry restoration* is described in the two important cases of first and second order phase transitions. In fact, the main features of first and second order phase transitions are outlined with the simple (and realistic) example of a temperature dependent potential which can be approximated by a renormalizable polynomial in the classical field. In first order phase transitions, bubble nucleation from the false to the true vacuum proceeds via quantum penetration of the barrier. At zero temperature this phenomenon is known as quantum tunnelling, and at finite temperature as thermal tunnelling. Both quantum and thermal tunnelling are described in some detail. In both cases the semiclassical description of the decay is provided by the bounce solution and the decay rate by the euclidean action. For quantum tunnelling (appropriate for the case of supercooled systems) explicit expressions are provided for the case of the thin wall approximation, where analytic formulae can be given for the euclidean action and the critical radius of the bubble. For thermal tunnelling (appropriate for the case of the electroweak phase

transition) a discussion on the evolution with temperature of the bounce solution is given: it is shown that just after the critical temperature thin wall bubbles are first formed. Only if the end of the phase transition is postponed, thick wall bubbles will be formed. Analytic formulae are given for the case of the thin wall approximation (as *e.g.* for the radius of the critical bubble) and also (without assuming the thin wall approximation) for the case of the renormalizable potential which served to exemplify the first and second order phase transitions. The beginning of the phase transition (one bubble per horizon nucleated) and the end of phase transition (all the space filled with bubbles) are dictated by comparison of the bubble nucleation rate with the expansion rate of the universe. This comparison is also done in this section with the result that the end of the phase transition should happen when the euclidean action is ~ 100. In particular cases this evaluation should serve to know whether the formed bubbles have thin or thick walls.

The problem of the breakdown of perturbative expansion at the critical temperature is treated in **Section 6**. Using the simplest theory of one self-interacting real scalar field we have first exhibited the appearance of infra-red divergences from higher-loop diagrams at finite temperature and heuristically shown that the one-loop approximation is not valid at the critical temperature. A new temperature-dependent expansion parameter is defined, which enables to prove, up to a certain order, the dominance of daisy over non-daisy diagrams. Resumming an infinite number of Feynman diagrams at finite temperature we obtain an *improved* theory, whose expansion parameter is the newly obtained temperature-dependent expansion parameter. We have constructed the improved theory to leading order, using functional and diagrammatic methods, and shown the role of the Debye mass on it. We have explicitly shown that both methods yield the same result. We have also made some comments about how to go to the next-to-leading order in the improved theory. The latter being a very controversial point we did not want to draw any final conclusion on it. Finally we have explicitly computed the case of the Standard Model, which will be useful in the next sections, to leading order in the improved theory, and given the expressions of the Debye masses for Higgs and Goldstone bosons, and the longitudinal components of gauge bosons.

Section 7 is devoted to a review of baryon asymmetry generation at the critical temperature of various phase transitions and the restrictions it imposes on them. We first summarize the problem of baryon asymmetry generation in the standard cosmological model and the classical Sakharov's conditions for baryogenesis. We then explore two different scenarios for baryogenesis: the standard out-of-equilibrium decay scenario and baryogenesis at the electroweak phase transition. The former (the standard out-of-equilibrium decay scenario) is based on the decay, out of equilibrium, of a particle whose decays products violate baryon

number and CP. The decaying particle can be either a gauge or Higgs boson of a grand unified theory or a gauge singlet coupled to the observable matter by gravitational interactions. In both cases we have deduced the necessary constraints in the corresponding theory. The latter scenario (baryogenesis at the electroweak phase transition) is more appealing since it is related to the physics which is being explored nowadays at present colliders. It is based on the fact that baryon and lepton numbers are anomalous global symmetries in the Standard Model that are violated by non-perturbative effects. At zero temperature these effects are negligible, but at finite temperature they are strong, mediated by sphalerons, and can trigger, in principle, enough baryon asymmetry as it is required by the nucleosynthesis constraints. We study the baryon violation rate beyond and below the critical temperature. The latter being controlled by the sphaleron barrier, we present the result of the calculation of the sphaleron energy at finite temperature in the context of the Standard Model as a function of the Higgs mass. Below the critical temperature the sphaleron mediated baryon violation rate should be out of equilibrium to avoid wash out of baryon asymmetry. This condition is performed by comparison of the actual baryon violation rate at the critical temperature of the electroweak phase transition with the expansion rate of the universe at that temperature, and provides an upper bound on the Higgs mass (which is one of the parameters controlling the strength of the first order phase transition). The case of the Standard Model is analyzed in some detail, including plasma effects to leading order. The result translates into an upper bound on the Higgs mass which is definitively below the LEP experimental lower bound.

Motivated by the previous, negative, result we have analyzed in **Section 8** two particularly interesting and motivated extensions of the Standard Model. First, the case of the Standard Model with a complex singlet with zero vacuum expectation value. It is almost the simplest extension of the Standard Model one can think of. In this case we have shown that the out of equilibrium condition for the sphaleron mediated baryon asymmetry rate translates into an upper bound which is still beyond the present experimental limit. In particular we have shown that the previous condition can be fulfilled for Higgs masses below the W mass, which is also the range of validity we expect for our perturbative results to be reliable. Secondly, we have analyzed the case of the minimal supersymmetric standard model. It is the minimal extension of the Standard Model where the gauge hierarchy problem is resolved. In this case, and imposing the most favorable conditions on the supersymmetric parameters, we have found a little window for pseudoscalar masses greater than ~ 400 GeV and $\tan\beta \sim 2$. Since a modest improvement in the present experimental bound on the Higgs mass would make this window to disappear, our results do not lead to optimism, though we do not want to draw a final negative conclusion for the case of the minimal supersymmetric standard model.

2 The effective potential at zero temperature

The effective potential for quantum field theories was originally introduced by Euler, Heisenberg and Schwinger [1], and applied to studies of spontaneous symmetry breaking by Goldstone, Salam, Weinberg and Jona-Lasinio [2]. Calculations of the effective potential were initially performed at one-loop by Coleman and E. Weinberg [3] and at higher-loop by Jackiw [4] and Iliopoulos, Itzykson and Martin [5]. More recently the effective potential has been the subject of a vivid investigation, especially related to its invariance under the renormalization group. I will try to review, in this section, the main ideas and update the latest developments on the effective potential.

2.1 Generating functionals

To fix the ideas, let us consider the theory described by a scalar field ϕ with a lagrangian density $\mathcal{L}\{\phi(x)\}$ and an action

$$S[\phi] = \int d^4x \mathcal{L}\{\phi(x)\} \tag{2.1}$$

The generating functional (vacuum-to-vacuum amplitude) is given by the path-integral representation,

$$Z[j] = \langle 0_{\text{out}} \mid 0_{\text{in}} \rangle_j \equiv \int d\phi \exp\{i(S[\phi] + \phi j)\} \tag{2.2}$$

where we are using the notation

$$\phi j \equiv \int d^4x \phi(x) j(x) \tag{2.3}$$

Using (2.2) one can obtain the connected generating functional $W[j]$ defined as,

$$Z[j] \equiv \exp\{iW[j]\} \tag{2.4}$$

and the effective action $\Gamma[\overline{\phi}]$ as the Legendre transform of (2.4)

$$\Gamma[\overline{\phi}] = W[j] - \int d^4x \frac{\delta W[j]}{\delta j(x)} j(x) \tag{2.5}$$

where

$$\overline{\phi}(x) = \frac{\delta W[j]}{\delta j(x)} \tag{2.6}$$

In particular, from (2.5) and (2.6), the following equality can be easily proven,

$$\frac{\delta \Gamma[\overline{\phi}]}{\delta \overline{\phi}} = \frac{\delta W[j]}{\delta j} \frac{\delta j}{\delta \overline{\phi}} - j - \overline{\phi} \frac{\delta j}{\delta \overline{\phi}} = -j \tag{2.7}$$

where we have made use of the notation (2.3). Eq.(2.7) implies in particular that,

$$\left.\frac{\delta\Gamma[\overline{\phi}]}{\delta\overline{\phi}}\right|_{j=0} = 0 \tag{2.8}$$

which defines de vacuum of the theory in the absence of external sources.

We can now expand $Z[j]$ ($W[j]$) in a power series of j, to obtain its representation in terms of Green functions G_n (connected Green functions $G^c_{(n)}$) as,

$$Z[j] = \sum_{n=0}^{\infty} \frac{i^n}{n!} \int d^4x_1 \dots d^4x_n j(x_1) \dots j(x_n) G_{(n)}(x_1, \dots, x_n) \tag{2.9}$$

and

$$iW[j] = \sum_{n=0}^{\infty} \frac{i^n}{n!} \int d^4x_1 \dots d^4x_n j(x_1) \dots j(x_n) G^c_{(n)}(x_1, \dots, x_n) \tag{2.10}$$

Similarly the effective action can be expanded in powers of $\overline{\phi}$ as

$$\Gamma[\overline{\phi}] = \sum_{n=0}^{\infty} \frac{1}{n!} \int d^4x_1 \dots d^4x_n \overline{\phi}(x_1) \dots \overline{\phi}(x_n) \Gamma^{(n)}(x_1, \dots, x_n) \tag{2.11}$$

where $\Gamma^{(n)}$ are the one-particle irreducible (1PI) Green functions.

We can Fourier transform $\Gamma^{(n)}$ and $\overline{\phi}$ as,

$$\Gamma^{(n)}(x_1, \dots, x_n) = \int \prod_{i=1}^{n} \left[\frac{d^4p_i}{(2\pi)^4} \exp\{ip_i x_i\} \right] (2\pi)^4 \delta^{(4)}(p_1 + \dots + p_n) \Gamma^{(n)}(p_1, \dots, p_n) \tag{2.12}$$

$$\tilde{\phi}(p) = \int d^4x e^{-ipx} \overline{\phi}(x) \tag{2.13}$$

and obtain for (2.5) the expression,

$$\Gamma[\overline{\phi}] = \sum_{n=0}^{\infty} \int \prod_{i=1}^{n} \left[\frac{d^4p_i}{(2\pi)^4} \tilde{\phi}(-p_i) \right] (2\pi)^4 \delta^{(4)}(p_1 + \dots + p_n) \Gamma^{(n)}(p_1, \dots, p_n) \tag{2.14}$$

In a translationally invariant theory,

$$\overline{\phi}(x) = \phi_c \tag{2.15}$$

the field $\overline{\phi}$ is constant. Removing an overall factor of space-time volume, we define the effective potential $V_{\text{eff}}(\phi_c)$ as,

$$\Gamma[\phi_c] = -\int d^4x V_{\text{eff}}(\phi_c) \tag{2.16}$$

Using now the definition of Dirac δ-function,

$$\delta^{(4)}(p) = \int \frac{d^4x}{(2\pi)^4} e^{-ipx} \tag{2.17}$$

and (2.15) in (2.13) we obtain,

$$\tilde{\phi}_c(p) = (2\pi)^4 \phi_c \delta^{(4)}(p). \tag{2.18}$$

Replacing (2.18) in (2.14) we can write the effective action for constant field configurations as,

$$\Gamma(\phi_c) = \sum_{n=0}^{\infty} \frac{1}{n!} \phi_c^n (2\pi)^4 \delta^{(4)}(0) \Gamma^{(n)}(p_i = 0) = \sum_{n=0}^{\infty} \frac{1}{n!} \phi_c^n \Gamma^{(n)}(p_i = 0) \int d^4x \tag{2.19}$$

and comparing it with (2.16) we obtain the final expression,

$$V_{\text{eff}}(\phi_c) = -\sum_{n=0}^{\infty} \frac{1}{n!} \phi_c^n \Gamma^{(n)}(p_i = 0) \tag{2.20}$$

which will be used for explicit calculations of the effective potential.

Let us finally mention that there is an alternative way of expanding the effective action: it can also be expanded in powers of momentum, about the point where all external momenta vanish. In configuration space that expansion reads as:

$$\Gamma[\overline{\phi}] = \int d^4x \left[-V_{\text{eff}}(\overline{\phi}) + \frac{1}{2} (\partial_\mu \overline{\phi}(x))^2 Z(\overline{\phi}) + \cdots \right] \tag{2.21}$$

2.2 The one-loop effective potential

We are now ready to compute the effective potential. In particular the zero-loop contribution is simply the classical (tree-level) potential. The one-loop contribution is readily computed using the previous techniques and can be written in closed form for any field theory containing spinless particles, spin-$\frac{1}{2}$ fermions and gauge bosons. Here we will follow closely the calculation of ref. [3].

2.2.1 Scalar fields

We consider the simplest model of one self-interacting real scalar field, described by the lagrangian

$$\mathcal{L} = \frac{1}{2} \partial^\mu \phi \partial_\mu \phi - V_0(\phi) \tag{2.22}$$

with a tree-level potential

$$V_0 = \frac{1}{2} m^2 \phi^2 + \frac{\lambda}{4!} \phi^4 \tag{2.23}$$

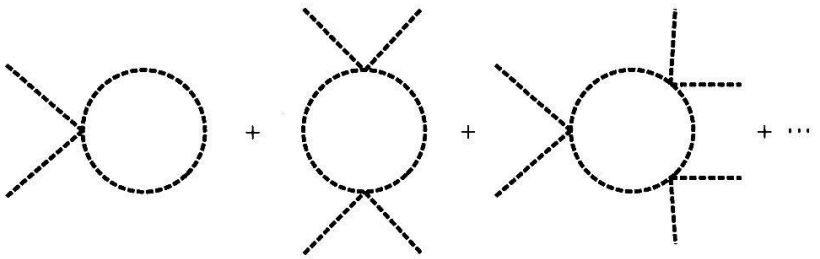

Figure 1: **1PI diagrams contributing to the one-loop effective potential of (2.22)**

The one-loop correction to the tree-level potential should be computed as the sum of all 1PI diagrams with a single loop and zero external momenta. Diagrammatically they are displayed in fig. 1, where each vertex has 2 external legs.

The nth diagram has n propagators, n vertices and $2n$ external legs. The n propagators will contribute a factor of $i^n(p^2-m^2+i\epsilon)^{-n}$ [1]. The external lines contribute a factor of ϕ_c^{2n} and each vertex a factor of $-i\lambda/2$, where the factor $1/2$ comes from the fact that interchanging the 2 external lines of the vertex does not change the diagram. There is a global symmetry factor $\frac{1}{2n}$, where $\frac{1}{n}$ comes from the symmetry of the diagram under the discrete group of rotations $\mathbf{Z}_n$ and $\frac{1}{2}$ from the symmetry of the diagram under reflection. Finally there is an integration over the loop momentum and an extra global factor of i from the definition of the generating functional.

Using the previous rules the one-loop effective potential can be computed as,

$$V_{\rm eff}(\phi_c) = V_0(\phi_c) + V_1(\phi_c),$$

with

$$V_1(\phi_c) = i\sum_{n=1}^{\infty}\int\frac{d^4p}{(2\pi)^4}\frac{1}{2n}\left[\frac{\lambda\phi_c^2/2}{p^2-m^2+i\epsilon}\right]^n = -\frac{i}{2}\int\frac{d^4p}{(2\pi)^4}\log\left[1-\frac{\lambda\phi_c^2/2}{p^2-m^2+i\epsilon}\right] \tag{2.24}$$

After a Wick rotation

$$p^0 = ip_E^0,\ p_E = (-ip^0,\vec{p}\,),\ p^2 = (p^0)^2 - \vec{p}^{\,2} = -p_E^2, \tag{2.25}$$

eq. (2.24) can be cast as,

$$V_1(\phi_c) = \frac{1}{2}\int\frac{d^4p_E}{(2\pi)^4}\log\left[1+\frac{\lambda\phi_c^2/2}{p_E^2+m^2}\right] \tag{2.26}$$

[1] We are using the Bjorken and Drell's [6] notation and conventions.

Finally, using the *shifted* mass

$$m^2(\phi_c) = m^2 + \frac{1}{2}\lambda\phi_c^2 = \frac{d^2V_0(\phi_c)}{d\phi_c^2} \tag{2.27}$$

and dropping the subindex E from the euclidean momenta, we can write the final expression of the one-loop contribution to the effective potential as,

$$V_1(\phi_c) = \frac{1}{2}\int \frac{d^4p}{(2\pi)^4}\log\left[p^2 + m^2(\phi_c)\right] \tag{2.28}$$

where a field independent term has been neglected.

The result of eq. (2.28) can be trivially generalized to the case of N_s **complex** scalar fields described by the lagrangian,

$$\mathcal{L} = \partial^\mu\phi^a\partial_\mu\phi_a^\dagger - V_0(\phi^a, \phi_a^\dagger). \tag{2.29}$$

The one-loop contribution to the effective potential in the theory described by the lagrangian (2.29) is given by

$$V_1 = \frac{1}{2}Tr\int \frac{d^4p}{(2\pi)^4}\log\left[p^2 + M_s^2(\phi^a, \phi_b^\dagger)\right] \tag{2.30}$$

where

$$(M_s^2)_b^a \equiv V_b^a = \frac{\partial^2 V}{\partial\phi_a^\dagger\partial\phi^b} \tag{2.31}$$

and $Tr\ M_s^2 = 2\ V_a^a$, where the factor of 2 comes from the fact that each complex field contains two degrees of freedom. Similarly $Tr\ \mathbf{1}$=2 N_s.

2.2.2 Fermion fields

We consider now a theory with fermion fields described by the lagrangian,

$$\mathcal{L} = i\overline{\psi}_a\gamma\cdot\partial\psi^a - \overline{\psi}_a(M_f)_b^a\psi^b \tag{2.32}$$

where the mass matrix $(M_f)_b^a(\phi_c^i)$ is a function of the scalar fields linear in ϕ_c^i: $(M_f)_b^a = \Gamma_{bi}^a\phi_c^i$.

The diagrams contributing to the one-loop effective potential are depicted in fig. 2. Diagrams with an odd number of vertices are zero because of the γ-matrices property: $tr(\gamma^{\mu_1}\cdots\gamma^{\mu_{2n+1}}) = 0$.

The diagram with $2n$ vertices has $2n$ fermionic propagators. The propagators yield a factor

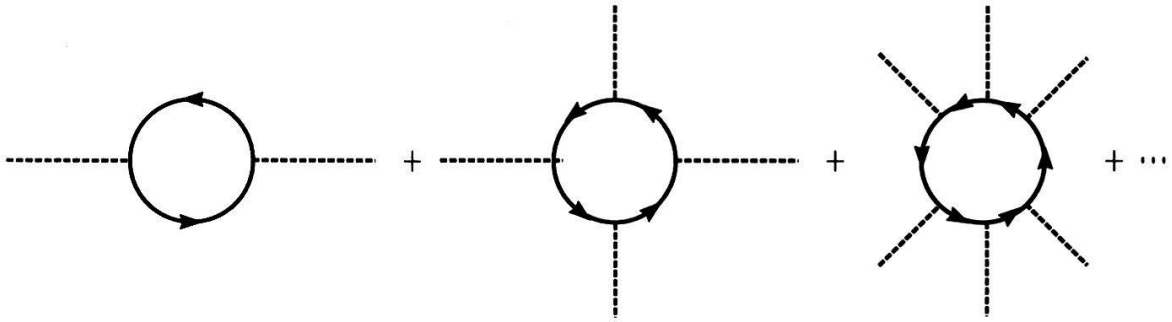

Figure 2: **1PI diagrams contributing to the one-loop effective potential of (2.32)**

$$Tr_s[i^{2n}(\gamma\cdot p)^{2n}(p^2+i\epsilon)^{2n}]$$

where Tr_s refers to spinor indices. The vertices contribute as

$$Tr[-i^{2n}M_f(\phi_c)^{2n}]$$

where Tr runs over the different fermionic fields. There is also a combinatorial factor $\frac{1}{2n}$ (from the cyclic and anticyclic symmetry of diagrams) and an overall -1 coming from the fermions loop. One finally obtains the total factor

$$-\frac{1}{2n}\frac{Tr(M_f^{2n})}{p^{2n}}\cdot Tr_s\mathbf{1}.$$

The factor $Tr_s\mathbf{1}$ just counts the number of degrees of freedom of the fermions. It is equal to 4 if Dirac fermions are used, and 2 if Weyl fermions (and σ-matrices) are present. So we will write,

$$Tr_s\mathbf{1}=2\lambda \tag{2.33}$$

where $\lambda=1$ ($\lambda=2$) for Weyl (Dirac) fermions. On the other hand we have grouped terms pairwise in the matrix product and used,

$$\tilde{p}^2=p^2$$

where $\tilde{p}$ stands either for $p\cdot\gamma$ or $p\cdot\sigma$, depending on the kind of fermions we are using.

Collecting everything together we can write the one-loop contribution to the effective potential from fermion fields as,

$$V_1(\phi_c)=-2\lambda iTr\sum_{n=1}^{\infty}\int\frac{d^4p}{(2\pi)^4}\frac{1}{2n}\left[\frac{M_f^2}{p^2}\right]^n=2\lambda\frac{i}{2}Tr\int\frac{d^4p}{(2\pi)^4}\log\left[1-\frac{M_f^2}{p^2}\right] \tag{2.34}$$

As in the case of the scalar theory, after making a Wick rotation to the Euclidean momenta space, and neglecting an irrelevant field independent term, we can cast (2.34) as

$$V_1=-2\lambda\frac{1}{2}Tr\int\frac{d^4p}{(2\pi)^4}\log\left[p^2+M_f^2(\phi_c)\right] \tag{2.35}$$

2.2.3 Gauge bosons

Consider now a theory described by the lagrangian,

$$\mathcal{L} = -\frac{1}{4}Tr(F_{\mu\nu}F^{\mu\nu}) + \frac{1}{2}Tr(D_\mu\phi_a)^\dagger D^\mu\phi^a + \cdots \tag{2.36}$$

In the Landau gauge, which does not require ghost-compensating terms, the free gauge-boson propagator is

$$\Pi^\mu{}_\nu = -\frac{i}{p^2 + i\epsilon}\Delta^\mu{}_\nu \tag{2.37}$$

with

$$\Delta^\mu{}_\nu = g^\mu{}_\nu - \frac{p^\mu p_\nu}{p^2} \tag{2.38}$$

satisfying the property $p_\mu\Delta^\mu{}_\nu = 0$ and $\Delta^n = \Delta$, $n = 1, 2, \ldots$.

The only vertex which contributes to one-loop is

$$\mathcal{L} = \frac{1}{2}(M_{gb})^2_{\alpha\beta}A^\alpha_\mu A^{\mu\beta} + \cdots \tag{2.39}$$

where

$$(M_{gb})^2_{\alpha\beta}(\phi_c) = g_\alpha g_\beta Tr\left[\left(T^i_{\alpha\ell}\phi_i\right)^\dagger T^\ell_{\beta j}\phi^j\right] \tag{2.40}$$

In this way the diagrams contributing to the one-loop effective potential are depicted in fig. 3.

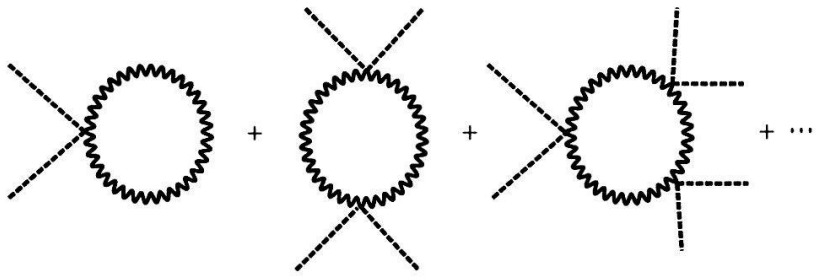

Figure 3: **1PI diagrams contributing to the one-loop effective potential of (2.36)**

A few comments about eq. (2.40): **(i)** g_α is the gauge coupling constant associated to the gauge field A^α_μ; if the gauge group is simple, *e.g.* $SU(5)$, $SO(10)$, $E_6, \ldots$, then all gauge couplings are equal; otherwise there is a distinct gauge coupling per group factor. **(ii)** T_α are the generators of the Lie algebra of the gauge group in the representation of the ϕ-fields and the trace in (2.40) is over indices of that representation.

Taking into account the combinatorial factors, the graph with n propagators and n vertices yields a total factor

$$\frac{1}{2n}\frac{Tr((M_{gb})^2)^n}{p^{2n}}Tr(\Delta)$$

where

$$Tr(\Delta) = 3 \tag{2.41}$$

which is the number of degrees of freedom of a massive gauge boson. Collecting together all factors, and making the Wick rotation to the euclidean momenta space, we can cast the effective potential from gauge bosons as,

$$V_1 = Tr(\Delta)\frac{1}{2}Tr\int\frac{d^4p}{(2\pi)^4}\log\left[p^2 + (M_{gb})^2(\phi_c)\right] \tag{2.42}$$

2.3 The higher-loop effective potential

Calculating the effective potential by summing infinite series of Feynman graphs at zero external momentum is an extremely onerous task beyond the one-loop approximation. However, as has been shown in ref. [4], this task is trivial for the case of one-loop, and affordable for the case of higher-loop. Here we will just summarize the result of ref. [4] [2].

We will start considering the theory described by a real scalar field, with a lagrangian $\mathcal{L}$ given in (2.22-2.23), and an action as in (2.1). We will define another lagrangian $\hat{\mathcal{L}}$ by the following procedure:

$$\int d^4x\hat{\mathcal{L}}\{\phi_c;\phi(x)\} \equiv S[\phi_c+\phi] - S[\phi_c] - \phi\frac{\delta S[\phi_c]}{\delta\phi_c} \tag{2.43}$$

where we have used in the last term the notation (2.3). In (2.43), ϕ_c is an x-independent shifting field. The second term in (2.43) makes the vacuum energy equal to zero, and the third term is there to cancel the tadpole part of the shifted action.

If we denote by $\mathcal{D}\{\phi_c; x-y\}$ the propagator of the shifted theory,

$$i\mathcal{D}^{-1}\{\phi_c; x-y\} = \left.\frac{\delta^2 S[\phi]}{\delta\phi(x)\delta\phi(y)}\right|_{\phi=\phi_c} \tag{2.44}$$

and

$$i\mathcal{D}^{-1}\{\phi_c; p\}$$

[2] The interested reader can find in [4] all calculational details.

its Fourier transform, the effective potential is found to be given by [4]:

$$V_{\rm eff}(\phi_c) = V_0(\phi_c) - \frac{i}{2}\int \frac{d^4p}{(2\pi)^4} \log\det i\mathcal{D}^{-1}\{\phi_c;p\} + i\left\langle \exp\left[i\int d^4x \hat{\mathcal{L}}_I\{\phi_c;\phi(x)\}\right]\right\rangle \quad (2.45)$$

The first term in (2.45) is just the classical tree-level potential. The second term is the one-loop potential, where the determinant operates on any possible internal indices defining the propagator. The third term summarizes the following operation: Compute all 1PI vacuum diagrams, with conventional Feynman rules, using the propagator of the shifted theory $\mathcal{D}\{\phi_c;p\}$ and the interaction provided by the interaction lagrangian $\hat{\mathcal{L}}_I\{\phi_c;\phi(x)\}$, and delete the overall factor of space-time volume $\int d^4x$ from the effective action (2.16). It can be shown that the last term in (2.45) starts at two-loop. Every term in (2.45) resums an infinite number of Feynman diagrams of the unshifted theory.

In the simple example of the lagrangian (2.22-2.23) it can be easily seen that the shifted potential is given by

$$\hat{V}\{\phi_c;\phi\} = \frac{1}{2}m^2(\phi_c)\phi^2 + \frac{\lambda}{3!}\phi_c\phi^3 + \frac{\lambda}{4!}\phi^4 \quad (2.46)$$

where the shifted mass is defined in (2.27). The shifted propagator is found to be

$$i\mathcal{D}^{-1}\{\phi_c;p\} = p^2 - m^2(\phi_c) \quad (2.47)$$

and the second term of (2.45) easily computed to be

$$V_1(\phi_c) = -\frac{i}{2}\int \frac{d^4p}{(2\pi)^4} \log[p^2 - m^2(\phi_c)] \quad (2.48)$$

which is easily seen to coincide with (2.24), up to field independent terms, so that after the Wick rotation we recover the result (2.28).

The two-loop effective potential is harder than the one-loop term, but affordable. The result can be found in ref. [4]. Diagrammatically, the one- and two-loop effective potentials are given in fig. 4, where it is understood that we are using the Feynman rules of the shifted

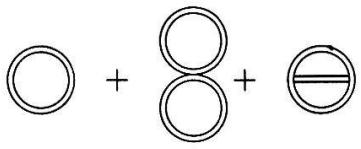

Figure 4: **One and two-loop diagrams contributing to the effective potential of (2.45)**

theory, as stated above.

Of course, the previous rules apply also to theories containing fermions and gauge bosons. The Feynman rules of the shifted theory applied to all 1PI diagrams provide the total effective potential according to (2.45). In particular it is trivial to obtain the one-loop effective potential for fermions and gauge bosons, as given by eqs. (2.35) and (2.42), respectively. Notice that the masses $M_f^2(\phi_c)$, in (2.35), and $M_{gb}^2(\phi_c)$, in (2.42) are the masses in the corresponding shifted theories. Diagrammatically (2.35) and (2.42) can be represented in the shifted theory as vacuum diagrams with one fermion and one gauge boson loop, respectively.

2.4 Renormalizations conditions

The final expression of the effective potential we have deduced in the previous section, eqs.(2.28), (2.35) and (2.42), is ultraviolet-divergent. To make sense out of it we have to follow the renormalization procedure of quantum field theories. First of all, to give a sense to the ultraviolet behaviour of the theory we have to make it finite: *i.e.* we have to **regularize** the theory. Second of all, all infinities have to be absorbed by appropriate **counterterms**, which were not explicitly written in our previous expressions. The way these infinities are absorbed by the counterterms depend on the definition of the **renormalized parameters**, *i.e.* on the choice of the **renormalization conditions**. Finally the theory, written as a function of the renormalized parameters, is finite.

In this way, the first step towards renormalizing the theory is choosing the regularization scheme. We will first present the straightforward regularization using a cut-off of momenta.

2.4.1 Cut-off regularization

We will illustrate this scheme with the simplest theory: a massless real scalar field, with a lagrangian

$$\mathcal{L} = \frac{1}{2}(1+\delta Z)(\partial_\mu \phi)^2 - \frac{1}{2}\delta m^2 \phi^2 - \frac{\lambda + \delta\lambda}{4!}\phi^4 \tag{2.49}$$

where δZ, δm^2 and $\delta\lambda$ are the usual wave-function, mass and coupling constant renormalization counterterms. They have to be defined self-consistently order by order in the loop expansion. Here we will compute everything to one-loop order.

The conventional definition of the renormalized mass of the scalar field is the negative inverse propagator at zero momentum. In view of (2.20) we can write it as:

$$m_R^2 = -\Gamma^{(2)}(p=0) = \left.\frac{d^2 V}{d\phi_c^2}\right|_{\phi_c=0} \tag{2.50}$$

We can also define the renormalized coupling as the four-point function at zero external momentum,

$$\lambda_R = -\Gamma^{(4)}(p=0) = \left.\frac{d^4V}{d\phi_c^4}\right|_{\phi_c=0} \tag{2.51}$$

and the standard condition for the field renormalization is,

$$Z(0) = 1 \tag{2.52}$$

Now we will compute the effective potential (2.28) cutting off the integral at $p^2 = \Lambda^2$. First of all we can integrate over angular variables. For that we can use,

$$\int d^n p f(\rho) = \frac{\pi^{n/2}}{\Gamma(\frac{n}{2})} \int f(\rho) d\rho \tag{2.53}$$

where $\rho = |p|^2$, and we can cast (2.28) as

$$V_1(\phi_c) = \frac{1}{32\pi^2} \int_0^{\Lambda^2} \rho \log[\rho + m^2(\phi_c)] d\rho. \tag{2.54}$$

This indefinite integral can be solved with the help of [7]

$$\int x \log(a+x) = \frac{1}{2}(x^2 - a^2)\log(a+x) - \frac{1}{2}\left(\frac{x^2}{2} - ax\right)$$

Neglecting now in (2.54) field independent terms, and terms which vanish in the limit $\Lambda \to \infty$, we finally obtain,

$$V_1(\phi_c) = \frac{1}{32\pi^2} m^2(\phi_c)\Lambda^2 + \frac{1}{64\pi^2} m^4(\phi_c) \log \frac{m^2(\phi_c)}{\Lambda^2} \tag{2.55}$$

Using now (2.55) we can write the one-loop effective potential of the theory (2.49) as,

$$V = \frac{1}{2}\delta m^2 \phi_c^2 + \frac{\lambda + \delta\lambda}{4!}\phi_c^4 + \frac{\lambda\phi_c^2}{64\pi^2}\Lambda^2 + \frac{\lambda^2\phi_c^4}{256\pi^2}\left(\log\frac{\lambda\phi_c^2}{2\Lambda^2} - \frac{1}{2}\right) \tag{2.56}$$

We will impose now a variant of the renormalization conditions (2.50), (2.51) and (2.52). For the renormalized mass we can impose it to vanish, *i.e.*,

$$\left.\frac{d^2V}{d\phi_c^2}\right|_{\phi_c=0} = 0 \tag{2.57}$$

For the renormalized gauge coupling λ, we cannot use eq. (2.51) at a value of the field equal to zero. There is nothing wrong with using a different renormalization prescription and using a different subtraction point. We can use,

$$\lambda = \left.\frac{d^4V}{d\phi_c^4}\right|_{\phi_c=\mu} \tag{2.58}$$

where μ is some mass scale. Different choices of the scale lead to different definitions of the coupling constant, *i.e.* to different parametrizations of the same theory, but in principle any value of μ is as good as any other.

Imposing now the conditions (2.57) and (2.58) to (2.56) we can write the counterterms as,

$$\delta m^2 = -\frac{\lambda}{32\pi^2}\Lambda^2 \tag{2.59}$$

and

$$\delta\lambda = -\frac{11\lambda^2}{32\pi^2} - \frac{3\lambda^2}{32\pi^2}\log\frac{\lambda^2\mu^2}{\pi\Lambda^2} \tag{2.60}$$

Using now (2.59) and (2.60) in (2.56) we can write the one-loop effective potential in the previous renormalization scheme as,

$$V_{\text{eff}} = \frac{\lambda}{4!}\phi_c^4 + \frac{\lambda^2\phi_c^4}{256\pi^2}\log\left(\frac{\phi_c^2}{\mu^2} - \frac{25}{6}\right) \tag{2.61}$$

A similar renormalization scheme can be defined also for theories with fermions and/or gauge bosons. However for gauge theories the regularization provided by the cut-off explicitly break gauge invariance so that the dimensional regularization is better suited for them. In the next section we will review the calculation of the effective potential in the dimensional regularization and define the so-called $\overline{\text{MS}}$ scheme.

2.4.2 Dimensional regularization

This regularization scheme was introduced by t'Hooft and Veltman [8]. It consists in making an analytic continuation of Feynman integrals to the complex plane in the number of space-time dimensions n. The integrals have singularities which arise as poles in $1/(n-4)$ and have to be subtracted out. The particular prescription for subtraction is called a **renormalization scheme**. In working with the effective potential it is customary to use the so-called $\overline{\text{MS}}$ renormalization scheme [10].

We will compute now the one-loop effective potential (2.28) using dimensional regularization, *i.e.*

$$V_1(\phi_c) = \frac{1}{2}(\mu^2)^{2-\frac{n}{2}}\int\frac{d^np}{(2\pi)^n}\log\left[p^2 + m^2(\phi_c)\right] \tag{2.62}$$

where μ is a scale with mass dimension which needs to be introduced to balance the dimension of the integration measure. It is simpler to compute the tadpole

$$V' = \frac{1}{2}(\mu^2)^{2-\frac{n}{2}}\int\frac{d^np}{(2\pi)^n}\frac{1}{p^2 + m^2(\phi_c)} \tag{2.63}$$

where the meaning of V' is the derivative with respect to $m^2(\phi_c)$, using the basic formula of dimensional regularization,

$$\int d^n p \frac{(p^2)^\alpha}{(p^2+M^2)^\beta} = \pi^{\frac{n}{2}} (M^2)^{\frac{n}{2}+\alpha-\beta} \frac{\Gamma(\alpha+\frac{n}{2})\Gamma(\beta-\alpha-\frac{n}{2})}{\Gamma(\frac{n}{2})\Gamma(\beta)} \tag{2.64}$$

and integrating the resulting integral with respect to $m^2(\phi_c)$. One can then write the regularized potential (2.62) as,

$$V_1(\phi_c) = -\frac{1}{32\pi^2} \frac{1}{\frac{n}{2}(\frac{n}{2}-1)} \left(\frac{m^2(\phi_c)}{4\pi\mu^2}\right)^{\frac{n}{2}-2} \Gamma\left(2-\frac{n}{2}\right) \tag{2.65}$$

We can expand (2.65) in powers of $2-n/2$ and use the expansion

$$\Gamma(z) = \frac{1}{z} - \gamma_E + \mathcal{O}(z) \tag{2.66}$$

where $\gamma_E = 0.5772\ldots$ is the Euler-Masccheroni constant [7]. We obtain for (2.65)

$$V_1(\phi_c) = \frac{m^4(\phi_c)}{64\pi^2} \left\{ -\left[\frac{1}{2-\frac{n}{2}} - \gamma_E + \log 4\pi\right] + \log\frac{m^2(\phi_c)}{\mu^2} - \frac{3}{2} + \mathcal{O}(\frac{n}{2}-2) \right\} \tag{2.67}$$

Now the $\overline{\text{MS}}$ renormalization scheme consists in subtracting the term proportional to

$$C_{uv} \equiv \left[\frac{1}{2-\frac{n}{2}} - \gamma_E + \log 4\pi\right] \tag{2.68}$$

in the regularized potential (2.67). Therefore the divergent piece,

$$-\frac{m^4(\phi_c)}{64\pi^2} \left\{ \left[\frac{1}{2-\frac{n}{2}} - \gamma_E + \log 4\pi\right] \right\}$$

has to be absorbed by the counterterms. Therefore the final expression for the one-loop potential, written in terms of the renormalized parameters, is

$$V_1(\phi_c) = \frac{1}{64\pi^2} m^4(\phi_c) \left\{ \log\frac{m^2(\phi_c)}{\mu^2} - \frac{3}{2} \right\} \tag{2.69}$$

For instance, in the theory described by lagrangian (2.49), the counterterms are given by,

$$\begin{aligned} \delta m^2 &= 0 \\ \delta\lambda &= \frac{3\lambda^2}{32\pi^2} \left[\frac{1}{2-\frac{n}{2}} - \gamma_E + \log 4\pi\right] \end{aligned} \tag{2.70}$$

and the effective potential is,

$$V_{\rm eff} = \frac{\lambda}{4!}\phi_c^4 + \frac{\lambda^2\phi_c^4}{256\pi^2}\log\left(\frac{\lambda\phi_c^2}{2\mu^2} - \frac{3}{2}\right) \tag{2.71}$$

The scale μ along this section is related to the renormalization group behaviour of the renormalized couplings and masses.

For a theory with fermion fields, one needs a trace operation in dimensional regularization, as $Tr\mathbf{1} = f(n)$. For instance, for an even dimension one could choose, $f(n) = 2^{n/2}$ for Dirac fermions, and $f(n) = 2^{n/2-1}$ for Weyl fermions. However the difference $f(n) - f(4)$ is only relevant for divergent graphs and can therefore be absorbed by a renormalization-group transformation. It is usually convenient to choose $f(n) = f(4) = 2\lambda$ for all values of n [11]. The effective potential (2.35) can be computed as in (2.62), leading to,

$$V_1(\phi_c) = -\lambda\frac{M_f^4(\phi_c)}{32\pi^2}\left\{-\left[\frac{1}{2-\frac{n}{2}} - \gamma_E + \log 4\pi\right] + \log\frac{M_f^2(\phi_c)}{\mu^2} - \frac{3}{2} + \mathcal{O}(\frac{n}{2}-2)\right\} \tag{2.72}$$

In the $\overline{\rm MS}$ renormalization scheme, after subtracting the term proportional to (2.68) we obtain,

$$V_1(\phi_c) = -\lambda\frac{1}{32\pi^2}M_f^4(\phi_c)\left\{\log\frac{M_f^2(\phi_c)}{\mu^2} - \frac{3}{2}\right\} \tag{2.73}$$

Similarly, in a theory with gauge bosons as in (2.36), the effective potential (2.42) is computed as,

$$V_1(\phi_c) = Tr(\Delta)\frac{M_{gb}^4(\phi_c)}{64\pi^2}\left\{-\left[\frac{1}{2-\frac{n}{2}} - \gamma_E + \log 4\pi\right] + \log\frac{M_{gb}^2(\phi_c)}{\mu^2} - \frac{3}{2} + \mathcal{O}(\frac{n}{2}-2)\right\} \tag{2.74}$$

where

$$Tr(\Delta) = n - 1 \tag{2.75}$$

In the $\overline{\rm MS}$ renormalization scheme, subtracting as usual the term proportional to (2.68) one obtains the effective potential,

$$V_1(\phi_c) = 3\frac{1}{64\pi^2}M_{gb}^4(\phi_c)\left\{\log\frac{M_{gb}^2(\phi_c)}{\mu^2} - \frac{5}{6}\right\} \tag{2.76}$$

A variant of the $\overline{\rm MS}$ renormalization scheme is the $\overline{\rm DR}$ renormalization scheme [9], where the dimensional regularization is applied only to the scalar part of the integrals, while all fermion and tensor indices are considered in four dimensions. In this case $Tr(\Delta)$ is taken

equal to 3, as in (2.41), and subtracting from (2.74) the term proportional to (2.68) one obtains,

$$V_1(\phi_c) = 3\frac{1}{64\pi^2} M_{gb}^4(\phi_c) \left\{ \log \frac{M_{gb}^2(\phi_c)}{\mu^2} - \frac{3}{2} \right\} \tag{2.77}$$

2.5 One-loop effective potential for the Standard Model

In this subsection we will apply the above ideas to compute the one loop effective potential for the Standard Model of electroweak interactions. The spin-zero fields of the Standard Model are described by the $SU(2)$ doublet,

$$\Phi = \frac{1}{\sqrt{2}} \begin{pmatrix} \chi_1 + i\chi_2 \\ \phi_c + h + i\chi_3 \end{pmatrix} \tag{2.78}$$

where ϕ_c is the real constant background, h the Higgs field, and χ_a (a=1,2,3) are the three Goldstone bosons. The tree level potential reads, in terms of the background field, as

$$V_0(\phi_c) = -\frac{m^2}{2}\phi_c^2 + \frac{\lambda}{4}\phi_c^4 \tag{2.79}$$

with positive λ and m^2, and the tree level minimum corresponding to

$$v^2 = \frac{m^2}{\lambda}.$$

The spin-zero field dependent masses are

$$\begin{aligned} m_h^2(\phi_c) &= 3\lambda\phi_c^2 - m^2 \\ m_\chi^2(\phi_c) &= \lambda\phi_c^2 - m^2 \end{aligned} \tag{2.80}$$

so that $m_h^2(v) = 2\lambda v^2 = 2m^2$ and $m_\chi^2(v) = 0$. The gauge bosons contributing to the one-loop effective potential are $W^\pm$ and Z, with tree level field dependent masses,

$$\begin{aligned} m_W^2(\phi_c) &= \frac{g^2}{4}\phi_c^2 \\ m_Z^2(\phi_c) &= \frac{g^2 + g'^2}{4}\phi_c^2 \end{aligned} \tag{2.81}$$

Finally, the only fermion which can give a significant contribution to the one loop effective potential is the top quark, with a field-dependent mass

$$m_t^2(\phi_c) = \frac{h_t^2}{2}\phi_c^2 \tag{2.82}$$

where h_t is the top quark Yukawa coupling.

The one-loop effective potential $V_1(\phi_c)$ can be computed using eqs. (2.28), (2.35) and (2.42). As we have said in the previous subsection, these integrals are ultraviolet divergent. They have to be regularized and the divergent contributions cancelled by the counterterms

$$V_1^{\text{c.t.}} = \delta\Omega + \frac{\delta m^2}{2}\phi_c^2 + \frac{\delta\lambda}{4}\phi_c^4 \tag{2.83}$$

where we have introduced a counterterm $\delta\Omega$ for the vacuum energy or cosmological constant (see next section).

The final expression for the effective potential is finite and depends on the used regularization and, correspondingly, on the renormalization conditions. Next we will describe the two most commonly used renormalization conditions for the Standard Model.

2.5.1 $\overline{\text{MS}}$ renormalization

In this case we can use eqs. (2.67), (2.72) and (2.74) for the contribution to $V_1(\phi_c)$ of the scalars, fermions and gauge bosons, respectively. In the $\overline{\text{MS}}$ renormalization scheme we subtract the terms proportional to C_{uv}, see eq. (2.68), which are cancelled by the counterterms in (2.83). One easily arrives to the finite effective potential provided by

$$V(\phi_c) = V_0(\phi_c) + \frac{1}{64\pi^2}\sum_{i=W,Z,h,\chi,t} n_i m_i^4(\phi_c)\left[\log\frac{m_i^2(\phi_c)}{\mu^2} - C_i\right] \tag{2.84}$$

where C_i are constants given by,

$$\begin{aligned} C_W = C_Z &= \frac{5}{6} \\ C_h = C_\chi = C_t &= \frac{3}{2} \end{aligned} \tag{2.85}$$

and n_i are the degrees of freedom

$$n_W = 6,\ n_Z = 3,\ n_h = 1,\ n_\chi = 3,\ n_t = -12 \tag{2.86}$$

The counterterms which cancel the infinities are provided by,

$$\begin{aligned} \delta\Omega &= \frac{m^4}{64\pi^2}\left(n_h + n_\chi\right)C_{uv} \\ \delta m^2 &= -\frac{3\lambda m^2}{16\pi^2}\left(n_h + \frac{1}{3}n_\chi\right)C_{uv} \\ \delta\lambda &= \frac{3}{16\pi^2}\left[\frac{2g^4 + (g^2+g'^2)^2}{16} - h_t^4 + \left(3n_h + \frac{1}{3}n_\chi\right)\lambda^2\right]C_{uv} \end{aligned} \tag{2.87}$$

where C_{uv} is defined in (2.68). We have explicitly written in (2.87) the contribution to the counterterms from the Higgs sector, n_h and n_χ. The latter give rise entirely to the mass counterterms δm^2 and $\delta\Omega$. For Higgs masses lighter than W masses, the Higgs sector can be ignored in the one loop radiative corrections (as it is usually done) and the massive counterterms are not generated.

2.5.2 Cut-off regularization

A very useful scheme [12] is obtained by regularizing the theory with a cut-off and imposing that the minimum, at $v = 246.22\ GeV$, and the Higgs mass does not change with respect to their tree level values, *i.e.*,

$$\begin{aligned} \left.\frac{d(V_1 + V_1^{c.t.})}{d\phi_c}\right|_{\phi_c=v} &= 0 \\ \left.\frac{d^2(V_1 + V_1^{c.t.})}{d\phi_c^2}\right|_{\phi_c=v} &= 0 \end{aligned} \tag{2.88}$$

Now we can use (2.55) to write

$$V_1(\phi_c) = \frac{1}{32\pi^2} \sum_{i=W,Z,t,h,\chi} n_i \left[m_i^2(\phi_c)\Lambda^2 + \frac{m_i^4(\phi_c)}{2} \log \frac{m_i^2(\phi_c)}{\Lambda^2} \right] \tag{2.89}$$

Imposing now the conditions (2.88) the infinities in (2.89) cancel against those in $V_1^{c.t.}$, and the resulting ϕ_c-dependent potential is finite, and given by,

$$V(\phi_c) = V_0(\phi_c) + \frac{1}{64\pi^2} \sum_i \left\{ m_i^4(\phi_c) \left(\log \frac{m_i^2(\phi_c)}{m_i^2(v)} - \frac{3}{2} \right) + 2m_i^2(v) m_i^2(\phi_c) \right\} \tag{2.90}$$

The counterterms $\delta\Omega$, δm^2 and $\delta\lambda$ in (2.83) turn out to be given by

$$\begin{aligned} \delta\lambda &= -\frac{1}{16\pi^2} \sum_i n_i \left(\frac{m_i^2(v) - b_i}{v^2} \right)^2 \left(\log \frac{m_i^2(v)}{\Lambda^2} + \frac{3}{2} \right) \\ \delta m^2 &= -\frac{1}{16\pi^2} \sum_i n_i \frac{m_i^2 - b_i}{v^2} \left[\Lambda^2 - m_i^2(v) + b_i \left(\log \frac{m_i^2(v)}{\Lambda^2} + \frac{3}{2} \right) \right] \\ \delta\Omega &= \frac{m^2}{32\pi^2} \sum_{i=h,\chi} n_i \left[\Lambda^2 - m_i^2(v) + \frac{1}{2} b_i \left(\log \frac{m_i^2(v)}{\Lambda^2} + \frac{3}{2} \right) \right] \end{aligned} \tag{2.91}$$

where $b_W = b_Z = b_t = 0$ and $b_h = b_\chi = -m^2$.

We can see again in (2.91) that ignoring the contribution to the one loop effective potential from the Higgs sector results in the non appearance of a cosmological constant. However,

unlike the $\overline{\rm MS}$ scheme, δm^2 is also generated by the contribution of the gauge boson and top quark loops. Of course the one loop counterterms we are computing along this section are only useful for two loop calculations.

2.6 Improved effective potential and renormalization group

As we have seen in the previous section, the calculation of the effective action involves a mass μ which is not physical in the sense that all the theory should be independent of the chosen value of μ. In fact a change in μ should be accompanied by a change in the renormalized parameters (couplings and masses) such that all the theory remains unchanged. This statement for the effective action can be expressed as an equation [3]

$$\left[\mu\frac{\partial}{\partial\mu}+\beta_i\frac{\partial}{\partial\lambda_i}-\gamma\phi_c\frac{\delta}{\delta\phi_c}\right]\Gamma[\phi_c]=0 \tag{2.92}$$

for an appropriate choice of the coefficients β_i and γ, where λ_i denotes collectively all couplings and masses of the theory. In the last term of (2.92) we have made use of the notation (2.3).

We define the effective potential $\hat{V}$ as in eq. (2.20),

$$\hat{V}\equiv\hat{V}(\mu,\lambda_i,\phi_c)=\hat{V}(\mu,\lambda_i,0)-\sum_{n=1}^{\infty}\frac{1}{n!}\phi_c^n\Gamma^{(n)}(p_i=0) \tag{2.93}$$

The role of the vacuum energy $\hat{\Omega}$,

$$\hat{\Omega}=\hat{V}(\mu,\lambda_i,0)$$

has been recently stressed in ref. [13]. Using now the renormalization group equation (RGE) satisfied by the effective action (2.92), we obtain the RGE satisfied by $\hat{V}$ as

$$\left[\mu\frac{\partial}{\partial\mu}+\beta_i\frac{\partial}{\partial\lambda_i}-\gamma\phi_c\frac{\partial}{\partial\phi_c}\right]\hat{V}=\left[\mu\frac{\partial}{\partial\mu}+\beta_i\frac{\partial}{\partial\lambda_i}\right]\hat{\Omega} \tag{2.94}$$

If we make a ϕ_c-independent shift to $\hat{V}$ such that,

$$\begin{aligned}V&=\hat{V}+\Delta\hat{\Omega}(\mu,\lambda_i)\\ \Omega&\equiv\hat{\Omega}+\Delta\hat{\Omega}\end{aligned} \tag{2.95}$$

with the condition,

$$\left[\mu\frac{\partial}{\partial\mu}+\beta_i\frac{\partial}{\partial\lambda_i}\right]\Omega=0 \tag{2.96}$$

then the potential V satisfies the well known RGE,

$$\left[\mu\frac{\partial}{\partial\mu}+\beta_i\frac{\partial}{\partial\lambda_i}-\gamma\phi_c\frac{\partial}{\partial\phi_c}\right]V=0 \tag{2.97}$$

The formal solutions to eqs. (2.96) and (2.97) can be written as,

$$\begin{aligned} V\equiv V(\mu,\lambda_i,\phi_c)&=V(\mu(t),\lambda_i(t),\phi(t))\\ \Omega\equiv\Omega(\mu,\lambda_i)&=\Omega(\mu(t),\lambda_i(t)) \end{aligned} \tag{2.98}$$

where

$$\begin{aligned} \mu(t) &= \mu\exp(t)\\ \phi(t) &= \phi_c\xi(t)\\ \xi(t) &= \exp\left\{-\int_0^t\gamma(\lambda_i(t'))dt'\right\}\\ \beta_i(\lambda(t)) &= \frac{d\lambda_i(t)}{dt} \end{aligned} \tag{2.99}$$

with the boundary conditions,

$$\begin{aligned} \mu(0) &= \mu\\ \phi(0) &= \phi_c \end{aligned} \tag{2.100}$$

$$\begin{aligned} \xi(0) &= 1\\ \lambda_i(0) &= \lambda_i \end{aligned} \tag{2.101}$$

In fact eqs. (2.96) and (2.97) can be simply written as,

$$\begin{aligned} \frac{d}{dt}\Omega &= 0\\ \frac{d}{dt}V &= 0 \end{aligned} \tag{2.102}$$

which state that Ω and V are scale-independent. Of course the same happens to all derivatives of V,

$$V^{(n)}(\mu,\lambda_i,\phi_c)\equiv\frac{\partial^n V(\mu,\lambda_i,\phi_c)}{\partial\phi_c^n} \tag{2.103}$$

which by virtue of (2.99) satisfies

$$V^{(n)}=\xi(t)^n\frac{\partial^n}{\partial\phi(t)^n}V(\mu(t),\lambda_i(t),\phi(t)) \tag{2.104}$$

The RGE satisfied by $V^{(n)}$ can be obtained from (2.97) and the property,

$$\frac{\partial^n}{\partial\phi_c^n}\left[-\gamma\phi_c\frac{\partial}{\partial\phi_c}\right]=\left[-\gamma\phi_c\frac{\partial}{\partial\phi_c}\right]\frac{\partial^n}{\partial\phi_c^n}-n\gamma\frac{\partial^n}{\partial\phi_c^n}$$

It is given by,

$$\left[\mu\frac{\partial}{\partial\mu}+\beta_i\frac{\partial}{\partial\lambda_i}-\gamma\phi_c\frac{\partial}{\partial\phi_c}\right]V^{(n)}=n\gamma V^{(n)} \tag{2.105}$$

which implies that $V^{(n)}$ is scale independent.

In particular the scale independence of $V^{(n)}$, $n=0,1,\ldots$, means that we can fix the scale t at any value, even ϕ_c-dependent. Suppose we fix t by the arbitrary conditions,

$$\begin{aligned}\mu(t) &= f(\phi_c)\\ t=t(\phi_c) &= \log\{f(\phi_c)/\mu\}\\ \phi(t) &= \xi(t(\phi_c))\phi_c\end{aligned} \tag{2.106}$$

Using (2.106) we can write the effective potential and its derivatives (2.103) as ϕ_c-functions,

$$V(\phi_c)\equiv V\left[f(\phi_c),\lambda_i(t(\phi_c)),\phi(t(\phi_c))\right] \tag{2.107}$$

and

$$V^{(n)}(\phi_c)\equiv\xi(t(\phi_c))^n\frac{\partial^n}{\partial\phi(t)^n}V(\mu(t),\lambda_i(t),\phi(t))\Big|_{t=t(\phi_c)} \tag{2.108}$$

Using eq. (2.105) one can easily prove that [14],

$$V^{(n)}(\phi_c)=\frac{d^nV(\phi_c)}{d\phi_c^n} \tag{2.109}$$

Fixing the scale is a matter of convention. Fixing the scale, as we have just described, as a function of ϕ_c (*i.e.* giving different scales for different values of the field) is usually done to optimize the validity of the perturbative expansion, *i.e.* minimizing the value of radiative corrections to the effective potential around the minimum of the field. A very interesting result obtained in ref. [13] is: *The RGE improved effective potential exact up to (next-to-leading)^L log order* [3] *is obtained using the L-loop effective potential and the (L+1)-loop RGE β-functions.*

[3]The convention is (next-to-leading)^0 ≡leading, *i.e.* $L=0$. For $L=1$ the potential is exact to next-to-leading log.

3 Field Theory at Finite Temperature

The formalism used in conventional quantum field theory is suitable to describe observables (*e.g.* cross-sections) measured in empty space-time, as particle interactions in an accelerator. However, in the early stages of the universe, at high temperature, the environment had a non-negligible matter and radiation density, making the hypotheses of conventional field theories impracticable. For that reason, under those circumstances, the methods of conventional field theories are no longer in use, and should be replaced by others, closer to thermodynamics, where the background state is a thermal bath. This field has been called field theory at finite temperature and it is extremely useful to study all phenomena which happened in the early universe: phase transitions, inflationary cosmology, ... Excellent articles [15, 16], review articles [17, 18] and textbooks [26] exist which discuss different aspects of these issues. In this section we will review the main methods which will be useful for the theory of phase transitions at finite temperature.

3.1 Grand-canonical ensemble

In this section we shall give some definitions borrowed from thermodynamics and statistical mechanics. The **microcanonical ensemble** is used to describe an isolated system with fixed energy E, particle number N and volume V. The **canonical ensemble** describes a system in contact with a heat reservoir at temperature T: the energy can be exchanged between them and T, N and V are fixed. Finally, in the **grand canonical ensemble** the system can exchange energy and particles with the reservoir: T, V and the chemical potentials are fixed.

Consider now a dynamical system characterized by a hamiltonian [4] H and a set of conserved (mutually commuting) charges Q_A. The equilibrium state of the system at rest in the large volume V is described by the **grand-canonical density operator**

$$\rho = \exp(-\Phi) \exp\left\{ -\sum_A \alpha_A Q_A - \beta H \right\} \tag{3.1}$$

where

$$\Phi \equiv \log Tr \exp\left\{ -\sum_A \alpha_A Q_A - \beta H \right\} \tag{3.2}$$

is called the Massieu function (Legendre transform of the entropy), α_A and β are Lagrange

[4] All operators will be considered in the Heisenberg picture.

multipliers given by,

$$\begin{aligned} \beta &= T^{-1} \\ \alpha_A &= -\beta\mu_A \end{aligned} \tag{3.3}$$

T is the temperature and μ_A are the chemical potentials.

Using (3.1) one defines the **grand canonical average** of an arbitrary operator $\mathcal{O}$, as

$$\langle\mathcal{O}\rangle \equiv Tr(\mathcal{O}\rho) \tag{3.4}$$

satisfying the property $\langle\mathbf{1}\rangle = 1$. For instance, charge densities q_A and energy density E are defined as,

$$\begin{aligned} q_A &= \frac{1}{V}\langle Q_A\rangle = -\frac{1}{V}\frac{\partial\Phi}{\partial\alpha_A} \\ E &= \frac{1}{V}\langle H\rangle = -\frac{1}{V}\frac{\partial\Phi}{\partial\beta} \end{aligned} \tag{3.5}$$

while pressure, P, and entropy, S, densities are

$$\begin{aligned} P &= \frac{1}{\beta V}\langle\Phi\rangle = \frac{1}{\beta V}\Phi \\ S &= -\frac{1}{V}\langle\log\rho\rangle \end{aligned} \tag{3.6}$$

leading to the relation

$$E = -P + TS + \sum_A q_A\mu_A \tag{3.7}$$

In the following of this section we will always consider the case of zero chemical potential. It will be re-introduced when necessary.

3.2 Generating functionals

As in the previous section, we will start considering the case of a real scalar field $\phi(x)$, carrying no charges ($\mu_A = 0$), with hamiltonian H, *i.e.*

$$\phi(x) = e^{itH}\phi(0,\vec{x})e^{-itH} \tag{3.8}$$

where the time $x^0 = t$ is analytically continued to the complex plane.

We define the thermal Green function as the grand canonical average of the ordered product of the n field operators

$$G^{(C)}(x_1,\ldots,x_n) \equiv \langle T_C\phi(x_1),\ldots,\phi(x_n)\rangle \tag{3.9}$$

where the T_C ordering means that fields should be ordered along the path C in the complex t-plane. For instance the product of two fields is defined as,

$$T_C\phi(x)\phi(y) = \theta_C(x^0 - y^0)\phi(x)\phi(y) + \theta_C(y^0 - x^0)\phi(y)\phi(x) \tag{3.10}$$

If we parameterize C as $t = z(\tau)$, where τ is a real parameter, T_C ordering means standard ordering along τ. Therefore the step and delta functions can be given as,

$$\begin{aligned} \theta_C(t) &= \theta(\tau) \\ \delta_C(t) &= \left(\frac{\partial z}{\partial \tau}\right)^{-1} \delta(\tau) \end{aligned} \tag{3.11}$$

The rules of the functional formalism can be applied as usual, with the prescription,

$$\frac{\delta j(y)}{\delta j(x)} = \delta_C(x^0 - y^0)\delta^{(3)}(\vec{x} - \vec{y}) \tag{3.12}$$

and the generating functional $Z^\beta[j]$ for the full Green functions, defined as in the case of field theory at zero temperature (eq. 2.9),

$$Z^\beta[j] = \sum_{n=0}^{\infty} \frac{i^n}{n!} \int_C d^4x_1 \ldots d^4x_n j(x_1)\ldots j(x_n) G^{(C)}(x_1, \ldots, x_n) \tag{3.13}$$

can also be written as,

$$Z^\beta[j] = \left\langle T_C \exp\left\{ i \int_C d^4x j(x)\phi(x) \right\} \right\rangle \tag{3.14}$$

which is normalized to $Z^\beta[0] = \langle \mathbf{1} \rangle = 1$, as in (3.4), and where the integral along t is supposed to follow the path C in the complex plane.

Similarly, the generating functional for connected Green functions $W^\beta[j]$ is defined as in (2.4)

$$Z^\beta[j] \equiv \exp\{iW^\beta[j]\} \tag{3.15}$$

and the generating functional for 1PI Green functions $\Gamma^\beta[\overline{\phi}]$, as in (2.5), by the Legendre transformation,

$$\Gamma^\beta[\overline{\phi}] = W^\beta[j] - \int_C d^4x \frac{\delta W^\beta[j]}{\delta j(x)} j(x) \tag{3.16}$$

where the current $j(x)$ is eliminated in favor of the classical field $\overline{\phi}(x)$ as in (2.6)

$$\overline{\phi}(x) = \frac{\delta W^\beta[j]}{\delta j(x)} \tag{3.17}$$

In (3.17) it is understood that the rule (3.12) for the functional derivative is to be used.

It follows from (3.16) and (3.17) that (see eq. (2.7))

$$\frac{\delta\Gamma^{\beta}[\overline{\phi}]}{\delta\overline{\phi}(x)} = -j(x) \tag{3.18}$$

and that

$$\overline{\phi}(x) = \langle\phi(x)\rangle \tag{3.19}$$

is the grand canonical average of the field $\phi(x)$.

As in eq. (2.8) symmetry violation is signaled by

$$\left.\frac{\delta\Gamma^{\beta}[\overline{\phi}]}{\delta\overline{\phi}}\right|_{j=0} = 0 \tag{3.20}$$

for a value of the field different from zero.

Again, as in field theory at zero temperature, in a translationally invariant theory $\overline{\phi}(x) = \phi_c$ is a constant. In this case, by removing the overall factor of space-time volume arising in each term of $\Gamma^{\beta}[\phi_c]$, we can define the effective potential at finite temperature as in (2.16),

$$\Gamma^{\beta}[\phi_c] = -\int d^4x V^{\beta}_{\text{eff}}(\phi_c) \tag{3.21}$$

and symmetry breaking occurs when

$$\frac{\partial V^{\beta}_{\text{eff}}(\phi_c)}{\partial\phi_c} = 0 \tag{3.22}$$

for $\phi_c \neq 0$.

3.3 Green functions

3.3.1 Scalar fields

Not all the contours are allowed if we require Green functions to be analytic with respect to t. Using (3.10) we can write the two-point Green function as,

$$G^{(C)}(x-y) = \theta_C(x^0-y^0)G_+(x-y) + \theta_C(y^0-x^0)G_-(x-y) \tag{3.23}$$

where

$$\begin{aligned} G_+(x-y) &= \langle\phi(x)\phi(y)\rangle \\ G_-(x-y) &= G_+(y-x) \end{aligned} \tag{3.24}$$

Now, take the complete set of states $|n\rangle$ with eigenvalues E_n

$$H|n\rangle = E_n|n\rangle.$$

One can readily compute (3.24) at the point $\vec{x} = \vec{y} = 0$ as

$$G_+(x^0 - y^0) = e^{-\Phi} \sum_{m,n} |\langle m|\phi(0)|n\rangle|^2 \, e^{-iE_n(x^0-y^0)} e^{iE_m(x^0-y^0+i\beta)} \tag{3.25}$$

so that the convergence of the sum implies that

$$-\beta < Im(x^0 - y^0) < 0$$

which requires $\theta_C(x^0 - y^0) = 0$ for $Im(x^0 - y^0) > 0$. From (3.24) it follows that the similar property for the convergence of $G_-(x^0 - y^0)$ is that,

$$0 < Im(x^0 - y^0) < \beta$$

which requires $\theta_C(y^0 - x^0) = 0$ for $Im(x^0 - y^0) < 0$, and the final condition for the convergence of the complete Green function on the strip

$$-\beta \leq Im(x^0 - y^0) \leq \beta \tag{3.26}$$

is that we define the function $\theta_C(t)$ such that

$$\theta_C(t) = 0 \quad \text{for} \quad Im(t) \geq 0.$$

The latter condition implies that C must be such that *a point moving along it has a monotonously decreasing or constant imaginary part.*

A very important periodicity relation affecting Green functions can be easily deduced from the very definition of $G_+(x)$ and $G_-(x)$, eq. (3.24). By using the definition of the grand canonical average and the cyclic permutation property of the trace of a product of operators, it can be easily deduced,

$$G_+(t - i\beta, \vec{x}) = G_-(t, \vec{x}) \tag{3.27}$$

which is known as the Kubo-Martin-Schwinger relation [20].

We can now compute the two-point Green function (3.23) for a free scalar field,

$$\phi(x) = \int \frac{d^3p}{(2\pi)^{3/2}(2\omega_p)^{1/2}} \left[a(p)e^{-ipx} + a^\dagger(p)e^{ipx}\right] \tag{3.28}$$

where

$$\omega_p = \sqrt{\vec{p}^{\,2} + m^2}, \tag{3.29}$$

which satisfies the equation

$$\left[\partial^\mu\partial_\mu + m^2\right] G^{(C)}(x-y) = -i\delta_C(x-y) \equiv -i\delta_C(x^0-y^0)\delta^{(3)}(\vec{x}-\vec{y}) \tag{3.30}$$

From (3.28), and using (3.23) we can write the two-point Green function as,

$$\begin{aligned} G^{(C)}(x-y) \;=\; & \int \frac{d^3k}{(2\pi)^{3/2}(2\omega_k)^{1/2}} \int \frac{d^3p}{(2\pi)^{3/2}(2\omega_p)^{1/2}} \cdot \\ & \left\{\theta_C(x^0-y^0)\left[e^{-ikx+ipy}\langle a(k)a^\dagger(p)\rangle + e^{ikx-ipy}\langle a^\dagger(k)a(p)\rangle\right] \cdot \right. \\ & \left. \theta_C(y^0-x^0)\left[e^{ikx-ipy}\langle a(p)a^\dagger(k)\rangle + e^{-ikx+ipy}\langle a^\dagger(p)a(k)\rangle\right]\right\} \end{aligned} \tag{3.31}$$

Using the time derivative of (3.28),

$$\dot{\phi}(y) = i\int \frac{d^3p}{(2\pi)^{3/2}}\left(\frac{\omega_p}{2}\right)^{1/2}\left[a^\dagger(p)e^{ipx} - a(p)e^{-ipx}\right] \tag{3.32}$$

and the equal time commutation relation,

$$\left[\phi(t,\vec{x}),\dot{\phi}(t,\vec{y})\right] = i\delta^{(3)}(\vec{x}-\vec{y}) \tag{3.33}$$

one easily obtains the commutation relation for creation and annihilation operators,

$$\left[a(p),a^\dagger(k)\right] = \delta^{(3)}(\vec{p}-\vec{k}) \tag{3.34}$$

and defining the Hamiltonian of the field as,

$$H = \int \frac{d^3p}{(2\pi)^3}\omega_p a^\dagger(p)a(p) \tag{3.35}$$

one can obtain, using (3.34) the thermodynamical averages,

$$\begin{aligned} \langle a^\dagger(p)a(k)\rangle &= n_B(\omega_p)\delta^{(3)}(\vec{p}-\vec{k}) \\ \langle a(p)a^\dagger(k)\rangle &= [1+n_B(\omega_p)]\delta^{(3)}(\vec{p}-\vec{k}) \end{aligned} \tag{3.36}$$

where $n_B(\omega)$ is the Bose distribution function,

$$n_B(\omega) = \frac{1}{e^{\beta\omega}-1} \tag{3.37}$$

We will give here a simplified derivation of expression (3.36). Consider the simpler example of a quantum mechanical state occupied by bosons of the **same** energy ω. There may be any number of bosons in that state and no interaction between the particles: we will denote that state by $|n\rangle$. The set $\{|n\rangle\}$ is complete. Creation and annihilation operators are

denoted by $a^\dagger$ and a, respectively. They act on the states $|n\rangle$ as, $a^\dagger|n\rangle = \sqrt{n+1}|n+1\rangle$ and $a|n\rangle = \sqrt{n}|n-1\rangle$, and satisfy the commutation relation,

$$\left[a, a^\dagger\right] = 1 \tag{3.38}$$

The hamiltonian and number operators are defined as $H = \omega N$ and $N = a^\dagger a$, with eigenvalues ωn and n, respectively.

It is very easy to compute now $\langle a^\dagger a\rangle$ and $\langle aa^\dagger\rangle$ as in (3.36) using the completeness of $\{|n\rangle\}$. In particular,

$$Tr(e^{-\beta H}) = \sum_{n=0}^{\infty}\langle n|e^{-\beta H}|n\rangle = \sum_{n=0}^{\infty} e^{-\beta\omega n} = \frac{1}{1-e^{-\beta\omega}}$$

and

$$Tr(e^{-\beta H}a^\dagger a) = \sum_{n=0}^{\infty} n e^{-\beta\omega n} = \frac{e^{-\beta\omega}}{(1-e^{-\beta\omega})^2}$$

from where,

$$\langle a^\dagger a\rangle = n_B(\omega) \tag{3.39}$$

and, using (3.38),

$$\langle aa^\dagger\rangle = 1 + n_B(\omega) \tag{3.40}$$

as we wanted to prove.

Using now (3.36) we can cast the two-point Green function (3.31) as,

$$\begin{aligned} G^{(C)}(x-y) \;=\; & \int \frac{d^3p}{(2\pi)^3 2\omega_p}\Big[\theta_C(x^0-y^0)e^{-ip(x-y)} + \theta_C(y^0-x^0)e^{ip(x-y)} \\ & + n_B(\omega_p)\left(e^{ip(x-y)} + e^{-ip(x-y)}\right)\Big] \end{aligned} \tag{3.41}$$

where $n_B(\omega_p)$ is defined in (3.37). Making use now of the properties,

$$n_B(-\omega) = -e^{\beta\omega}n_B(\omega) = -[1+n_B(\omega)]$$

and

$$\delta(p^2-m^2) = \frac{1}{2\omega_p}\left[\delta(p^0+\omega_p) + \delta(p^0-\omega_p)\right] \tag{3.42}$$

one can write (3.41) as,

$$G^{(C)}(x-y) = \int \frac{d^4p}{(2\pi)^4}\rho(p)e^{-ip(x-y)}\left[\theta_C(x^0-y^0) + n_B(p^0)\right] \tag{3.43}$$

where the function $\rho(p)$ is defined by,

$$\rho(p) = 2\pi[\theta(p^0) - \theta(-p^0)]\delta(p^2-m^2) \tag{3.44}$$

Now the particular value of the Green function (3.43) depends on the chosen contour C. We will show later on two particular contours giving rise to the so-called imaginary and real time formalisms. Before coming to them we will describe how the previous formulae apply to the case of fermion fields.

3.3.2 Fermion fields

We will replace here (3.23) and (3.24) by,

$$\begin{aligned} S^{(C)}_{\alpha\beta}(x-y) &\equiv \langle T_C \psi_\alpha(x)\overline{\psi}_\beta(y)\rangle \\ &= \theta_C(x^0-y^0)S^+_{\alpha\beta} + \theta_C(y^0-x^0)S^-_{\alpha\beta} \end{aligned} \tag{3.45}$$

where α and β are spinor indices, and

$$S^+_{\alpha\beta}(x-y) = \langle \psi_\alpha(x)\overline{\psi}_\beta(y)\rangle \tag{3.46}$$

are the reduced Green function, which satisfy the Kubo-Martin-Schwinger relation,

$$S^+_{\alpha\beta}(t-i\beta,\vec{x}) = -S^-_{\alpha\beta}(t,\vec{x}) \tag{3.47}$$

The calculation of the two-Green function for a free fermion field, satisfying the equation

$$(i\gamma\cdot\partial - m)_{\alpha\sigma}\, S^{(C)}_{\sigma\beta}(x-y) = i\delta_C(x-y)\delta_{\alpha\beta} \tag{3.48}$$

follows lines similar to eqs. (3.28) to (3.44). In particular, one can define a Green function $S^{(C)}$ as

$$S^{(C)}_{\alpha\beta}(x-y) \equiv (i\gamma\cdot\partial + m)_{\alpha\beta} S^{(C)}(x-y) \tag{3.49}$$

where $S^{(C)}(x-y)$ satisfies the Klein-Gordon propagator equation (3.30). One can obtain for $S^{(C)}$ the expression,

$$\begin{aligned} S^{(C)}(x-y) &= \int \frac{d^3p}{(2\pi)^3 2\omega_p}\Big[\theta_C(x^0-y^0)e^{-ip(x-y)} + \theta_C(y^0-x^0)e^{ip(x-y)} \\ &\quad -n_F(\omega_p)\left(e^{ip(x-y)} + e^{-ip(x-y)}\right)\Big] \end{aligned} \tag{3.50}$$

which can be cast as,

$$S^{(C)}(x-y) = \int \frac{d^4p}{(2\pi)^4}\rho(p)e^{-ip(x-y)}\left[\theta_C(x^0-y^0) - n_F(p^0)\right] \tag{3.51}$$

where $n_F(\omega)$ is the Fermi distribution function

$$n_F(\omega) = \frac{1}{e^{\beta\omega}+1} \tag{3.52}$$

which satisfies the equation,

$$n_F(-\omega) = e^{\beta\omega} n_F(\omega) = 1 - n_F(\omega)$$

Eq. (3.52 can be derived similarly to (3.39) as the mean number of fermions for a Fermi gas. This time the Pauli exclusion principle forbids more than one fermion occupying a single state, so that only the states $|0\rangle$ and $|1\rangle$ exist. They are acted on by creation and annihilation operators $b^\dagger$ and b, respectively as:

$$b^\dagger|0\rangle = |1\rangle,$$

$$b^\dagger|1\rangle = 0,$$

$$b|0\rangle = 0,$$

$$b|1\rangle = |0\rangle,$$

and satisfy anticommutation rules,

$$\left\{b, b^\dagger\right\} = 1 \tag{3.53}$$

Defining the hamiltonian and number operators as $H = \omega N$ and $N = b^\dagger b$, we can compute now the statistical averages of $\langle b^\dagger b\rangle$ and $\langle bb^\dagger\rangle$ using the completeness of $\{|n\rangle\}$.

$$Tr(e^{-\beta H}) = \sum_{n=0}^{1} \langle n|e^{-\beta H}|n\rangle = \sum_{n=0}^{1} e^{-\beta\omega n} = 1 + e^{-\beta\omega}$$

and

$$Tr(e^{-\beta H} b^\dagger b) = \sum_{n=0}^{1} n e^{-\beta\omega n} = e^{-\beta\omega}$$

from where,

$$\langle b^\dagger b\rangle = n_F(\omega) \tag{3.54}$$

and, using (3.53),

$$\langle bb^\dagger\rangle = 1 - n_F(\omega) \tag{3.55}$$

as we wanted to prove.

3.4 Imaginary time formalism

The calculation of the propagators in the previous sections depends on the chosen path C going from an initial arbitrary time t to $t - i\beta$, provided by the Kubo-Martin-Schwinger periodicity properties (3.27) and (3.47) of Green functions. The simplest path is to take

a straight line along the imaginary axis $t = -i\tau$. It is called Matsubara contour, since Matsubara [21] was the first to set up a perturbation theory based upon this contour. In that case eq. (3.11) reads as,

$$\delta_C(t) = i\delta(\tau) \tag{3.56}$$

The two-point Green functions for scalar (3.43) and fermion (3.51) fields can be written as,

$$G(\tau, \vec{x}) = \int \frac{d^4p}{(2\pi)^4} \rho(p) e^{i\vec{p}\vec{x}} e^{-\tau p^0} \left[\theta(\tau) + \eta n(p^0)\right] \tag{3.57}$$

where the symbol η stands for

$$\begin{aligned} \eta_B &= 1 \quad \text{for bosons} \\ \eta_F &= -1 \quad \text{for fermions} \end{aligned} \tag{3.58}$$

Analogously, $n(p^0)$ stands either for $n_B(p^0)$, as given by (3.37) for bosons, or $n_F(p^0)$, as given by (3.52) for fermions. It can be defined as a function of η as,

$$n(\omega) = \frac{1}{e^{\beta\omega} - \eta} \tag{3.59}$$

The Green function (3.57) can be decomposed as in (3.23)

$$G(\tau, \vec{x}) = G_+(\tau, \vec{x})\theta(\tau) + G_-(\tau, \vec{x})\theta(-\tau) \tag{3.60}$$

Using now the Kubo-Martin-Schwinger relations, eqs. (3.27) and (3.47), we can write,

$$G(\tau + \beta) = \eta G(\tau) \text{ for } -\beta \leq \tau \leq 0 \tag{3.61}$$

$$G(\tau - \beta) = \eta G(\tau) \text{ for } 0 \leq \tau \leq \beta \tag{3.62}$$

which means that the propagator for bosons (fermions) is periodic (antiperiodic) in the *time* variable τ, with period β.

It follows that the Fourier transform of (3.57)

$$\tilde{G}(\omega_n, \vec{p}) = \int_{\alpha-\beta}^{\alpha} d\tau \int d^3x e^{i\omega_n\tau - i\vec{x}\vec{p}} G(\tau, \vec{x}) \tag{3.63}$$

(where $0 \leq \alpha \leq \beta$) is independent of α and the discrete frequencies satisfy the relation,

$$\eta e^{i\omega_n\beta} = 1 \tag{3.64}$$

i.e.

$$\omega_n = 2n\pi\beta^{-1} \tag{3.65}$$

for bosons, and

$$\omega_n = (2n+1)\pi\beta^{-1} \tag{3.66}$$

for fermions.

Inserting now (3.57) into (3.63) we can obtain the propagator in momentum space $\tilde{G}$. The integral over τ can be easily done with the result,

$$\int_{\alpha-\beta}^{\alpha} d\tau e^{(i\omega_n - p^0)\tau}\left[\theta(\tau) + \frac{\eta}{e^{\beta p^0} - \eta}\right] = \frac{1}{p^0 - i\omega_n} \tag{3.67}$$

where we have made use of eq. (3.64). We see that the integral (3.67) is independent of α, as anticipated, and does not depend on η. Inserting now (3.67) into (3.63) and making use of the property,

$$[\theta(p^0) - \theta(-p^0)]\delta(p^2 - m^2) = \frac{1}{2\omega_p}[\delta(p^0 + \omega_p) - \delta(p^0 - \omega_p)] \tag{3.68}$$

we can write the propagator in momentum space as,

$$\tilde{G}(\omega_n, \vec{p}) = \frac{1}{\vec{p}^{\,2} + m^2 + \omega_n^2} \tag{3.69}$$

where ω_n is given by (3.65) for bosons and by (3.66) for fermions.

We can now define the euclidean propagator, $\Delta(-i\tau, \vec{x})$, by

$$G(\tau, \vec{x}) = i\Delta(-i\tau, \vec{x}) \tag{3.70}$$

where $G(\tau, \vec{x})$ is the propagator defined in (3.57). Therefore, using (3.69), we can write the inverse Fourier transformation,

$$\Delta(x) = \frac{1}{\beta}\sum_{n=-\infty}^{\infty}\int \frac{d^3p}{(2\pi)^3} e^{-i\omega_n\tau + i\vec{p}\vec{x}} \frac{-i}{\vec{p}^{\,2} + m^2 + \omega_n^2} \tag{3.71}$$

where the Matsubara frequencies ω_n are defined in (3.65) for bosons and in (3.66) for fermions.

From (3.71) one can deduce the Feynman rules for the different fields in the imaginary time formalism. We can summarize them in the following way:

$$\begin{aligned}
\text{Boson propagator} &: \frac{i}{p^2 - m^2};\ p^\mu = [2ni\pi\beta^{-1}, \vec{p}\,] \\
\text{Fermion propagator} &: \frac{i}{\gamma\cdot p - m};\ p^\mu = [(2n+1)i\pi\beta^{-1}, \vec{p}\,] \\
\text{Loop integral} &: \frac{i}{\beta}\sum_{n=-\infty}^{\infty}\int \frac{d^3p}{(2\pi)^3} \\
\text{Vertex function} &: -i\beta(2\pi)^3\delta_{\sum\omega_i}\delta^{(3)}(\sum_i \vec{p}_i)
\end{aligned} \tag{3.72}$$

There is a standard trick to perform infinite summations as in (3.72). For the case of bosons we can have frequency sums as,

$$\frac{1}{\beta}\sum_{n=-\infty}^{\infty} f(p^0 = i\omega_n) \tag{3.73}$$

with $\omega_n = 2n\pi\beta^{-1}$. Since the function

$$\frac{1}{2}\beta\coth(\frac{1}{2}\beta z)$$

has poles at $z = i\omega_n$ and is analytic and bounded everywhere else, we can write (3.73) as,

$$\frac{1}{2\pi i\beta}\int_\gamma dz f(z)\frac{\beta}{2}\coth(\frac{1}{2}\beta z)$$

where the contour γ encircles anticlockwise all the previous poles of the imaginary axis. We are assuming that $f(z)$ does not have singularities along the imaginary axis (otherwise the previous expression is obviously not correct). The contour γ can be deformed to a new contour consisting in two straight lines: the first one starting at $-i\infty+\epsilon$ and going to $i\infty+\epsilon$, and the second one starting at $i\infty-\epsilon$ and ending at $-i\infty-\epsilon$. Rearranging the exponentials in the hyperbolic cotangent one can write the previous expression as,

$$\frac{1}{2\pi i}\int_{i\infty-\epsilon}^{-i\infty-\epsilon} dz f(z)\left[-\frac{1}{2}-\frac{1}{e^{-\beta z}-1}\right]+$$
$$\frac{1}{2\pi i}\int_{-i\infty+\epsilon}^{i\infty+\epsilon} dz f(z)\left[\frac{1}{2}+\frac{1}{e^{\beta z}-1}\right]$$

Now changing the variable $z \to -z$ in the first integral, the previous expression can be written as,

$$\frac{1}{2\pi i}\int_{-i\infty}^{i\infty} dz\frac{1}{2}[f(z)+f(-z)]+\frac{1}{2\pi i}\int_{-i\infty+\epsilon}^{i\infty+\epsilon} dz[f(z)+f(-z)]\frac{1}{e^{\beta z}-1}$$

and the contour of the second integral can be deformed to a contour C which encircles clockwise all singularities of the functions $f(z)$ and $f(-z)$ in the right half plane. Therefore we can write (3.73) as

$$\frac{1}{\beta}\sum_{n=-\infty}^{\infty} f(p^0 = i\omega_n) = \int_{-i\infty}^{i\infty}\frac{dz}{4\pi i}[f(z)+f(-z)]+\int_C\frac{dz}{2\pi i}n_B(z)[f(z)+f(-z)] \tag{3.74}$$

where $n_B(z)$ is the Bose distribution function (3.37).

Eq. (3.74) can be generalized for both bosons and fermions as,

$$\frac{1}{\beta}\sum_{n=-\infty}^{\infty} f(p^0 = i\omega_n) = \int_{-i\infty}^{i\infty}\frac{dz}{4\pi i}[f(z)+f(-z)]+\eta\int_C\frac{dz}{2\pi i}n(z)[f(z)+f(-z)] \tag{3.75}$$

where the symbol η is defined in (3.58) and the distribution functions $n(z)$ in (3.59). Eq. (3.75) shows that the frequency sum naturally separates into a T independent piece, which should coincide with the similar quantity computed in the field theory at zero temperature, and a T dependent piece which vanishes in the limit $T \to 0$, *i.e.* $\beta \to \infty$.

3.5 Real time formalism

The obvious disadvantage of the imaginary time formalism is to compute Green functions along imaginary time, so that going to the real time has to be done through a process of analytic continuation. However, a direct evaluation of Green function in the real time is possible by a judicious choice of the contour C in (3.9). The family of such real time contours is depicted in fig. 5 where the contour C is

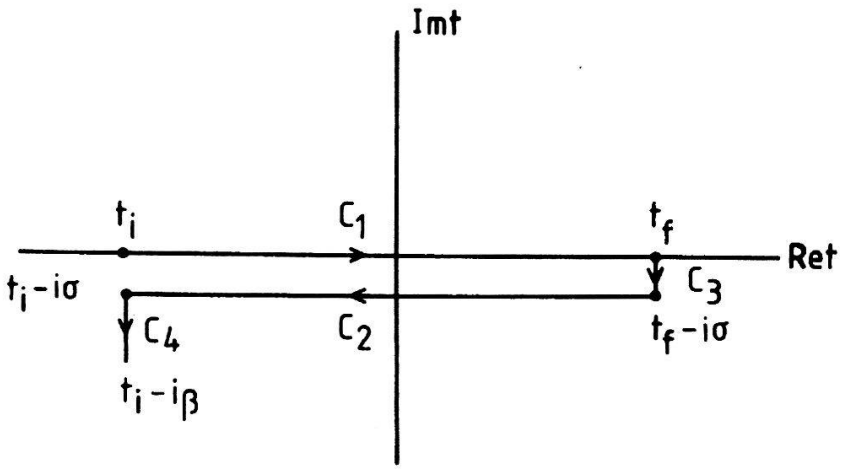

Figure 5: **Contour used in the real time formalism**

$$C = C_1 \bigcup C_2 \bigcup C_3 \bigcup C_4$$

where C_1 goes from the initial time t_i to the final time t_f, C_3 from t_f to $t_f - i\sigma$, with $0 \leq \sigma \leq \beta$, C_2 from $t_f - i\sigma$ to $t_i - i\sigma$, and C_4 from $t_i - i\sigma$ to $t_i - i\beta$. Different choices of σ lead to an equivalence class of quantum field theories at finite temperature [22]. For instance the choice $\sigma = 0$ leads to the Keldish perturbation expansion [23], while the choice

$$\sigma = \beta/2 \tag{3.76}$$

is the preferred one to compute Green function.

Computing the Green function for scalar (3.43) and fermion (3.51) fields taking the path depicted in fig. 5 is a matter of calculation, as we did for the imaginary time formalism in (3.57)-(3.69). One can prove that the contribution from the contours C_3 and C_4 can be neglected [18, 24]. Therefore, for the propagator between x^0 and y^0 there are four possibilities depending on whether they are on C_1 or C_2. Correspondingly, there are four propagators which are labelled by (11), (12), (21) and (22).

Making the choice (3.76), the propagators for scalar fields (3.43) can be written, in momentum space, as

$$G(p) \equiv \begin{pmatrix} G^{(11)}(p) & G^{(12)}(p) \\ G^{(21)}(p) & G^{(22)}(p) \end{pmatrix} = M_B(\beta,p) \begin{pmatrix} \Delta(p) & 0 \\ 0 & \Delta^*(p) \end{pmatrix} M_B(\beta,p) \tag{3.77}$$

where $\Delta(p)$ is the boson propagator at zero temperature,

$$\Delta(p) = \frac{i}{p^2 - m^2 + i\epsilon} \tag{3.78}$$

and the matrix $M_B(\beta,p)$ is given by,

$$M_B(\beta,p) = \begin{pmatrix} \cosh\theta(p) & \sinh\theta(p) \\ \sinh\theta(p) & \cosh\theta(p) \end{pmatrix} \tag{3.79}$$

where

$$\begin{aligned} \sinh\theta(p) &= e^{-\beta\omega_p/2}\left(1 - e^{-\beta\omega_p}\right)^{-1/2} \\ \cosh\theta(p) &= \left(1 - e^{-\beta\omega_p}\right)^{-1/2} \end{aligned} \tag{3.80}$$

Using now (3.77), (3.79), (3.80), and the property

$$\frac{1}{x + i\epsilon} = \mathcal{P}\frac{1}{x} + \pi\delta(x)$$

where $\mathcal{P}$ means the principal part, one can easily write the expression for the four bosonic propagators, as

$$\begin{aligned} G^{(11)}(p) &= \Delta(p) + 2\pi n_B(\omega_p)\delta(p^2 - m^2) \\ G^{(22)}(p) &= G^{(11)*} \\ G^{(12)} &= 4\pi e^{\beta\omega_p/2} n_B(\omega_p)\delta(p^2 - m^2) \\ G^{(21)} &= G^{(12)} \end{aligned} \tag{3.81}$$

Similarly, the propagators for fermion fields can be written as

$$\begin{aligned} S(p)_{\alpha\beta} &\equiv \begin{pmatrix} S^{(11)}_{\alpha\beta}(p) & G^{(12)}_{\alpha\beta}(p) \\ G^{(21)}_{\alpha\beta}(p) & G^{(22)}_{\alpha\beta}(p) \end{pmatrix} \\ &= M_F(\beta,p) \begin{pmatrix} (\gamma\cdot p + m)_{\alpha\beta}\Delta(p) & 0 \\ 0 & (\gamma\cdot p + m)_{\alpha\beta}\Delta^*(p) \end{pmatrix} M_F(\beta,p) \end{aligned} \tag{3.82}$$

where $\Delta_B(p)$ is given by (3.78), and the matrix $M_F(\beta,p)$ by,

$$M_F(\beta,p) = \begin{pmatrix} \cosh\theta(p) & \sinh\theta(p) \\ \sinh\theta(p) & \cosh\theta(p) \end{pmatrix} \tag{3.83}$$

with

$$\begin{aligned} \sinh\theta(p) &= e^{-\beta\omega_p/2}\left(1+e^{-\beta\omega_p}\right)^{-1/2} \\ \cosh\theta(p) &= [\theta(p^0)-\theta(-p^0)]\left(1+e^{-\beta\omega_p}\right)^{-1/2} \end{aligned} \tag{3.84}$$

In the same way, using now (3.82), (3.83), and (3.84) one can easily write the expression for the four fermionic propagators, as

$$\begin{aligned} S^{(11)}(p) &= (\gamma\cdot p+m)\left(\Delta(p)-2\pi n_F(\omega_p)\delta(p^2-m^2)\right) \\ S^{(22)}(p) &= S^{(11)*} \\ S^{(12)} &= -4\pi(\gamma\cdot p+m)[\theta(p^0)-\theta(-p^0)]e^{\beta\omega_p/2}n_F(\omega_p)\delta(p^2-m^2) \\ G^{(21)} &= -G^{(12)} \end{aligned} \tag{3.85}$$

As one can see from (3.81) and (3.85), the main feature of the real time formalism is that the propagators come in two terms: one which is the same as in the zero temperature field theory, and a second one where all the temperature dependence is contained. This is welcome. However the propagators (12), (21) and (22) are unphysical since one of their time arguments has an imaginary component. They are required for the consistency of the theory. The only physical propagator is the (11) component in (3.81) and (3.85).

Now the Feynman rules in the real time formalism are very similar to those in the zero temperature field theory. In fact all diagrams have the same topology as in the zero temperature field theory and the same symmetry factors. However, associated to every field there are two possible vertices, 1 and 2, and four possible propagators, (11), (12), (21) and (22) connecting them. All of them have to be considered for the consistency of the theory. In the Feynman rules, type 2 vertices are hermitian conjugate with respect to type 1 vertices. The golden rule is that: *Physical legs must always be attached to type 1 vertices.* Apart from the previous prescription, one must sum over all the configurations of type 1 and type 2 vertices, and use the propagator $G^{(ab)}$ or $S^{(ab)}$ to connect vertex a with vertex b.

There is now a general agreement in the sense that the imaginary time formalism and the real time formalism should give the same physical answer [25]. Using one or the other is sometimes a matter of taste, though in some cases the choice is dictated by calculational simplicity depending on the physical problem one is dealing with.

4 The effective potential at finite temperature

In this section we will construct the (one-loop) effective potential at finite temperature, using all the tools provided in the previous sections. As we will see, in particular, the effective potential at finite temperature contains the effective potential at zero temperature computed in section 2. The usefulness of this construction is addressed to the theory of phase transitions at finite temperature. The latter being essential for the understanding of phenomena as: inflation, baryon asymmetry generation, quark-gluon plasma transition in QCD,... We will compare different methods leading to the same result, including the use of both the imaginary and the real time formalisms. This exercise can be useful mainly to face more complicated problems than those which will be developed in this course.

4.1 Scalar fields

We will consider here the simplest model of one self-interacting scalar fields described by the lagrangian (2.22) and (2.23). We have to compute the diagrams contained in fig. 1 using the Feynman rules described in (3.72), for the imaginary time formalism, or in (3.81) for the real time formalism. We will write the result as,

$$V_{\rm eff}^{\beta}(\phi_c) = V_0(\phi_c) + V_1^{\beta}(\phi_c) \tag{4.1}$$

where $V_0(\phi_c)$ is the tree level potential.

4.1.1 Imaginary time formalism

We will compute the diagrams in fig.1. Using the Feynman rules in eq. (3.72), eq. (2.28) translates into,

$$V_1^{\beta}(\phi_c) = \frac{1}{2\beta}\sum_{n=-\infty}^{\infty}\int\frac{d^3p}{(2\pi)^3}\log(\omega_n^2+\omega^2) \tag{4.2}$$

where ω_n are the bosonic Matsubara frequencies defined in eq. (3.65) and

$$\omega^2 = \vec{p}^{\,2} + m^2(\phi_c) \tag{4.3}$$

m^2 being defined in (2.27).

The sum over n in (4.2) diverges, but the infinite part does not depend on ϕ_c. The finite part, which contains the ϕ_c dependence, can be computed by the following method [15].

Define,

$$v(\omega) = \sum_{n=-\infty}^{\infty} \log(\omega_n^2 + \omega^2) \tag{4.4}$$

then,

$$\frac{dv}{d\omega} = \sum_{n=-\infty}^{\infty} \frac{2\omega}{\omega_n^2 + \omega^2} \tag{4.5}$$

Using the identity,

$$\begin{aligned} f(y) = \sum_{n=-\infty}^{\infty} \frac{y}{y^2 + n^2} &= -\frac{1}{2y} + \frac{1}{2}\pi \coth \pi y \\ &= -\frac{1}{2y} + \frac{\pi}{2} + \pi \frac{e^{-2\pi y}}{1 - e^{-2\pi y}} \end{aligned} \tag{4.6}$$

with $y = \beta\omega/2\pi$ we obtain,

$$\frac{\partial v}{\partial \omega} = 2\beta \left[\frac{1}{2} + \frac{e^{-\beta\omega}}{1 - e^{-\beta\omega}} \right] \tag{4.7}$$

and

$$v(\omega) = 2\beta \left[\frac{w}{2} + \frac{1}{\beta} \log \left(1 - e^{-\beta\omega} \right) \right] + \omega - \text{independent terms} \tag{4.8}$$

Substituting finally (4.8) into (4.2) one gets,

$$V_1^{\beta}(\phi_c) = \int \frac{d^3p}{(2\pi)^3} \left[\frac{\omega}{2} + \frac{1}{\beta} \log \left(1 - e^{-\beta\omega} \right) \right] \tag{4.9}$$

One can easily prove that the first integral in (4.9) is the one-loop effective potential at zero temperature. For that we have to prove the identity,

$$-\frac{i}{2} \int_{-\infty}^{\infty} \frac{dx}{2\pi} \log(-x^2 + \omega^2 - i\epsilon) = \frac{\omega}{2} + \text{constant} \tag{4.10}$$

i.e.

$$\omega \int_{-\infty}^{\infty} \frac{dx}{2\pi i} \frac{1}{-x^2 + \omega^2 - i\epsilon} = \frac{1}{2} \tag{4.11}$$

Integral (4.11) can be performed closing the integration interval $(-\infty, \infty)$ in the complex x plane along a contour going anticlockwise and picking the pole of the integrand at $x = -\sqrt{\omega^2 - i\epsilon}$ with a residue $1/2\omega$. Using the residues theorem eq.(4.11) can be easily checked. Now we can use identity (4.10) to write the temperature independent part of (4.9) as

$$\frac{1}{2} \int \frac{d^3p}{(2\pi)^3} \omega = -\frac{i}{2} \int \frac{d^4p}{(2\pi)^4} \log(-p_o^2 + \omega^2 - i\epsilon) \tag{4.12}$$

and, after making the Wick rotation $p^0 = ip_E$ in (4.12) we obtain,

$$\frac{1}{2} \int \frac{d^3p}{(2\pi)^3} \omega = \frac{1}{2} \int \frac{d^4p}{(2\pi)^4} \log[p^2 + m^2(\phi_c)] \tag{4.13}$$

which is the same result we obtained in the zero temperature field theory, see eq. (2.28).

Now the temperature dependent part in (4.9) can be easily written as,

$$\frac{1}{\beta}\int\frac{d^3p}{(2\pi)^3}\log\left(1-e^{-\beta\omega}\right)=\frac{1}{2\pi^2\beta^4}J_B[m^2(\phi_c)\beta^2] \tag{4.14}$$

where the thermal bosonic function J_B is defined as,

$$J_B[m^2\beta^2]=\int_0^\infty dx\ x^2\log\left[1-e^{-\sqrt{x^2+\beta^2m^2}}\right] \tag{4.15}$$

The integral (4.15) and therefore the thermal bosonic effective potential admits a high-temperature expansion which will be very useful for practical applications. It is given by

$$\begin{aligned}J_B(m^2/T^2) &= -\frac{\pi^4}{45}+\frac{\pi^2}{12}\frac{m^2}{T^2}-\frac{\pi}{6}\left(\frac{m^2}{T^2}\right)^{3/2}-\frac{1}{32}\frac{m^4}{T^4}\log\frac{m^2}{a_bT^2} \\ &\quad -2\pi^{7/2}\sum_{\ell=1}^{\infty}(-1)^\ell\frac{\zeta(2\ell+1)}{(\ell+1)!}\Gamma\left(\ell+\frac{1}{2}\right)\left(\frac{m^2}{4\pi^2T^2}\right)^{\ell+2}\end{aligned} \tag{4.16}$$

where $a_b=16\pi^2\exp(3/2-2\gamma_E)$ ($\log a_b=5.4076$) and ζ is the Riemann ζ-function.

There is a very simple way of computing the effective potential: it consists in *computing its derivative* **in the shifted theory** *and then integrating*! In fact the derivative of the effective potential

$$\frac{dV_1^\beta}{d\phi_c}$$

is described diagrammatically by the tadpole diagram of fig. 6. In fact using the Feynman rules in (3.72) one can easily write for the tadpole of fig. 6 the expression,

Figure 6: **Tadpole diagram for scalar loop**

$$\frac{dV_1^\beta}{d\phi_c}=\frac{\lambda\phi_c}{2}\frac{1}{\beta}\sum_{n=-\infty}^{\infty}\int\frac{d^3p}{(2\pi)^3}\frac{1}{\omega_n^2+\omega^2} \tag{4.17}$$

or, using the expression (2.27) for $m^2(\phi_c)$,

$$\frac{dV_1^\beta}{dm^2(\phi_c)} = \frac{1}{2\beta}\sum_{n=-\infty}^{\infty}\int\frac{d^3p}{(2\pi)^3}\frac{1}{\omega_n^2+\omega^2} \tag{4.18}$$

Now we can perform the infinite sum in (4.18) using the result in eq. (3.74) with a function f defined as,

$$f(z) = \frac{1}{\omega^2 - z^2} \tag{4.19}$$

and obtain for the tadpole (4.18) the result

$$\frac{dV_1^\beta}{dm^2(\phi_c)} = \int\frac{d^3p}{(2\pi)^3}\left\{\frac{1}{2}\int_{-i\infty}^{i\infty}\frac{dz}{2\pi i}\frac{1}{\omega^2-z^2} + \int_C\frac{dz}{2\pi i}\frac{1}{e^{\beta z}-1}\frac{1}{\omega^2-z^2}\right\} \tag{4.20}$$

The first term in (4.20) gives the β-independent part of the tadpole contribution as,

$$\frac{1}{2}\int_{-i\infty}^{i\infty}\frac{dz}{2\pi i}\frac{1}{\omega^2-z^2} \tag{4.21}$$

We can now close the integration contour of (4.21) anticlockwise and pick the pole of (4.19) at $z=-\omega$ with a residue $1/2\omega$. The result of (4.21) is

$$\frac{1}{4\omega} \tag{4.22}$$

The second term in (4.20) gives the β-dependent part of the tadpole contribution. Here the integration contour encircles the pole at $z=\omega$ with a residue

$$-\frac{1}{2\omega}\frac{1}{e^{\beta\omega}-1} \tag{4.23}$$

Adding (4.22) and (4.23) we obtain for the tadpole the final expression,

$$\frac{dV_1(\phi_c)}{dm^2(\phi_c)} = \frac{1}{2}\int\frac{d^3p}{(2\pi)^3}\left[\frac{1}{2\omega}+\frac{1}{\omega}\frac{1}{e^{\beta\omega}-1}\right] \tag{4.24}$$

Now, integration of (4.24) with respect to $m^2(\phi_c)$ leads to the expression (4.9) for the thermal effective potential and, therefore, to the final expression given by (4.13) and (4.14).

4.1.2 Real time formalism

As we will see in this section, the final result for the effective potential (4.9) can be also obtained using the real time formalism. Let us compute the tadpole diagram of fig. 6. Since physical legs must be attached to type 1 vertices, the vertex in fig. 6 must be considered of type 1, and the propagator circulating around the loop has to be considered as a (11)

propagator. Application of the Feynman rules (3.81) to the tadpole diagram of fig. 6 leads to the expression [5]

$$\frac{dV_1^\beta}{d\phi_c} = \frac{\lambda\phi_c}{2}\int\frac{d^4p}{(2\pi)^4}\left[\frac{i}{p^2-m^2(\phi_c)+i\epsilon}+2\pi n_B(\omega)\delta(p^2-m^2(\phi_c))\right] \tag{4.25}$$

or, using as before the expression (2.27) for $m^2(\phi_c)$,

$$\frac{dV_1^\beta}{dm^2(\phi_c)} = \frac{1}{2}\int\frac{d^4p}{(2\pi)^4}\left[\frac{-i}{-p^2+m^2(\phi_c)-i\epsilon}+2\pi n_B(\omega)\delta(p^2-m^2(\phi_c))\right] \tag{4.26}$$

Now the β-independent part of (4.26), after integration on $m^2(\phi_c)$ contributes to the effective potential as

$$-\frac{i}{2}\int\frac{d^4p}{(2\pi)^4}\log(-p^2+m^2(\phi_c)-i\epsilon) \tag{4.27}$$

Finally using eq. (4.10) to perform the p^0 integral, we can cast eq. (4.27) as

$$\int\frac{d^3p}{(2\pi)^3}\frac{\omega}{2} \tag{4.28}$$

which coincides with the first term in (4.9).

Integration over p^0 in the β-dependent part of (4.26) can be easily performed with the help of the identity (3.42) leading to,

$$\int\frac{d^3p}{(2\pi)^3}\frac{1}{2\omega}n_B(\omega) \tag{4.29}$$

which, upon integration over $m^2(\phi_c)$ leads to the second term of eq. (4.9).

We have checked that trivially the real time and imaginary time formalisms lead to the same expression of the thermal effective potential, in the one loop approximation.

4.2 Fermion fields

We will consider here a theory with fermion fields described by the lagrangian (2.32). As in the scalar case, we have to compute the diagrams contained in fig. 2, using the Feynman rules either for the imaginary or for the real time formalism, and decompose the thermal effective potential as in (4.1).

[5] We are replacing in (3.81) the value of ω_p given by (3.29) by the corresponding value ω given by (4.3) in the shifted theory.

4.2.1 Imaginary time formalism

The calculation of the diagrams in fig. 2, using the Feynman rules (3.72), yields,

$$V_1^\beta(\phi_c) = -\frac{2\lambda}{2\beta}\sum_{n=-\infty}^{\infty}\int\frac{d^3p}{(2\pi)^3}\log(\omega_n^2+\omega^2) \tag{4.30}$$

where ω_n are the fermionic Matsubara frequencies defined in eq. (3.66) and

$$\omega^2 = \vec{p}^{\,2} + M_f^2. \tag{4.31}$$

The sum over n is done with the help of the same trick employed in (4.4)-(4.8). Let $f(y)$ be given by (4.6), then,

$$\begin{aligned}\sum_{m=2,4,\ldots}\frac{y}{y^2+m^2} &= \sum_{n=1}^{\infty}\frac{y}{y^2+4n^2} = \frac{1}{2}f\left(\frac{y}{2}\right)\\ \sum_{m=1,3,\ldots}\frac{y}{y^2+m^2} &= f(y) - \frac{1}{2}f\left(\frac{y}{2}\right)\end{aligned} \tag{4.32}$$

and using (4.6) we get,

$$\sum_{m=1,3,\ldots}\frac{y}{y^2+m^2} = \frac{\pi}{4} - \frac{\pi}{2}\frac{1}{e^{\pi y}+1} \tag{4.33}$$

The function $v(\omega)$ in this case can be written as,

$$v(\omega) = 2\sum_{n=1,3,\ldots}\log\left[\frac{\pi^2n^2}{\beta^2}+\omega^2\right] \tag{4.34}$$

and its derivative,

$$\frac{\partial v}{\partial\omega} = \frac{4\beta}{\pi}\sum_{1,3,\ldots}\frac{y}{y^2+n^2} \tag{4.35}$$

where $y = \beta\omega/\pi$. Then using (4.33) we get

$$\frac{\partial v}{\partial\omega} = 2\beta\left[\frac{1}{2} - \frac{1}{1+e^{\beta\omega}}\right] \tag{4.36}$$

and, after integration with respect to ω,

$$v(\omega) = 2\beta\left[\frac{w}{2} + \frac{1}{\beta}\log\left(1+e^{-\beta\omega}\right)\right] + \omega - \text{independent terms} \tag{4.37}$$

Replacing finally (4.37) into (4.30) one gets,

$$V_1^\beta(\phi_c) = -2\lambda\int\frac{d^3p}{(2\pi)^3}\left[\frac{\omega}{2} + \frac{1}{\beta}\log\left(1+e^{-\beta\omega}\right)\right] \tag{4.38}$$

The first integral in (4.38) can be proven, as in (4.10)-(4.13), to lead to the one-loop effective potential at zero temperature (2.35). The second integral, which contains all the temperature dependent part, can be written as,

$$-2\lambda\frac{1}{\beta}\int\frac{d^3p}{(2\pi)^3}\log\left(1+e^{-\beta\omega}\right)=-2\lambda\frac{1}{2\pi^2\beta^4}J_F[M_f^2(\phi_c)\beta^2] \tag{4.39}$$

where the thermal fermionic function J_F is defined as,

$$J_F[m^2\beta^2]=\int_0^\infty dx\ x^2\log\left[1+e^{-\sqrt{x^2+\beta^2m^2}}\right] \tag{4.40}$$

As in the scalar field, the integral (4.40) and therefore the thermal fermionic effective potential admits a high-temperature expansion which will be very useful for practical applications. It is given by

$$\begin{aligned}J_F(m^2/T^2) &= \frac{7\pi^4}{360}-\frac{\pi^2}{24}\frac{m^2}{T^2}-\frac{1}{32}\frac{m^4}{T^4}\log\frac{m^2}{a_fT^2} \\ &-\frac{\pi^{7/2}}{4}\sum_{\ell=1}^{\infty}(-1)^\ell\frac{\zeta(2\ell+1)}{(\ell+1)!}\left(1-2^{-2\ell-1}\right)\Gamma\left(\ell+\frac{1}{2}\right)\left(\frac{m^2}{\pi^2T^2}\right)^{\ell+2}\end{aligned} \tag{4.41}$$

where $a_f=\pi^2\exp(3/2-2\gamma_E)$ ($\log a_f=2.6351$) and ζ is the Riemann ζ-function.

As we did in the case of the scalar field, there is a very simple way of obtaining the effective potential, computing the tadpole of fig. 7 in the shifted theory, and integrating over

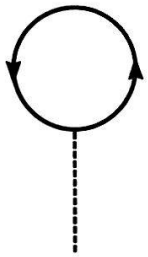

Figure 7: **Tadpole diagram for fermion loop**

ϕ_c. Using for the fermion propagator (3.72)

$$i\frac{\gamma\cdot p+M_f}{p^2-M_f^2}$$

and the trace formula,

$$Tr\left(\gamma\cdot p+M_f\right)=2\lambda M_f$$

we can write for the tadpole the expression,

$$\frac{dV_1^\beta}{d\phi_c} = -2\lambda\Gamma M_f \frac{1}{\beta}\sum_{n=-\infty}^{\infty}\int\frac{d^3p}{(2\pi)^3}\frac{1}{\omega_n^2+\omega^2} \tag{4.42}$$

or, using the expression $M_f(\phi_c) = \Gamma\phi_c$, where Γ is the Yukawa coupling,

$$\frac{dV_1^\beta}{dM_f^2(\phi_c)} = -2\lambda\frac{1}{2\beta}\sum_{n=-\infty}^{\infty}\int\frac{d^3p}{(2\pi)^3}\frac{1}{\omega_n^2+\omega^2} \tag{4.43}$$

Now the infinite sum in (4.43) can be done with the help of (3.75), with $f(z)$ given by (4.19), as

$$\frac{dV_1^\beta}{dM_f^2(\phi_c)} = -2\lambda\int\frac{d^3p}{(2\pi)^3}\left\{\frac{1}{2}\int_{-i\infty}^{i\infty}\frac{dz}{2\pi i}\frac{1}{\omega^2-z^2} - \int_C\frac{dz}{2\pi i}\frac{1}{e^{\beta z}+1}\frac{1}{\omega^2-z^2}\right\} \tag{4.44}$$

The first term of (4.44) reproduces the zero temperature result (2.35), after M_f^2 integration, by closing the integration contour of (4.21) anticlockwise and picking the pole at $z=-\omega$ with a residue $1/2\omega$. The second term in (4.44) gives the β-dependent part of the tadpole contribution. Here the integration contour C encircles the pole at $z=\omega$ with a residue

$$(-2\lambda)\frac{1}{2\omega}\frac{1}{e^{\beta\omega}+1} \tag{4.45}$$

Adding all of them together, we obtain for the tadpole the final expression

$$\frac{dV_1(\phi_c)}{dM_f^2(\phi_c)} = -\lambda\int\frac{d^3p}{(2\pi)^3}\left[\frac{1}{2\omega} - \frac{1}{\omega}\frac{1}{e^{\beta\omega}+1}\right] \tag{4.46}$$

and, upon integration with respect to M_f^2 we obtain the result previously presented in eq. (4.38).

4.2.2 Real time formalism

As for the case of scalar fields, the thermal effective potential for fermions (4.38) can also be very easily obtained using the real time formalism. We compute again the tadpole diagram of fig. 7, where the vertex between the two fermions and the scalar is of type 1 and the fermion propagator circulating along the loop is a (11) propagator. Application of the Feynman rules (3.85) leads to the expression

$$\frac{dV_1^\beta}{d\phi_c} = -\Gamma Tr\int\frac{d^4p}{(2\pi)^4}(\gamma\cdot p + M_f)\left[\frac{i}{p^2-M_f^2+i\epsilon} - 2\pi n_F(\omega)\delta(p^2-M_f^2)\right] \tag{4.47}$$

or, using as before the expression for M_f^2,

$$\frac{dV_1^\beta}{dM_f^2(\phi_c)} = -\frac{Tr\mathbf{1}}{2}\int\frac{d^4p}{(2\pi)^4}\left[\frac{-i}{-p^2+M_f^2-i\epsilon} - 2\pi n_F(\omega)\delta(p^2-M_f^2)\right] \tag{4.48}$$

Now the β-independent part of (4.48), after integration on M_f^2, contributes to the effective potential,

$$-Tr\mathbf{1}\int\frac{d^3p}{(2\pi)^3}\frac{\omega}{2} \tag{4.49}$$

which coincides with the first term in (4.38).

Integration over p^0 in the β-dependent part of (4.48) can be easily performed with the help of the identity (3.42) leading to,

$$-Tr\mathbf{1}\int\frac{d^3p}{(2\pi)^3}\frac{1}{2\omega}[-n_F(\omega)] \tag{4.50}$$

which, upon integration over M_f^2 leads to the second term of eq. (4.38).

4.3 Gauge bosons

The thermal effective potential for gauge bosons in a theory described by the lagrangian (2.36) is computed in the same way as for previous fields. The simplest thing is to compute the tadpole diagram of fig 8 using the shifted mass for the gauge boson. In the Landau

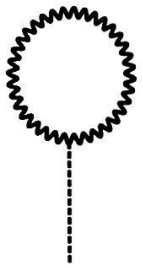

Figure 8: **Tadpole diagram for gauge-boson loop**

gauge, the gauge boson propagator reads as,

$$\Pi^\mu{}_\nu(p) = -\frac{i}{p^2-M_{gb}^2+i\epsilon}\Delta^\mu{}_\nu \tag{4.51}$$

where Δ is the projector defined in (2.38) with a trace equal to 3 (see eq. (2.41)). Therefore the final expression for the thermal effective potential is computed as,

$$V_1^\beta(\phi_c) = Tr(\Delta)\left\{\frac{1}{2}\int\frac{d^4p}{(2\pi)^4}\log[p^2+M_{gb}^2(\phi_c)] + \frac{1}{2\pi^2\beta^4}J_B[M_{gb}^2(\phi_c)\beta^2]\right\} \tag{4.52}$$

where the thermal bosonic function J_B in (4.15). The first term of (4.52) agrees with the zero temperature effective potential computed in (2.42), and the second one just counts that of a scalar field theory a number of times equal to the number of degrees of freedom (3) of the gauge boson.

4.4 The Standard Model case

The Standard Model of electroweak interactions was previously defined through eqs. (2.78)-(2.82), and the corresponding one loop effective potential at zero temperature computed through eqs. (2.83)-(2.91) using various renormalization schemes and the contribution of gauge and Higgs bosons and the top quark fermion to radiative corrections. Here we will compute the corresponding one loop effective potential at finite temperature. We will use the renormalization scheme of eq. (2.88), so that the renormalized effective potential at zero temperature is given by eq. (2.90), and consider only the contribution of W and Z bosons, and the top quark to radiative corrections. This is expected to be a good enough approximation for Higgs masses lighter than the W mass.

Using eqs (4.39) and (4.52) one can easily see that the finite-temperature part of the one-loop effective potential can be written as,

$$\Delta V^{(1)}(\phi_c,T)=\frac{T^4}{2\pi^2}\left[\sum_{i=W,Z} n_i J_B[m_i^2(\phi_c)/T^2]+n_t J_F[m_t^2(\phi_c)/T^2]\right] \tag{4.53}$$

where the function J_B and J_F where defined in eqs. (4.15) and (4.40), respectively.

Using now the high temperature expansions (4.16) and (4.41), and the one loop effective potential at zero temperature, eq. (2.90), one can write the total potential as,

$$V(\phi_c,T)=D(T^2-T_o^2)\phi_c^2-ET\phi_c^3+\frac{\lambda(T)}{4}\phi_c^4 \tag{4.54}$$

where the coefficients are given by

$$D=\frac{2m_W^2+m_Z^2+2m_t^2}{8v^2} \tag{4.55}$$

$$E=\frac{2m_W^3+m_Z^3}{4\pi v^3} \tag{4.56}$$

$$T_o^2=\frac{m_h^2-8Bv^2}{4D} \tag{4.57}$$

$$B=\frac{3}{64\pi^2v^4}\left(2m_W^4+m_Z^4-4m_t^4\right) \tag{4.58}$$

$$\lambda(T) = \lambda - \frac{3}{16\pi^2 v^4}\left(2m_W^4 \log\frac{m_W^2}{A_B T^2} + m_Z^4 \log\frac{m_Z^2}{A_B T^2} - 4m_t^4 \log\frac{m_t^2}{A_F T^2}\right) \tag{4.59}$$

where $\log A_B = \log a_b - 3/2$ and $\log A_F = \log a_F - 3/2$, and a_B, a_F are given in (4.16) and (4.41). All the masses which appear in the definition of the coefficients, eqs. (4.55) to (4.59), are the physical masses, *i.e.* the masses at the zero temperature minimum. The peculiar form of the potential, as given by eq. (4.54), will be useful to study the associated phase transition, as we will see in subsequent sections.

5 Finite temperature phase transitions in field theories

All cosmological applications of field theories are based on the theory of phase transitions at finite temperature, that we will briefly describe throughout this section. The main point here is that at finite temperature, the equilibrium value of the scalar field ϕ, $\langle\phi(T)\rangle$, does not correspond to the minimum of the effective potential $V_{\rm eff}^{T=0}(\phi)$, but to the minimum of the finite temperature effective potential $V_{\rm eff}^{\beta}(\phi)$, as given by (4.1). Thus, even if the minimum of $V_{\rm eff}^{T=0}(\phi)$ occurs at $\langle\phi\rangle = \sigma \neq 0$, very often, for sufficiently large temperatures, the minimum of $V_{\rm eff}^{\beta}(\phi)$ occurs at $\langle\phi(T)\rangle = 0$: this phenomenon is known as **symmetry restoration** at high temperature, and gives rise to the phase transition from $\phi(T) = 0$ to $\phi = \sigma$. It was discovered by Kirzhnits [26] in the context of the electroweak theory (symmetry breaking between weak and electromagnetic interactions occurs when the universe cools down to a critical temperature $T_c \sim 10^2\ GeV$) and subsequently confirmed and developed by other authors [27, 15, 16, 28].

The cosmological scenario can be drawn as follows: In the theory of the hot big bang, the universe is initially at very high temperature and, depending on the function $V_{\rm eff}^{\beta}(\phi)$, it can be in the **symmetric phase** $\langle\phi(T)\rangle = 0$, *i.e.* $\phi = 0$ can be the stable absolute minimum. At some critical temperature T_c the minimum at $\phi = 0$ becomes metastable and the phase transition may proceed. The first transition may be **first** or **second** order. First-order phase transitions have supercooled (out of equilibrium) symmetric states when the temperature decreases and are of use for baryogenesis purposes. Second-order phase transitions are used in the so-called new inflationary models [29]. We will illustrate these kinds of phase transitions with very simple examples.

5.1 First and second order phase transitions

We will illustrate the difference between **first** and **second** order phase transitions by considering first the simple example of a potential [6] described by the function,

$$V(\phi, T) = D(T^2 - T_o^2)\phi^2 + \frac{\lambda(T)}{4}\phi^4 \tag{5.1}$$

where D and T_o^2 are constant terms and λ is a slowly varying function of T [7]. A quick glance at (4.16) and (4.41) shows that the potential (5.1) can be part of the one-loop finite temperature effective potential in field theories. More explicit applications will be done later on.

At zero temperature, the potential

$$V(\phi, 0) = -T_o^2 D\phi^2 + \frac{\lambda}{4}\phi^4 \tag{5.2}$$

(where $\lambda \equiv \lambda(0)$) has a negative mass-squared term, which indicates that the state $\phi = 0$ is unstable, and the energetically favored state corresponds to the minimum of (5.2) at $\phi(0) = \pm\sqrt{\frac{2D}{\lambda}}T_o$, as shown in fig. 9, where the symmetry $\phi \leftrightarrow -\phi$ of the original theory is spontaneously broken.

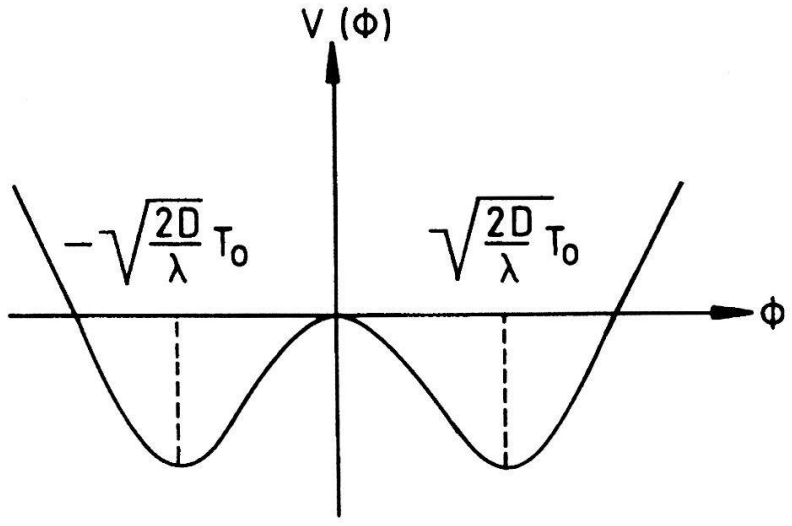

Figure 9: **Typical shape of the zero temperature potential (5.2) with spontaneous symmetry breaking**

[6] The ϕ independent terms in (5.1), *i.e.* $V(0, T)$, are not explicitly considered.

[7] The T dependence of λ will often be neglected in this section.

The curvature of the finite temperature potential (5.1) is now T-dependent,

$$m^2(\phi,T) = 3\lambda\phi^2 + 2D(T^2 - T_o^2) \tag{5.3}$$

and its stationary points, *i.e.* solutions to $dV(\phi,T)/d\phi = 0$, given by,

$$\begin{aligned} \phi(T) &= 0 \\ &\text{and} \\ \phi(T) &= \sqrt{\frac{2D(T_o^2 - T^2)}{\lambda(T)}} \end{aligned} \tag{5.4}$$

Therefore the critical temperature is given by T_o. At $T > T_o$, $m^2(0,T) > 0$ and the origin $\phi = 0$ is a minimum. At the same time only the solution $\phi = 0$ in (5.4) does exist. At $T = T_o$, $m^2(0,T_o) = 0$ and both solutions in (5.4) collapse at $\phi = 0$. The potential (5.1) becomes,

$$V(\phi,T_o) = \frac{\lambda(T_o)}{4}\phi^4 \tag{5.5}$$

At $T < T_o$, $m^2(0,T) < 0$ and the origin becomes a maximum. Simultaneously, the solution $\phi(T) \neq 0$ does appear in (5.4). This phase transition is called of **second order**, because there is no barrier between the symmetric and broken phases. Actually, when the broken phase is formed, the origin (symmetric phase) becomes a maximum. The typical potential (5.1) which describes a second order phase transition is illustrated in fig. 10. The phase

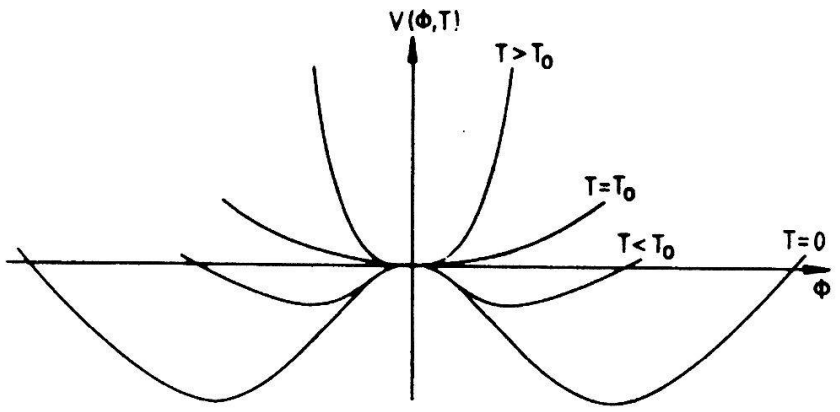

Figure 10: **The potential of eq. (5.1) describing a second order phase transition. The potential is normalized at $\phi = 0$ for all values of T**

transition may be achieved by a thermal fluctuation for a field located at the origin.

However, in many interesting theories there is a **barrier** between the symmetric and broken phases. This is characteristic of **first order** phase transitions. A typical example is provided by the potential [8],

$$V(\phi,T) = D(T^2 - T_o^2)\phi^2 - ET\phi^3 + \frac{\lambda(T)}{4}\phi^4 \tag{5.6}$$

where, as before, D, T_0 and E are T independent coefficients, and λ is a slowly varying T-dependent function. Notice that the difference between (5.6) and (5.1) is the cubic term with coefficient E. This term can be provided by the contribution to the effective potential of bosonic fields (4.16). The behaviour of (5.6) for the different temperatures is displayed in fig. 11, and its behaviour reviewed in refs. [12, 30]. At $T > T_1$ the only minimum is at

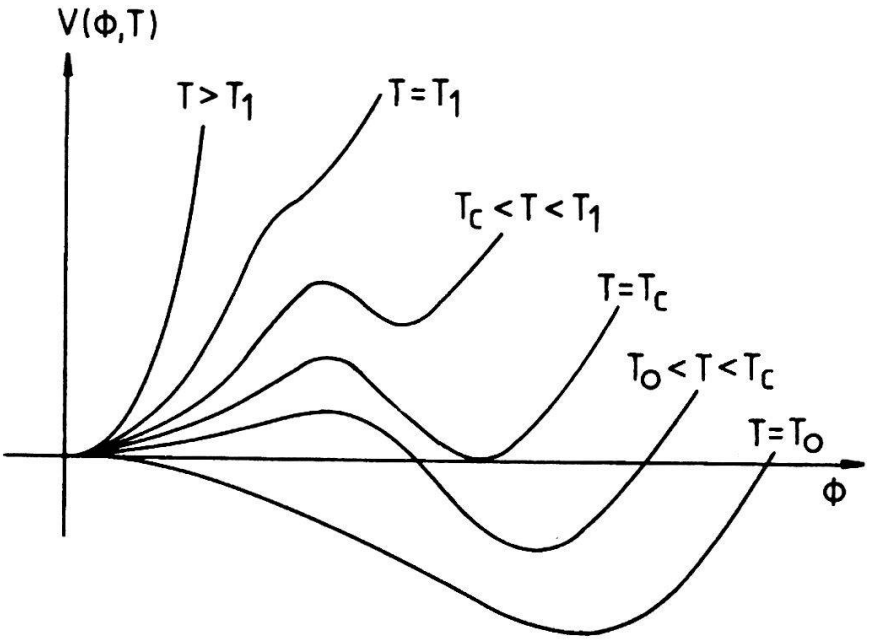

Figure 11: **A typical first order phase transition. The potential has been normalized at $\phi = 0$ for all values of T**

$\phi = 0$. At $T = T_1$

$$T_1^2 = \frac{8\lambda(T_1)DT_o^2}{8\lambda(T_1)D - 9E^2} \tag{5.7}$$

a local minimum at $\phi(T) \neq 0$ appears as an inflection point. The value of the field ϕ at $T = T_1$ is,

$$\langle\phi(T_1)\rangle = \frac{3ET_1}{2\lambda(T_1)} \tag{5.8}$$

[8] See, *e.g.* the one-loop effective potential for the Standard Model, eq. (4.54).

A barrier between the latter and the minimum at $\phi = 0$ starts to develop at lower temperatures. Then the point (5.8) splits into a maximum

$$\phi_M(T) = \frac{3ET}{2\lambda(T)} - \frac{1}{2\lambda(T)}\sqrt{9E^2T^2 - 8\lambda(T)D(T^2 - T_o^2)} \tag{5.9}$$

and a local minimum

$$\phi_m(T) = \frac{3ET}{2\lambda(T)} + \frac{1}{2\lambda(T)}\sqrt{9E^2T^2 - 8\lambda(T)D(T^2 - T_o^2)} \tag{5.10}$$

At a given temperature $T = T_c$

$$T_c^2 = \frac{\lambda(T_c)DT_o^2}{\lambda(T_c)D - E^2} \tag{5.11}$$

the origin and the minimum (5.10) become degenerate,

$$V(0, T_c) = V(\phi(T_c), T_c) \tag{5.12}$$

From (5.9) and (5.10) we find that

$$\phi_M(T_c) = \frac{ET_c}{\lambda(T_c)} \tag{5.13}$$

and

$$\phi_m(T_c) = \frac{2ET_c}{\lambda(T_c)} \tag{5.14}$$

For $T < T_c$ the minimum at $\phi = 0$ becomes metastable and the minimum at $\phi_m(T) \neq 0$ becomes the global one. At $T = T_o$ the barrier disappears, the origin becomes a maximum

$$\phi_M(T_o) = 0 \tag{5.15}$$

and the second minimum becomes equal to

$$\phi_m(T_o) = \frac{3ET_o}{\lambda(T_o)} \tag{5.16}$$

The phase transition starts at $T = T_c$ by tunnelling. However, if the barrier is high enough the tunnelling effect is very small and the phase transition does effectively start at a temperature $T_c > T_t > T_o$. In some models T_o can be equal to zero. The details of the phase transition depend therefore on the process of tunnelling from the false to the global minimum. These details will be studied in the rest of this section.

5.2 Bubble nucleation

The transition from the false to the true vacuum proceeds via quantum penetration of the barrier. We will use the term **quantum tunnelling** to refer to tunnelling at zero temperature, and **thermal tunnelling** to refer to tunnelling at finite temperature. It can be understood, in both cases, in terms of formation of bubbles of the broken phase in the sea of the symmetric phase. Once this has happened, the bubble spreads throughout the universe converting false vacuum into true one.

5.2.1 Quantum tunnelling

The dynamics of bubble nucleation at zero temperature has been studied by Coleman *et al.* [31, 32, 33]. It is found that the probability of decay of the false vacuum per unit time per unit volume has the form

$$\frac{\Gamma}{\nu} = Ae^{-\frac{B}{\hbar}}\left[1 + \mathcal{O}(\hbar)\right] \tag{5.17}$$

where the coefficients A [32] and B [31] depend on the theory under study. In this section we will study the value of B (which is the most relevant quantity in (5.17) in field theories) following closely the work of Coleman in ref. [31].

Consider first a **particle** of unit mass moving in **one** dimension with a lagrangian,

$$L = \frac{1}{2}\dot{q}^2 - V(q) \tag{5.18}$$

and a potential as the one in fig. 12. In semiclassical language, the particle penetrates the potential barrier and materializes at the escape point σ with zero kinetic energy, after which it propagates classically.

Just to simplify the analysis, take now the square potential shown in fig. 13. The wave function satisfies the Schrödinger equation,

$$\left[-\frac{\hbar^2}{2}\frac{\partial^2}{\partial x^2} + V(x)\right]\psi(x) = E\psi(x) \tag{5.19}$$

so that inside the region $0 \leq x \leq L$ the wave function is given (in natural units) by,

$$\psi(x) \sim e^{-\sqrt{2(V_0 - E)}x} \tag{5.20}$$

for $E < V_0$. The density probability for barrier penetration is thus, for $E = 0$,

$$P \sim |\psi(L)|^2 \sim e^{-2(2V_0)^{1/2}L} = e-2\int_0^L [2V(x)]^{1/2}dx \tag{5.21}$$

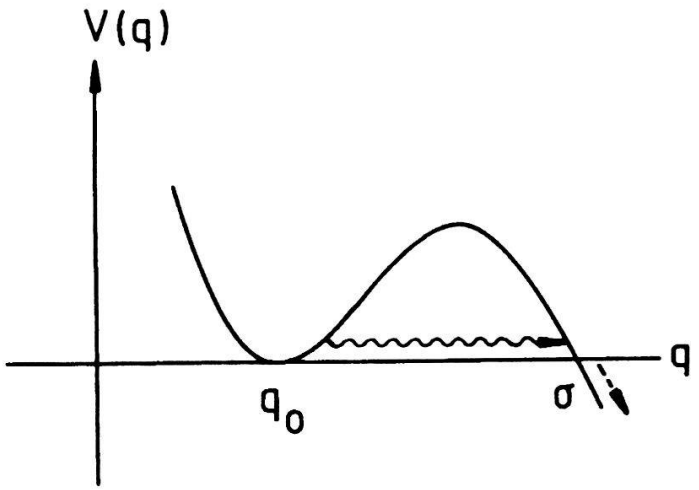

Figure 12: **Potential used in (5.18) to study the probability of quantum jump to overcome the barrier**

For an arbitrary potential $V(q)$ the coefficient B in (5.17) is given by

$$B = 2\int_{q_0}^{\sigma} dq(2V(q))^{1/2} \tag{5.22}$$

We can generalize this description to a **particle** moving in **N dimensions**: $\vec{q}(t)$. The lagrangian is,

$$L = \frac{1}{2}\dot{\vec{q}}\cdot\dot{\vec{q}} - V(\vec{q}) \tag{5.23}$$

and then, according to Banks, Bender and Wu [34],

$$B = 2\int_{\vec{q}_0}^{\vec{\sigma}} ds(2V)^{1/2} \tag{5.24}$$

where $ds^2 = d\vec{q}\cdot d\vec{q}$, $\vec{q}_0$ is a local minimum with $V(\vec{q}_0) = 0$ and $\vec{\sigma} \in \Sigma$, the surface of zeroes. The integral (5.24) is over the path for which B is a minimum, *i.e.* the path which satisfies

$$\delta\int_{\vec{q}_0}^{\vec{\sigma}} ds(2V)^{1/2} = 0 \tag{5.25}$$

This means that the **particle penetrates the barrier along the path of least resistance**.

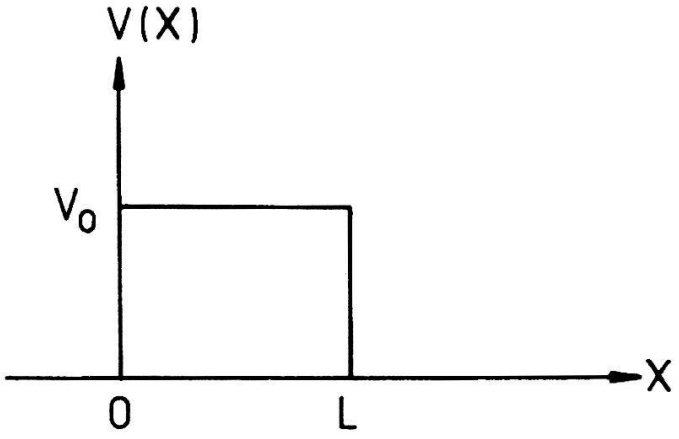

Figure 13: **Square potential**

We just have to determine now the paths satisfying (5.25). To do that Coleman [31] uses the fact that the solutions to the variational problem

$$\delta \int_{\vec{q}_0}^{\vec{\sigma}} ds \, [2(E-V)]^{1/2} = 0 \tag{5.26}$$

with fixed end points, are the paths in configuration space given by the Euler-Lagrange equations

$$\frac{d^2\vec{q}}{dt^2} = -\frac{\partial V}{\partial \vec{q}} \tag{5.27}$$

with

$$E = \frac{1}{2}\left[\frac{d\vec{q}}{dt}\right]^2 + V \tag{5.28}$$

The differences between (5.25) and (5.26) are:

- $E = 0$ in (5.25).
- The sign of V is reversed in (5.25).
- $\vec{\sigma}$ is not a fixed point in (5.25), but $\vec{\sigma} \in \Sigma$.

Ignoring the last point, the solutions to (5.25) are given by,

$$\frac{d^2\vec{q}}{d\tau^2} = \frac{\partial V}{\partial \vec{q}} \tag{5.29}$$

with

$$\frac{1}{2}\left[\frac{d\vec{q}}{d\tau}\right]^2 - V = 0 \tag{5.30}$$

Notice that (5.29) is the imaginary time version $\tau \equiv it$ of eq. (5.27), *i.e.* the Euler-Lagrange equation of the euclidean lagrangian,

$$L_E = \frac{1}{2}\left[\frac{d\vec{q}}{d\tau}\right]^2 + V \tag{5.31}$$

We will take the classical equilibrium as a boundary condition,

$$\lim_{\tau\to-\infty} \vec{q}(\tau) = \vec{q}_0 \tag{5.32}$$

and the imaginary time at which the particle reaches $\vec{\sigma}$ to be $\tau = 0$, *i.e.* from eq. (5.30),

$$\begin{aligned} \vec{q}(0) &= \vec{\sigma} \\ \left.\frac{d\vec{q}}{d\tau}\right|_{\tau=0} &= 0 \end{aligned} \tag{5.33}$$

so that the variation of (5.25) with respect to changes in the end point $\vec{\sigma}$ vanishes. On the other hand the motion of the particle for $\tau > 0$ is just the time reversal of its motion for $\tau < 0$. The particle **bounces** off Σ at $\tau = 0$ and returns to $\vec{q}_0$ at $\tau = +\infty$.

Using (5.30) and (5.31) we obtain,

$$L_E = 2V$$

and

$$ds(2V)^{1/2} = d\tau\ 2V = d\tau\ L_E$$

and so the coefficient B in (5.24)

$$B = \int_{-\infty}^{\infty} d\tau\ L_E = S_E \tag{5.34}$$

is the **total euclidean action for the bounce**, *i.e.* for the solution to the imaginary time equations of motion (5.29) satisfying the boundary conditions (5.32) and (5.33).

It is straightforward to generalize the above ideas to a field theory described by the lagrangian,

$$\mathcal{L} = \frac{1}{2}\partial^\mu\phi\partial_\mu\phi - V(\phi) \tag{5.35}$$

where the potential $V(\phi)$ has a false vacuum at ϕ_+ and a true vacuum at ϕ_-, as shown in fig. 14. The euclidean action is defined as,

$$S_E = \int d\tau d^3x \left[\frac{1}{2}\left(\frac{\partial\phi}{\partial\tau}\right)^2 + \frac{1}{2}\left(\vec{\nabla}\phi\right)^2 + V(\phi)\right] \tag{5.36}$$

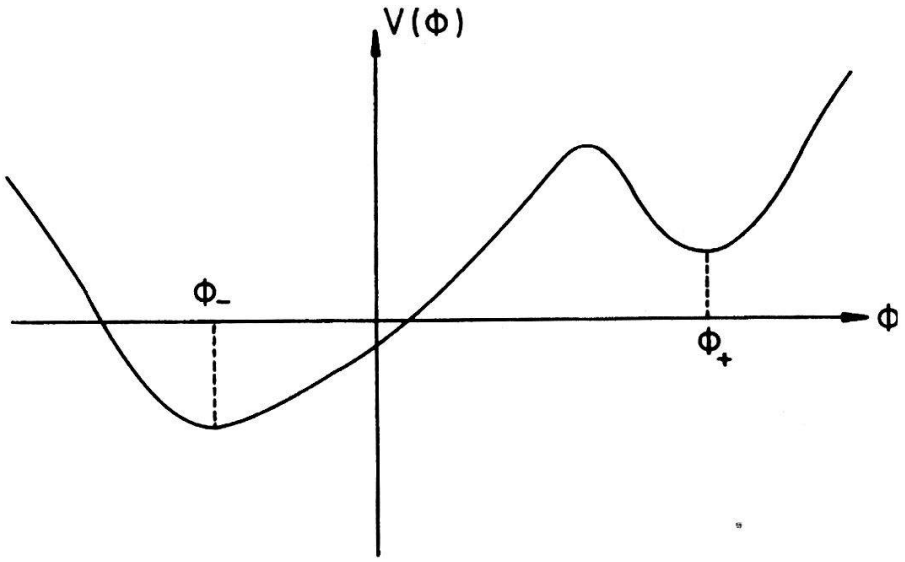

Figure 14: **Typical potential in (5.35) with two vacua: the true vacuum and the unstable (false) one**

and the **bounce** is a solution of the euclidean equation of motion

$$\left(\partial_\tau^2 + \vec{\nabla}^{\,2}\right)\phi = V'(\phi) \tag{5.37}$$

with boundary conditions (finiteness of the action)

$$\lim_{\tau\to\pm\infty} \phi(\tau,\vec{x}) = \phi_+ \tag{5.38}$$

and

$$\frac{\partial\phi}{\partial\tau}(0,\vec{x}) = 0 \tag{5.39}$$

Then the coefficient B in the vacuum decay amplitude is

$$B = S_E(\phi) - S_E(\phi_+) \tag{5.40}$$

Coleman, Glaser and Martin [35] have proven that the bounce is always $O(4)$ symmetric. This means that

$$\phi = \phi(\rho) \tag{5.41}$$

with $\rho = (\tau^2 + \vec{x}^{\,2})^{1/2}$. The euclidean action is then simplified to

$$S_E = 2\pi^2 \int_0^\infty \rho^3 d\rho \left[\frac{1}{2}\phi'^2 + V\right] \tag{5.42}$$

where $\phi' = d\phi/d\rho$, and the euclidean equation of motion (5.37) simplifies to

$$\phi'' + \frac{3}{\rho}\phi' = \frac{dV}{d\phi} \tag{5.43}$$

The boundary conditions (5.38-5.39) read now as

$$\lim_{\rho\to\infty}\phi(\rho) = \phi_+ \tag{5.44}$$

$$\left.\frac{d\phi}{d\rho}\right|_{\rho=0} = 0 \tag{5.45}$$

If we interpret ϕ as a particle position and ρ as a time, eq. (5.43) is the mechanical equation for a particle moving in the potential $-V$ and subject to a peculiar viscous damping force with a coefficient inversely proportional to the time. The corresponding physical situation can be seen in fig. 15 If the initial position is properly chosen, the particle will

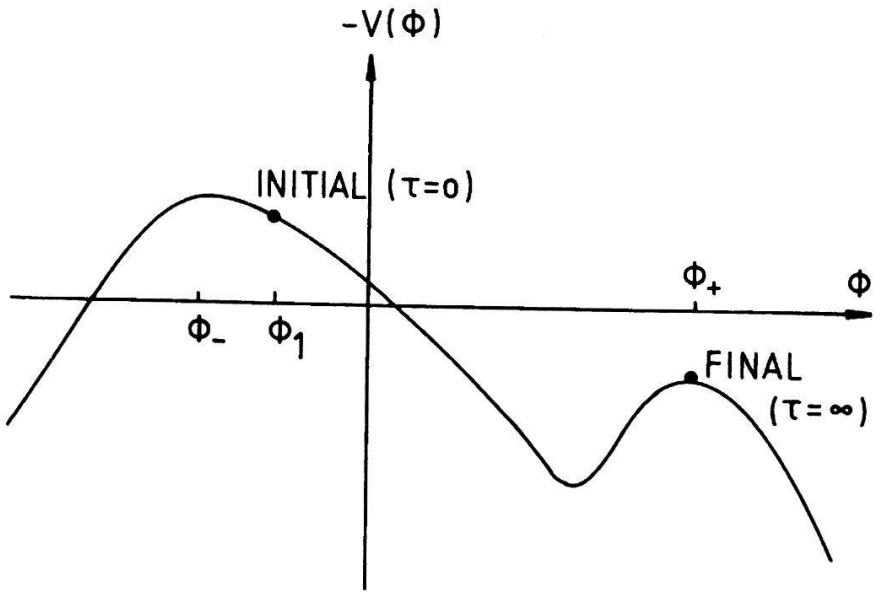

Figure 15: **Picture of the mechanical problem of a particle moving in the potential $-V$ and subject to a viscous damping force**

come to rest at time ∞ at ϕ_+, on the top of the right hand hill. If the particle is released to the right of ϕ_1, at some value of ϕ such that $-V(\phi) < -V(\phi_+)$, it will not have enough energy (the damping force does not affect this argument) to climb the hill at ϕ_+: it will **undershoot** and never rich ϕ_+. On the contrary, if the particle is released to the left of ϕ_1, and sufficiently close to ϕ_- we can arrange for it to stay arbitrarily close to ϕ_- for arbitrarily large ρ: in that case the damping force ($\sim \frac{1}{\rho}$) can be neglected, and the particle **overshoots** and passes through ϕ_+ at some finite time. By continuity there must be an intermediate

initial position for which it just comes to rest at ϕ_+. This initial position is the **bounce** at $\rho = 0$, $\phi_B(0)$.

In short, the **semiclassical description** of the decay of the false vacuum in field theory is similar to that in particle mechanics. The classical field makes a quantum jump (say at $t = 0$) to the state defined by $\phi(t = 0, \vec{x})$, where ϕ is the bounce, which satisfies eqs. (5.43), (5.44) and (5.45). In other words, $\phi(t = 0, \vec{x})$ is the initial position of a function $\phi(\rho)$ which satisfies the equation of motion (5.43) and reaches the top of the hill in infinite time, at rest. Afterwards it evolves according to the classical field equation,

$$-\frac{\partial^2}{\partial t^2}\phi + \vec{\nabla}^{\,2}\phi = V'(\phi) \tag{5.46}$$

Because the Minkowskian field equation (5.46) is simply the analytic continuation of the euclidean field equation (5.37), the solution to the equation (5.46) is just the analytic continuation of the bounce

$$\phi(t, \vec{x}) = \phi\left(\rho = \sqrt{\vec{x}^{\,2} - t^2}\right) \tag{5.47}$$

Therefore, $O(4)$ invariance of the bounce becomes $O(3,1)$ invariance of the classical solution. In other words, the growth of the bubble after its materialization looks the same to any Lorentz observer.

It is possible to obtain an explicit approximation for the bounce in the limit of small ϵ, with

$$\epsilon = V(\phi_+) - V(\phi_-) \tag{5.48}$$

We can write [31]

$$V(\phi) = V_0(\phi) + \mathcal{O}(\epsilon) \tag{5.49}$$

where V_0 is a function chosen such that

$$V_0(\phi_-) = V_0(\phi_+) \tag{5.50}$$

$$\left.\frac{dV_0}{d\phi}\right|_{\phi=\phi_\pm} = 0 \tag{5.51}$$

The field $\phi(\rho)$ obeys the approximate equation,

$$\phi'' = \frac{dV_0}{d\phi} \tag{5.52}$$

where we have neglected the ϕ' term in (5.43) [9]. Integration of (5.52) gives

$$\left[\frac{1}{2}\phi'^2 - V_0\right]' = 0 \tag{5.53}$$

[9] If $\epsilon \ll 1$ the initial bounce $\phi_B(0)$ is very close to ϕ_- for large ρ. Then the viscosity damping force can be very soon neglected.

whose value is determined by the condition $\phi(\infty) = \phi_+$, $\phi'(\infty) = 0$

$$\frac{1}{2}\phi'^2 - V_0 = -V_0(\phi_\pm) \tag{5.54}$$

Choosing as integration constant R such that

$$\phi(R) = \frac{1}{2}(\phi_+ + \phi_-) \tag{5.55}$$

we can integrate (5.54) and obtain

$$\int_{\frac{1}{2}(\phi_+ + \phi_-)}^{\phi} \frac{d\phi}{\sqrt{2(V_0 - V_0(\phi_\pm))}} = \rho - R \tag{5.56}$$

If R is large, the bounce looks like a ball of true vacuum, $\phi = \phi_-$, embedded in a sea of false vacuum $\phi = \phi_+$ with a wall separating them, as in fig. 16. The thickness of the wall is

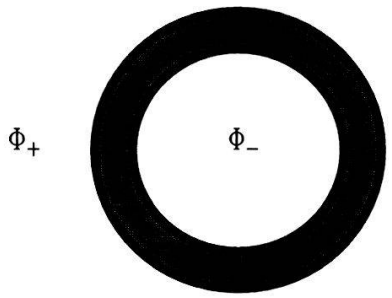

Figure 16: **Picture of the bounce solution in the thin wall approximation**

small compared to the radius R of the ball. In the thin wall approximation it is justified to neglect ϕ': it is zero outside the wall and negligible in the wall because R is large.

We determine the size of the **critical bubble** R_c by computing B and demanding it to be stationary under changes of R. Using (5.40)

$$B_{\text{out}} = S_E(\phi_+) - S_E(\phi_+) = 0 \tag{5.57}$$

and

$$\begin{aligned} B_{\text{in}} &= S_E(\phi_-) - S_E(\phi_+) \\ &= 2\pi^2 \int_0^R \rho^3 d\rho \, [V(\phi_-) - V(\phi_+)] = -\frac{\pi^2}{2} R^4 \epsilon \end{aligned} \tag{5.58}$$

and within the wall, in the thin wall approximation,

$$\begin{aligned} B_{\text{wall}} &= 2\pi^2 \int \rho^3 d\rho \left[\frac{1}{2}\phi'^2 + V_0(\phi) - V_0(\phi_+)\right] \\ &= 2\pi^2 R^3 S_1 \end{aligned} \tag{5.59}$$

where, using (5.54), S_1 is given by

$$S_1 = 2\int d\rho\,[V_0(\phi) - V_0(\phi_+)] \tag{5.60}$$

or, using (from eq. (5.54))

$$d\rho = \frac{d\phi}{\sqrt{2(V_0 - V_0(\phi_+))}}$$

one obtains

$$S_1 = \int_{\phi_-}^{\phi_+} d\phi\sqrt{2(V_0(\phi) - V_0(\phi_+))} \tag{5.61}$$

The coefficient B is thus given by

$$B = -\frac{1}{2}\pi^2 R^4\epsilon + 2\pi^2 R^3 S_1 \tag{5.62}$$

which is stationary at

$$R_c = \frac{3S_1}{\epsilon} \tag{5.63}$$

which is the radius of the **critical** bubble [10]. It can be easily checked that this extremum is not a minimum of the action, but a maximum. This corresponds to the fact that critical bubbles are unstable, either they expand or they contract. Using now (5.63) in (5.62), the coefficient B for the critical bubble is given by,

$$B_c = \frac{27\pi^2 S_1^4}{2\epsilon^3} \tag{5.64}$$

As a simple application we will compute the previous equations for the potential

$$V_0 = \frac{\lambda}{8}\left[\phi^2 - \frac{\mu^2}{\lambda}\right]^2 \tag{5.65}$$

The bounce solution is given by

$$\phi(\rho) = \frac{\mu}{\sqrt{\lambda}}\tanh\left[\frac{1}{2}\mu(\rho - R)\right] \tag{5.66}$$

the euclidean action in the wall by

$$S_1 = \frac{\mu^3}{3\lambda} \tag{5.67}$$

the radius of the critical bubble by

$$R_c = \frac{\mu^3}{\lambda\epsilon} \tag{5.68}$$

[10]Notice that, consistently with our approximation, r is large when ϵ is small.

and the coefficient B of the critical bubble by

$$B_c = \frac{\pi^2 \mu^{12}}{6\epsilon^3 \lambda^4} \tag{5.69}$$

Finally, the coefficient A in (5.17) can be computed following a scheme developed by Callan and Coleman [32]. The calculation is in general quite complicated and yields,

$$A = \left(\frac{S_E(\phi)}{2\pi}\right)^2 \left[\frac{\det'[-\Box_E + V''(\phi)]}{\det[-\Box_E + V''(\phi_+)]}\right]^{-1/2} \tag{5.70}$$

where prime indicates that zero eigenvalues of the operator are to be omitted when computing the determinant. In fact the four zero modes associated with the translational invariance of euclidean space give rise to the factor $(S_E(\phi)/2\pi)^2$ in (5.70).

5.2.2 Thermal tunnelling

The tunnelling rate at finite temperature is computed by following the same procedure as above, but using the rules of field theory at finite temperature [36]. In the previous section we defined the critical temperature T_c as the temperature at which the two minima of the potential $V(\phi, T)$ have the same depth (5.12). However, tunnelling with formation of bubbles of the field ϕ corresponding to the second minimum starts somewhat later, and goes sufficiently fast to fill the universe with bubbles of the new phase only at some lower temperature T_t when the corresponding euclidean action $S_E = S_3/T$ suppressing the tunnelling becomes O(130-140) [37, 76, 12], as we will see in the next section.

We will use as prototype the potential of eq. (5.6) which can trigger, as we showed in this section, a first order phase transition. In this case the false minimum is $\phi_+ = 0$, and the value of the potential at the origin is zero, $V(0, T) = 0$. The tunnelling probability per unit time per unit volume is given by [36]

$$\frac{\Gamma}{\nu} \sim A(T) e^{-S_3/T} \tag{5.71}$$

which is the direct translation of (5.17) and (5.40). In (5.71) the prefactor $A(T)$ is roughly of $\mathcal{O}(T^4)$ while S_3 is the three-dimensional euclidean action defined as (see (5.36))

$$S_3 = \int d^3x \left[\frac{1}{2}\left(\vec{\nabla}\phi\right)^2 + V(\phi, T)\right] \tag{5.72}$$

where $V(\phi, T)$ is the finite temperature effective potential defined in the previous section (see eq. (5.6)).

At very high temperature the **bounce** solution has $O(3)$ symmetry [36] and the euclidean action is then simplified to (see (5.42)),

$$S_3 = 4\pi \int_0^\infty r^2 dr \left[\frac{1}{2} \left(\frac{d\phi}{dr} \right)^2 + V(\phi(r), T) \right] \tag{5.73}$$

where $r^2 = \vec{x}^{\,2}$, and the euclidean equation of motion (5.37) yields (see (5.43)),

$$\frac{d^2\phi}{dr^2} + \frac{2}{r}\frac{d\phi}{dr} = V'(\phi, T) \tag{5.74}$$

with the boundary conditions (see (5.44-5.45))

$$\lim_{r\to\infty} \phi(r) = 0 \tag{5.75}$$

$$\left.\frac{d\phi}{dr}\right|_{r=0} = 0 \tag{5.76}$$

From here on we will follow the discussion in ref. [12]. Let us take $\phi_+ = 0$ outside a bubble. Then (5.73), which is also the surplus free energy of a true vacuum bubble, can be written as

$$S_3 = 4\pi \int_0^R r^2 dr \left[\frac{1}{2} \left(\frac{d\phi}{dr} \right)^2 + V(\phi(r), T) \right] \tag{5.77}$$

where R is the bubble radius. There are two contributions to (5.77): a surface term F_S, coming from the derivative term in (5.77), and a volume term F_V, coming from the second term in (5.77). They scale like,

$$S_3 \sim 2\pi R^2 \left(\frac{\delta\phi}{\delta R} \right)^2 \delta R + \frac{4\pi R^3 \langle V \rangle}{3} \tag{5.78}$$

where δR is the thickness of the bubble wall, $\delta\phi = \phi_m$ and $\langle V \rangle$ is the average of the potential inside the bubble.

For temperatures just below T_c, the height of the barrier $V(\phi_M, T)$ is large compared to the depth of the potential at the minimum, $-V(\phi_m, T)$. In that case, the solution of minimal action corresponds to minimizing the contribution to F_V coming from the region $\phi = \phi_M$. This amounts to a very small bubble wall $\delta R/R \ll 1$ and so a very quick change of the field from $\phi = 0$ outside the bubble to $\phi = \phi_m$ inside the bubble. Therefore, the first formed bubbles after T_c are **thin wall** bubbles.

Subsequently, when the temperature drops towards T_o the height of the barrier $V(\phi_M, T)$ becomes small as compared with the depth of the potential at the minimum $-V(\phi_m, T)$. In that case the contribution to F_V from the region $\phi = \phi_M$ is negligible, and the minimal action

corresponds to minimizing the surface term F_S. This amounts to a configuration where δR is as large as possible, *i.e.* $\delta R/R = \mathcal{O}(1)$: **thick wall** bubbles. So whether the phase transition proceeds through thin or thick wall bubbles depends on how large the bubble nucleation rate (5.71) is, or how small S_3 is, before thick bubbles are energetically favoured.

For the case of **thick bubbles**, $\delta R \sim R$ and the free energy of the bubble can be written as,

$$S_3 \sim 2\pi R(\delta\phi)^2 + \frac{4\pi R^3\langle V\rangle}{3} \tag{5.79}$$

The critical radius of the bubble, obtained as the maximum of the action (5.79), is given by

$$R_c \sim \frac{\delta\phi}{\sqrt{-2\langle V\rangle}} \tag{5.80}$$

and the action at the critical radius (5.80)

$$S_3 \sim \frac{(\delta\phi)^3}{\sqrt{-\langle V\rangle}} \tag{5.81}$$

In particular, for the potential (5.6) one can find [12]

$$S_3 \sim \frac{ET}{\lambda(T)^{3/2}}(1-\epsilon)^{3/2} \tag{5.82}$$

where

$$\epsilon(T) = \frac{T_c - T}{T_c - T_o} \tag{5.83}$$

For the case of **thin bubbles** one can adapt Coleman's procedure, as explained in the previous subsection, and obtain analytic formulae in the limit of $\epsilon(T) \ll 1$, where ϵ is the temperature ratio (5.83). In this limit we can neglect the term $\frac{2}{r}\frac{d\phi}{dr}$ in (5.74), as we did in the zero temperature case (see eq. (5.52)), and integration of (5.74) yields,

$$\frac{d\phi}{dr} = \sqrt{2V(\phi,T)} \tag{5.84}$$

where we have made use of boundary conditions (5.75) and (5.76). Using now (5.73) and (5.84) we can write the euclidean action as,

$$S_3 \sim 4\pi R^2 \int_{\phi(R-\delta R)}^{\phi(R+\delta R)} \sqrt{2V(\phi,T)}d\phi + 4\pi\int_0^R dr\, r^2 V(\phi_m,T) \tag{5.85}$$

Application to the potential (5.6), a straightforward calculation gives [12]

$$S_3(R) = \sqrt{2}\frac{8\pi}{3}\frac{(ET)^3R^2}{\lambda(T)^{5/2}} - \frac{16\pi\epsilon(T)}{3}\frac{(ET)^4R^3}{\lambda(T)^3} \tag{5.86}$$

The critical radius is obtained as usual maximizing the action (5.86). It yields,

$$R_c = \frac{\sqrt{2\lambda(T)}}{3ET\epsilon(T)} \tag{5.87}$$

while the action at the critical radius is given by

$$S_3 = \left(\frac{64\pi}{81}\right) \frac{ET}{(2\lambda(T))^{3/2}\epsilon(T)^2} \tag{5.88}$$

After using the thin wall approximation it is convenient to check its validity in all cases. For the potential (5.6) an analytic formula has been obtained in ref. [30] without assuming the thin wall approximation. It is given by,

$$\frac{S_3}{T} = \frac{13.72}{E^2}\left[D\left(1-\frac{T_o^2}{T^2}\right)\right]^{3/2} f\left[\frac{\lambda(T)D}{E^2}\left(1-\frac{T_o^2}{T^2}\right)\right] \tag{5.89}$$

where the function $f(x)$ is equal to 1 at $x = 0$ and blows up when x approaches 1. It is defined by

$$f(x) = 1 + \frac{x}{4}\left[1 + \frac{2.4}{1-x} + \frac{0.26}{(1-x)^2}\right] \tag{5.90}$$

A comparison of (5.88) with (5.89) will in general determine the validity of the thin wall approximation for theories with a potential which can be approximated by eq. (5.6). On the other hand the connection between zero temperature and finite temperature tunnelling is manifest. In particular at temperatures much less than the inverse radius the $O(4)$ solution has the least action. This can happen for theories with a supercooled symmetric phase: for instance in the presence of a barrier that does not disappear when the temperature drops to zero. At temperatures much larger than the inverse radius, the $O(3)$ solution has the least action.

5.3 Development of the phase transition

In the previous subsection we have established the free energy and the critical radius of a bubble large enough to grow after formation. The subsequent progress of the phase transition depends on the ratio of the rate of production of bubbles of true vacuum, as given by (5.17) and (5.71), over the expansion rate of the universe. For example if the former remains always smaller than the latter, then the state will be trapped in the supercooled false vacuum [11].

[11] In practice this happens whenever the life time of false vacuum decay is greater than the present age of the universe. Notice that for this to happen it is necessary that the barrier separating the false and true vacua does not disappear at zero temperature. Of course, as we have discussed in the previous subsections, this feature is not shared by the potentials described by (5.6).

Otherwise the phase transition will start at some temperature T_t by **bubble nucleation**. However this is not sufficient to claim that the phase transition really proceeds by bubble nucleation. For that it is necessary that bubbles **percolate** before the barrier disappear at the temperature T_o. In other words it is necessary that all space will be filled by bubbles before the barrier disappear. These issues will be briefly discussed in this subsection.

5.3.1 The beginning of the phase transition: bubble nucleation

The probability of bubble formation per unit time per unit volume is given by (5.71)

$$\frac{\Gamma}{\nu} = \omega T^4 e^{-B(T)} \tag{5.91}$$

where $B(T) = S_3(T)/T$ and the parameter ω will be taken of $\mathcal{O}(1)$ [12].

Since the progress of the phase transition should depend on the expansion rate of the universe, we have to describe the universe at temperatures close to the electroweak phase transition. A homogeneous and isotropic (flat) universe is described by a Robertson-Walker metric which, in comoving coordinates, is given by,

$$ds^2 = dt^2 - a(t)^2 \left(dr^2 + r^2 d\Omega^2\right) \tag{5.92}$$

where $a(t)$ is the scale factor of the universe. The universe expansion is governed by the equation

$$\left(\frac{\dot{a}}{a}\right)^2 = \frac{8\pi}{3M_{P\ell}^2}\rho \tag{5.93}$$

where $M_{P\ell}$ is the Planck mass,

$$M_{P\ell} = G_N^{-1/2} = 1.22 \times 10^{19}\ GeV \tag{5.94}$$

and ρ is the energy density. For temperatures $T \sim 10^2\ GeV$ the universe is radiation dominated, and its energy density is given by,

$$\rho = \frac{\pi^2}{30} g(T) T^4 \tag{5.95}$$

where

$$g(T) = g_B(T) + \frac{7}{8} g_F(T) \tag{5.96}$$

[12]The behaviour of (5.91) is dominated by the exponential and so the precise value of ω does not affect much the results of this section.

and $g_B(T)$ ($g_F(T)$) is the effective number of bosonic (fermionic) degrees of freedom at the temperature T. For the standard model we have

$$g_B^{SM} = 2(\text{polarizations}) \times 12(\text{gauge bosons}) + 2(\text{complex}) \times 2(\text{higgs bosons}) = 28 \quad (5.97)$$

$$g_F^{SM} = 3(\text{generations}) \times 2(\text{helicities})\,[3(\text{leptons}) + 3(\text{colors}) \times 4(\text{quarks})] = 90 \quad (5.98)$$

and so

$$g^{SM} = 106.75 \quad (5.99)$$

which can be considered as temperature independent.

The equation of motion (5.93) can be solved, and assuming an adiabatic expansion of the universe, $a(T_1)T_1 = a(T_2)T_2$, one obtains the following relationship,

$$t = \zeta \frac{M_{P\ell}}{T^2} \quad (5.100)$$

where

$$\zeta = \frac{1}{4\pi}\sqrt{\frac{45}{\pi g}} \sim 3 \times 10^{-2}$$

Using (5.100) the horizon length is given by

$$d_H(t) = 2\zeta \frac{M_{P\ell}}{T^2} \quad (5.101)$$

and the horizon volume

$$V_H(t) = 8\zeta^3 \frac{M_{P\ell}^3}{T^6} \quad (5.102)$$

The onset of nucleation happens at a temperature T_t such that **the probability for a single bubble to be nucleated within one horizon volume is ~ 1.** Using (5.100), (5.102) and (5.91), the probability for bubble nucleation in the temperature interval dT is given by

$$\frac{dP}{dT} \sim \omega \left(\frac{2\zeta M_{P\ell}}{T}\right)^4 \frac{1}{T} e^{-B(T)} \quad (5.103)$$

where, using (5.88) and (5.83), the exponent B can be written [13] as

$$B = \frac{64\pi}{81} \frac{E}{(2\lambda)^{3/2}} \left(\frac{T_c - T_o}{T_c - T}\right)^2 \quad (5.104)$$

Therefore, from (5.104) we can easily see that when T approaches T_c from below, then $B(T) \to \infty$, which reflects the fact that no phase transition can take place for $T > T_c$.

[13] We will assume here the thin wall approximation is valid.

Below T_c, $B(T)$ decreases as T decreases. Let us define T_t as the temperature at which the probability defined in (5.103) is $P(T_t) \sim 1$ and we will assume that T_t is reached before the barrier disappears, $T_t > T_o$. Then for $T < T_t$ we can effectively write $B_{\rm eff}(T) \to \infty$, and so the corresponding probability goes to zero. So the euclidean effective action $B_{\rm eff}(T)$ has a minimum at T_t [14] and we can integrate (5.103) using the steepest descent method around the point $B'(T_t) = 0$. This gives,

$$P(T_t) \sim \omega \left(\frac{2\zeta M_{P\ell}}{T_c}\right)^4 \left(\frac{T_c - T_t}{T_c}\right) \sqrt{\frac{\pi}{12B(T_t)}} e^{-B(T_t)} \tag{5.105}$$

We want now to evaluate (5.105) and impose the condition $P \sim 1$. To do that we can approximate $T_c - T_t \sim T_c - T_o$, since they are expected to be of the same order of magnitude, because the change in temperatures from T_c to T_o is a very small one. Then one can use the relation between T_c and T_o as given by (5.11) to write,

$$\frac{T_c - T_t}{T_c} \sim \frac{E^2}{\lambda D}$$

and finally we can write that $P \sim 1$ implies,

$$B(T_t) \sim 137 + \log \frac{10^2 E^2}{\lambda D} + 4 \log \frac{100\ GeV}{T_c} \tag{5.106}$$

where we have normalized $T_c \sim 100\ GeV$ and $E^2/(\lambda D) \sim 10^{-2}$ which are typical values which will be obtained in the standard model of electroweak interactions, as we will see later on.

5.3.2 The end of the phase transition: bubble percolation

In order to guarantee that the phase transition really proceeds by bubble nucleation it is necessary, but not sufficient, that at least one bubble of the true vacuum be formed per horizon volume before the barrier of the potential disappear at the temperature T_o. The sufficient condition is that at some temperature T^* greater than T_o all the space is filled with bubbles, which then percolate. The fraction of space in the old phase in a first order phase transition has been evaluated by Guth and E. Weinberg as [39]

$$p_{\rm old}(t) = e^{-h(t)} \tag{5.107}$$

[14] Notice that the physical origin of this minimum is different to the minimum obtained in ref. [39] which is due to the decrease of thermal effects at temperatures $\sim T_c/4$. At the electroweak phase transition the range in temperature from T_c to T_o is a tiny interval.

where

$$h(t) = \int_{t_c}^{t} dt_1 \frac{\Gamma(t_1)}{\nu} a^3(t_1) V(t_1, t) \tag{5.108}$$

and $V(t_1, t)$ being the volume at time t of a bubble nucleated at time t_1.

Suppose now that the bubble is propagating at the speed of light [15]. Then its radius R satisfies the relation $dt = a(t)dR$, from (5.92) and, therefore, neglecting the bubble initial size, the bubble radius at time t of a bubble nucleated at time t_1 is

$$R(t_1, t) = \int_{t_1}^{t} \frac{dt_2}{a(t_2)} \tag{5.109}$$

Using now (5.100) and the adiabaticity condition we can cast (5.109) as

$$R(T_1, T) = \frac{2\zeta}{a(T_1)T_1} M_{P\ell} \left(\frac{1}{T} - \frac{1}{T_1} \right) \tag{5.110}$$

and the volume at the temperature T of a bubble nucleated at temperature T_1,

$$V(T_1, T) = \frac{32\pi}{3} \frac{\zeta^3 M_{P\ell}^3}{a(T_1)^3 T_1^3} \left(\frac{1}{T} - \frac{1}{T_1} \right)^3 \tag{5.111}$$

Finally the function $h(T)$ in (5.108) can be written, using (5.91) and (5.111), as

$$h(T) = \frac{64\pi}{3} \zeta^4 \omega \left(\frac{M_{P\ell}}{T} \right)^4 \int_T^{T_c} \frac{T dT_1}{T_1^2} \left(1 - \frac{T}{T_1} \right)^3 e^{-B(T_1)} \tag{5.112}$$

When $h \to 0$, the fraction of space in the new phase

$$p_{\text{new}}(t) = 1 - p_{\text{old}}(t) = 1 - e{-}h(t) \tag{5.113}$$

is $\to 0$. On the other hand, when $h \to \infty$, the fraction of space in the new phase is $\to 1$. Of course, in practice this is realized when $h = \mathcal{O}(1)$. Suppose that this happens at a temperature T^*, where $T_o < T^* < T_c$. The euclidean action goes to infinity when $T \to T_c$ from below, and decreases for decreasing values of the temperature. So for temperatures T in the range $T^* < T < T_c$ the function $B(T)$ reaches its minimum value at $T = T^*$. For temperatures $T < T^*$ all the space has already turned to the new phase and the effective transition probability is zero since there is no available space. In this way, the effective action $B(T)$ has a minimum at $T = T^*$. Because $B(T)$ is a very rapidly changing function in the interval of temperatures between T_c and T_o, while the change of temperatures itself

[15] In fact assuming a velocity $\beta \lesssim 1$ is not changing significantly the results in this section. Only extremely non relativistic bubbles could change it.

is insignificant, we can make the integral in (5.112) using the steepest descent method. We obtain,

$$h(T^*) \sim \frac{4\pi}{3}\left(\frac{2\zeta M_{P\ell}}{T_c}\right)^4 \omega \left(\frac{T_c - T_o}{T_c}\right)^4 \sqrt{\frac{\pi}{12B(T^*)}} e^{-B(T^*)} \tag{5.114}$$

where we have made use of the fact that $T_c \sim T^* \sim T_o$. The condition $h(T^*) \sim 1$ in (5.114) translates into the condition on the euclidean action $B(T^*)$,

$$B(T^*) \sim 124 + 4\log\frac{10^2 E^2}{\lambda D} + 4\log\frac{100\ GeV}{T_c} + \log\omega \tag{5.115}$$

where we have normalized, as in (5.106), T_c and $E^2/\lambda D$ to the typical values obtained in the standard model of electroweak interactions. The phase transition completes between T_t and T^* very quickly.

6 Improved effective potential at finite temperature

The approach of ref. [16] to the finite temperature effective potential relied on the observation that **symmetry restoration implies that ordinary perturbation theory must break down at high temperature**. In fact, otherwise perturbation theory should hold and, since the tree level potential is temperature independent, radiative corrections (which are temperature dependent) should be unable to restore the symmetry. We will see that the failure of perturbative expansion is intimately linked to the appearance of infrared divergences for the zero Matsubara modes of bosonic degrees of freedom. This just means that the usual perturbative expansion in powers of the coupling constant fails at temperatures beyond the critical temperature. It has to be replaced by an improved perturbative expansion where an infinite number of diagrams are resummed at each order in the new expansion. We will review the actual situation in this section.

6.1 The breakdown of perturbative expansion

We will examine the simplest model of one self-interacting real scalar field, described by the lagrangian (2.22) and (2.23). The one-loop effective potential was computed in section 4.1. We will use now power counting arguments to investigate the high temperature behaviour of higher loop diagrams contributing to the effective potential [16, 40, 41]. After rescaling all loop momenta and energies by T, a loop amplitude with superficial divergence D takes the form,

$$T^D f(\frac{m}{T}) \tag{6.1}$$

If there are no infrared divergences when $m/T \to 0$, then the loop goes like T^D. For instance the diagram contributing to the self-energy of fig. 17 is quadratically divergent ($D = 2$),

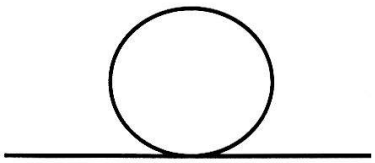

Figure 17: **One-loop contribution to the self-energy for the scalar theory**

and so behaves like

$$\lambda T^2 \tag{6.2}$$

For $D \leq 0$, there are infrared divergences associated to the zero modes of bosonic propagators in the imaginary time formalism [$n = 0$ in (3.72)] and the only T dependence comes from the T in front of the loop integral in (3.72). Then every logarithmically divergent or convergent loop contributes a factor of T. For instance the diagram contributing to the self-energy in fig. 18 contains two logarithmically divergent loops and so behaves like,

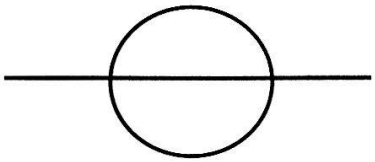

Figure 18: **Two-loop contribution to the self-energy for the scalar theory**

$$\lambda^2 T^2 = \lambda(\lambda T^2) \tag{6.3}$$

It is clear that to a fixed order in the loop expansion the largest graphs are those with the maximum number of quadratically divergent loops. These diagrams are obtained from the diagram in fig. 17 by adding n quadratically divergent loops on top of it, as shown in fig. 19. They behave as,

$$\lambda^{n+1} \frac{T^{2n+1}}{M^{2n-1}} = \lambda^2 \frac{T^3}{M} \left(\frac{\lambda T^2}{M^2} \right)^{n-1} \tag{6.4}$$

where M is the mass scale of the theory, and has been introduced to rescale the powers of the temperature [16]. As was clear from eq. (6.4), adding a quadratically divergent bubble to a

[16] In fact, the mass M has a different meaning for the improved and the unimproved theories, as we shall see. For the unimproved theory, M is the mass in the shifted lagrangian, $M^2 = m^2(\phi)$, while in the improved theory, M is given by the Debye mass, see eq. (6.41).

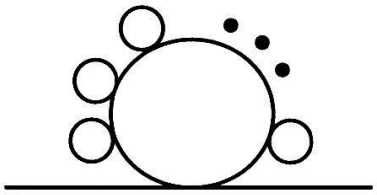

Figure 19: **Daisy (n+1)-loop contribution to the self-energy for the scalar theory**

propagator which is part of a logarithmically divergent or finite loop amounts to multiplying the diagram by

$$\alpha \equiv \lambda \frac{T^2}{M^2} \tag{6.5}$$

This means that for the one-loop approximation to be valid it is required that

$$\lambda \frac{T^2}{M^2} \ll 1$$

along with the usual requirement for the ordinary perturbation expansion

$$\lambda \ll 1$$

However at the critical temperature we have that $T_c \sim M/\sqrt{\lambda}$ [see *e.g.* eqs. (5.1)-(5.3)]. Therefore **at the critical temperature the one-loop approximation is not valid** and higher loop diagrams where multiple quadratically divergent bubbles are inserted cannot be neglected.

What about the diagrams which are not considered in the **improved** expansion? The two-loop diagram of fig. 18 is suppressed with respect to the diagram of fig. 17 by λ. On the other hand the multiple loop diagram obtained from that of fig. 18 by adding n quadratically divergent loops on top of it, see fig. 20, behaves as

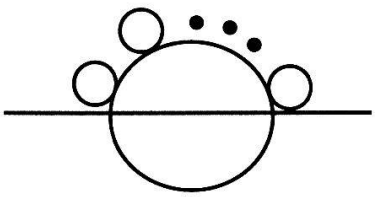

Figure 20: **Non-daisy (n+2)-loop contribution to the self-energy for the scalar theory**

$$\lambda^{n+2} \frac{T^{2n+2}}{M^{2n}} = \lambda^{n+1} \frac{T^{2n+1}}{M^{2n-1}} \left(\lambda \frac{T}{M}\right) \tag{6.6}$$

and it is suppressed with respect to the multiple loop diagram of eq. (6.4) by $\lambda T/M$ [17]. Therefore the validity of the improved expansion is guaranteed provided that,

$$\begin{aligned} \lambda &\ll 1 \\ \beta \equiv \lambda\frac{T}{M} &\ll 1 \end{aligned} \tag{6.7}$$

6.2 Improved theory: diagrammatic approach

We have seen that [16, 28] the perturbative expansion fails at temperatures close to the critical temperature, because of infrared (IR) divergences, and it was proposed to solve the IR problem by the resummation of an infinite set of the most IR divergent diagrams: *i.e.* those belonging to the daisy and superdaisy classes [15]. Improving the effective potential in different theories by the inclusion of daisy and superdaisy diagrams has produced a lot of activity in the field during the last years [40]-[54]. Since there has been some controversy about the correct resummation procedure concerning the leading infrared divergent graphs [44, 45, 48, 49, 51, 52, 53, 47], I will develop in this section the formalism [55] which was followed in [41, 50] as well as will compare it with different approaches recently used by other authors.

We will consider again, and for simplicity, the theory of a real scalar field Φ, described by the lagrangian (2.22) and the tree level potential

$$V_{\rm eff}^{(0)}(\Phi) = -\frac{m^2}{2}\Phi^2 + \frac{\lambda}{4}\Phi^4 \tag{6.8}$$

with positive λ and m^2. At the tree level, the field-dependent mass of the scalar field (after shifting $\Phi \to \Phi + \phi$) is $m^2(\phi) = 3\lambda\phi^2 - m^2$, and the minimum of $V_{\rm eff}^{(0)}$ corresponds to $v^2 = m^2/\lambda$, so that $m^2(v) = 2\lambda v^2 = 2m^2$.

At finite temperature, the one-loop effective potential can be written diagrammatically as[18],

$$V_{\rm eff}^{(1)} = \sum_{n=0}^{\infty} V_{[n]}^{(1)} = \frac{1}{2}$$  (6.9)

[17]Non-daisy contributions to the self-energy are suppressed, with respect to daisy contributions, by $\mathcal{O}(\beta)$, where β is defined in (6.7). The corresponding contributions to the vacuum diagrams (*i.e.* effective potential) are suppressed by $\mathcal{O}(\beta^2)$ [41].

[18]There is an overall negative sign in front of all diagrams contributing to the effective potential and self-energies that (for simplicity) will be dropped systematically from the figures, but will be taken into account in the calculation.

where n are the bosonic Matsubara frequencies and $V^{(1)}_{[n]}$ are the contributions to the one-loop effective potential from the different frequencies. They can be written to lowest order in $m(\phi)/T$ as (see eqs. (4.14) and (4.16))

$$V^{(1)}_{[0]} = \frac{1}{2}\bigcirc = -\frac{1}{12\pi}Tm^3(\phi) \tag{6.10}$$

$$\sum_{n=1}^{\infty} V^{(1)}_{[n]} = \frac{1}{2}\ \bigcirc\ = \frac{1}{24}T^2m^2(\phi) + \cdots \tag{6.11}$$

where big bubbles denote the contribution from zero modes and small bubbles the one from all non-zero modes. The contribution from all modes will be denoted by a big dotted bubble, *i.e.*

$$\bigodot = \bigcirc + \bigcirc \tag{6.12}$$

For the zero modes ($n = 0$) there is a severe infrared problem in the loop expansion for values of ϕ such that $m(\phi) \ll \lambda T$ at $\vec{p} = 0$. At one-loop the potential (6.10) is non-analytic at $m(\phi) = 0$, while the validity of the perturbative expansion breaks down at higher-loop order, which contribute powers of α and β [16, 40]

$$\alpha = \lambda\frac{T^2}{m^2(\phi)}, \quad \beta = \lambda\frac{T}{m(\phi)} \tag{6.13}$$

The usual way out is dressing the zero-modes with daisy and super-daisy diagrams [16]. This can be done by solving the gap equations. For the theory defined by eq. (6.8), and neglecting the terms represented by the ellipsis in (6.11), the gap equation can be diagrammatically written as,

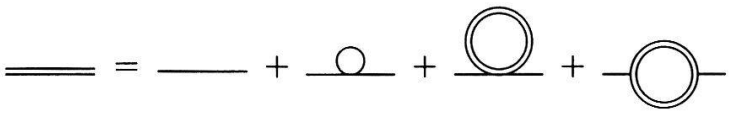

(6.14)

where a double line represents a dressed zero-mode propagator. Using the approximation in eq. (6.11) the self-energies can be written as

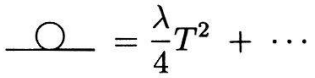

$$= \frac{\lambda}{4}T^2 + \cdots \tag{6.15}$$

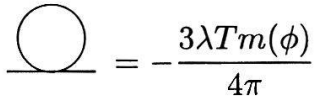

$$= -\frac{3\lambda T m(\phi)}{4\pi} \tag{6.16}$$

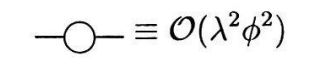

$$\equiv \mathcal{O}(\lambda^2\phi^2) \tag{6.17}$$

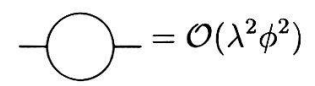

$$= \mathcal{O}(\lambda^2\phi^2) \tag{6.18}$$

and the gap equation (6.14), to $\mathcal{O}(\lambda)$, as

$$M^2 = m^2(\phi) + \frac{\lambda T^2}{4} - \frac{3\lambda T M}{4\pi} + \mathcal{O}(\lambda^2\phi^2) \tag{6.19}$$

where M is the solution to (6.19). In the approximation of eq. (6.11) the small bubbles are constant and proportional to T^2 (6.15) or zero (6.17) (the ellipsis is neglected), and so they do not have to be dressed. Going beyond this approximation, also small bubbles would need to be dressed. We will comment on this possibility later on.

Now we will see how the daisy and superdaisy diagrams amount to a resummation in the loop expansion of the effective potential which can therefore be written in terms of the solution to the gap equation (6.19). In the order of approximation we are working only the zero modes need to be dressed, and only $V^{(1)}_{[0]}$ in eq. (6.10) is improved, while $\sum_{n\neq 0} V^{(1)}_{[n]}$ in eq. (6.11) does not have any IR problem and can be considered as a good estimate. We will prove the resummation to four-loop order though also functional methods [56] can be used [48] as we will see.

The loop expansion of the effective potential will be written as

$$V_{\rm eff} = \sum_{\ell=0}^{\infty} V^{(\ell)}_{\rm eff} \; + \; {\rm non-(super)daisies} \tag{6.20}$$

where $V^{(\ell)}_{\rm eff}$ indicates the contribution to the effective potential from ℓ-loop daisy and superdaisy diagrams. Non-(super)daisy diagrams contribute to the effective potential to $\mathcal{O}(\beta^2)$ [40, 41]. At least, to $\mathcal{O}(\beta)$ it is consistent to keep only diagrams of daisy and superdaisy classes. $V^{(1)}_{\rm eff}$ was given in eq. (6.9), while $V^{(2)}_{\rm eff}$ and $V^{(3)}_{\rm eff}$ can be written as

$$V^{(2)}_{\rm eff} = \frac{1}{8}$$ 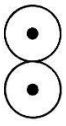 $$+ \frac{1}{12}$$ 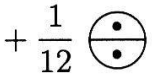 (6.21)

$$V^{(3)}_{\rm eff} = \frac{1}{16}$$ 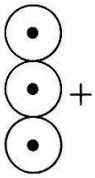 $$+ \frac{1}{8}$$  $$+ \frac{1}{16}$$  (6.22)

where we are putting dots everywhere to remember that all modes (zero and non-zero modes) are contributing in the loop propagators, and the numerical pre-factors in front of (6.21) and (6.22) are the symmetry factors of the corresponding diagrams.

Using the approximation in (6.15), (6.17), we can rearrange the loop expansion in (6.9), (6.21) and (6.22) as

$$V_{\rm eff}^{(\ell)} = V_{\rm daisy}^{(\ell)} + V_{\rm superdaisy}^{(\ell)} + \Delta^{(\ell)} \left[-\frac{1}{8} \right. \quad - \frac{1}{6} \left. \right] \tag{6.23}$$

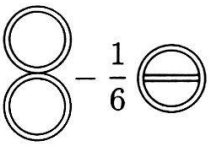

where $\Delta^{(\ell)}[\cdots]$ means the contribution to $[\cdots]$ from ℓ-loop diagrams and the double line is given by eq. (6.14). This decomposition is well defined for $\ell \geq 2$. Next we give the results for two and three-loop diagrams.

Two-loop

$$V_{\rm daisy}^{(2)} = \frac{1}{4} \quad + \frac{1}{4} \quad + \frac{1}{4} \tag{6.24}$$

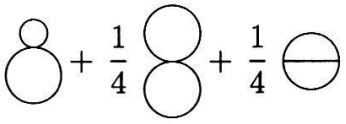

$$V_{\rm superdaisy}^{(2)} = 0 \tag{6.25}$$

$$\Delta^{(2)} = -\frac{1}{8} \quad - \frac{1}{6} \tag{6.26}$$

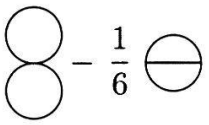

Three-loop

$$V_{\rm daisy}^{(3)} = \frac{1}{16} \quad + \frac{1}{8} \quad + \frac{1}{16} \quad + \frac{1}{8} \quad + \frac{1}{8} \quad + \frac{1}{16} \tag{6.27}$$

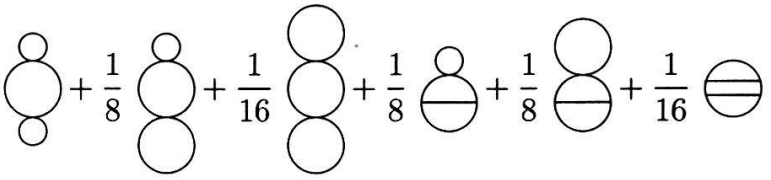

$$V_{\rm superdaisy}^{(3)} = \frac{1}{8} \quad + \frac{1}{8} \quad + \frac{1}{4} \quad + \frac{3}{8} \quad + \frac{1}{4} \tag{6.28}$$

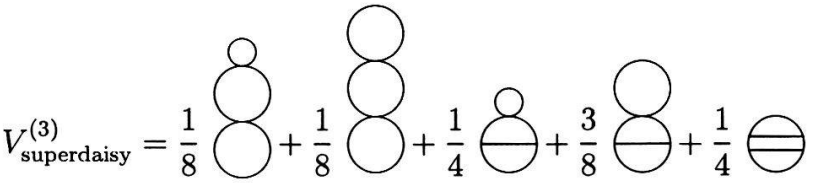

$$\Delta^{(3)} = -\frac{1}{8} \quad - \frac{1}{8} \quad - \frac{1}{4} \quad - \frac{3}{8} \quad - \frac{1}{4} \tag{6.29}$$

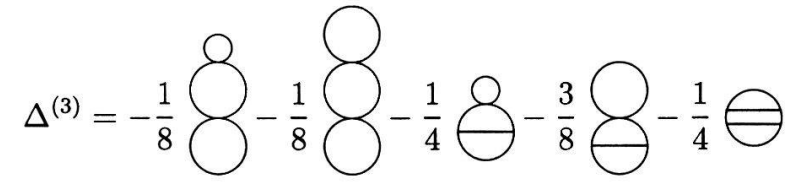

We can see from (6.21) and (6.24) that the symmetry factors for $\ell = 2$ do not match the combinatorics for daisy resummation. However including (6.26) the matching is accomplished as can be seen from the coefficients in (6.21) and the last two terms in (6.24) and (6.26)

$$\begin{aligned} \frac{1}{4} - \frac{1}{8} &= \frac{1}{8} \\ \frac{1}{4} - \frac{1}{6} &= \frac{1}{12} \end{aligned} \tag{6.30}$$

On the other hand, we have seen from (6.28,6.29) that $V^{(3)}_{\text{superdaisy}} + \Delta^{(3)} = 0$. The reason being that all the diagrams in (6.22) could be interpreted either as daisies or as superdaisies. Therefore we have considered all of them as daisies, because their coefficients match the correct combinatorics for resummation. This can be seen by comparison with the corresponding coefficients in (6.27) and it is a general feature of daisy diagrams for $\ell \geq 3$. However, for $\ell \geq 4$ there are diagrams that can never be considered as daisies. In that case the previous cancellation does not hold, but still the equation (6.23) is satisfied. As an example we will consider the theory at the origin (*i.e.* at $\phi = 0$) to four-loop order.

Four-loop

The contributions to (6.20) and (6.23) can be written as

$$V^{(4)}_{\text{eff}}(0) = \frac{1}{48}$$ 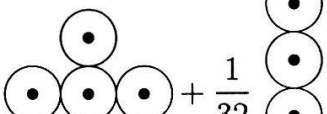 $$+ \frac{1}{32}$$ 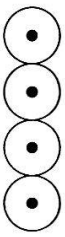 (6.31)

$$V^{(4)}_{\text{daisy}}(0) = \frac{1}{48}$$ 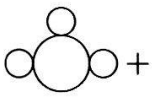 $$+ \frac{3}{48}$$ 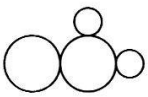 $$+ \frac{3}{48}$$ 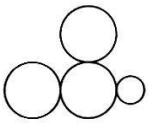 $$+ \frac{1}{48}$$ 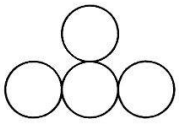 (6.32)

$$V^{(4)}_{\text{superdaisy}}(0) = \frac{1}{16}$$ 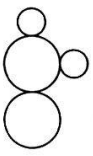 $$+ \frac{1}{8}$$ 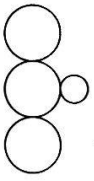 $$+ \frac{1}{16}$$ 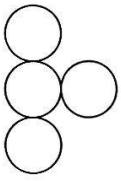 $$+ \frac{1}{16}$$ 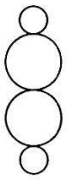 $$+ \frac{3}{16}$$  $$+ \frac{2}{16}$$ 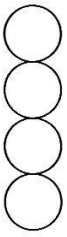 (6.33)

$$\Delta^{(4)}(0) = -\frac{1}{16}$$ 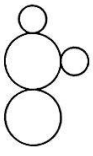 $$- \frac{1}{8}$$ 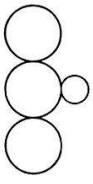 $$- \frac{1}{16}$$ 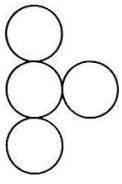 $$- \frac{1}{32}$$ 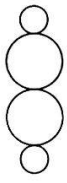 $$- \frac{1}{8}$$ 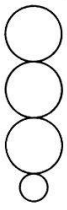 $$- \frac{3}{32}$$ 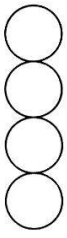 (6.34)

The first diagram in (6.31) can be (and it is) considered as a daisy diagram in (6.32). For that reason the coefficients of the first three terms in (6.33) and (6.34) are equal and opposite in sign. The second diagram in (6.31) can *never* be considered as a daisy diagram. So it

contributes to the last three terms of (6.33) and (6.34) in such a way that their coefficients match to those of the second term of (6.31). In particular

$$\begin{aligned} \frac{1}{16} - \frac{1}{32} &= \frac{1}{32} \\ \frac{3}{16} - \frac{1}{8} &= 2 \times \frac{1}{32} \\ \frac{2}{16} - \frac{3}{32} &= \frac{1}{32} \end{aligned} \tag{6.35}$$

for the last three terms, respectively.

All-loop

Summarizing the above results, we can write the final equation:

$V_{\text{eff}} = \frac{1}{2}$ $+ \frac{1}{2}$ 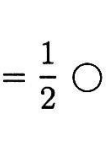 $- \frac{1}{8}$ 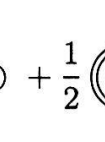 $- \frac{1}{6}$ 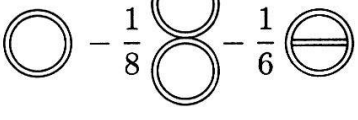 (6.36)

where the double line indicates the solution of the gap equation (6.14) and (6.19), in the approximation of eqs. (6.15) and (6.17). Using the explicit solution to (6.19) we can write (6.36) as

$$V_{\text{eff}} = -\frac{m^2}{2}\phi^2 + \frac{\lambda}{4}\phi^4 + \frac{1}{24}T^2 m^2(\phi) - \frac{1}{12\pi}TM^3 + \cdots - \frac{3\lambda}{64\pi^2}T^2M^2 + \mathcal{O}(\lambda^2\gamma T^4) \tag{6.37}$$

which agrees, as we will see later on, with the result of Amelino-Camelia and Pi [48], who used functional methods [56] and computed (6.14) and (6.19) to zeroth order in γ

$$\gamma \equiv \frac{\phi^2}{T^2} \tag{6.38}$$

In the improved theory of zero-modes defined by (6.19) and (6.37), the expansion parameters α and β in (6.13) become [19]

$$\alpha = \lambda \frac{T^2}{\mathcal{M}^2} \sim 1 \tag{6.39}$$

which is summed to all orders, and

$$\beta = \lambda \frac{T}{\mathcal{M}} \sim \lambda^{\frac{1}{2}} \tag{6.40}$$

[19] We will keep for notational simplicity the same names α and β for the expansion parameters in the improved (as in the unimproved) theory.

which remains as the only expansion parameter, where $\mathcal{M}$ is the Debye mass

$$\mathcal{M}^2 = m^2(\phi) + \frac{\lambda}{4}T^2 \tag{6.41}$$

By expanding the solution of eq. (6.19) to different orders in β we can obtain the effective potential (6.37) to the corresponding order of approximation. To illustrate the procedure we will first obtain the solution to $\mathcal{O}(\beta^0)$. In that case we have

$$M^2 = \mathcal{M}^2 \tag{6.42}$$

and the effective potential is given by

$$V_{\rm eff} = -\frac{m^2}{2}\phi^2 + \frac{\lambda}{4}\phi^4 + \frac{1}{24}T^2m^2(\phi) - \frac{1}{12\pi}T\mathcal{M}^3 + \cdots \tag{6.43}$$

This approximation has been worked out in [43]. The last two terms in (6.36) and (6.37) do not contribute to this order[20] since they start to $\mathcal{O}(\beta)$.

The solution to $\mathcal{O}(\beta)$ is equally easy to be worked out. From (6.19) one can write

$$M^2 = \mathcal{M}^2 - \frac{3\lambda}{4\pi}\mathcal{M}T + \mathcal{O}(\lambda^2\phi^2) \tag{6.44}$$

where the first term is the leading order result, eq. (6.42), and the second term is $\mathcal{O}(\beta)$. Replacing (6.44) in (6.37) and expanding again to $\mathcal{O}(\beta)$ we can obtain the corresponding approximation to the effective potential, given by

$$V_{\rm eff} = -\frac{m^2}{2}\phi^2 + \frac{\lambda}{4}\phi^4 + \frac{1}{24}T^2m^2(\phi) - \frac{1}{12\pi}T\mathcal{M}^3 + \cdots + \frac{(6-3)}{64\pi^2}\lambda T^2\mathcal{M}^2 + \mathcal{O}(\lambda^2\phi^2T^2) \tag{6.45}$$

This solution was presented in [50]. We can easily check that the last term in (6.45) is an $\mathcal{O}(\beta)$ correction to the fourth term. It comes partly from the expansion (6.44) and partly from the last two terms in (6.36).

There is another, recent, proposal by Arnold and O. Espinosa [52] who have advocated a hybrid method using a partial resummation of the leading contribution of $n \neq 0$ bubbles followed by an ordinary loop expansion [54]. One can define a *partially dressed* propagator as

(6.46)

where the tiny bubble propagator is defined as,

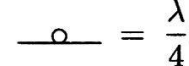

$$= \frac{\lambda}{4}T^2\,, \tag{6.47}$$

[20] In the language of ref. [50] there is no *combinatorial* term to this order.

and a *partially resummed* loop expansion as

$$V_{\rm eff} = V_{\rm eff}^{(0)} + \frac{1}{2}\,\bigcirc\!\!\bullet + \frac{1}{8}\,\bigcirc\!\!\bullet\!\!\bigcirc\!\!\bullet + \frac{1}{12}\,\bigcirc\!\!\bullet\!\!\bullet\!\!\bigcirc + \cdots \tag{6.48}$$

It is easy to check that using the approximation of eqs. (6.15)-(6.18), and ignoring overlapping momenta, one recovers, to $\mathcal{O}(\beta)$, the same result as that of eq. (6.45).

Other authors [45, 47] have proposed computing tadpoles, instead of vacuum diagrams, to exhibit some features of the improved theory, *e.g.* resummation properties and the absence of a linear term in $m(\phi)$ in the final effective potential. Since the tadpole is nothing else than the ϕ-derivative of the effective potential, there can be no difference between both formalisms. In fact, by comparison between the contents of this section and those in [47] one can easily see that the resummation properties of the tadpole diagrams are inherited from the corresponding ones in vacuum diagrams. However, in our opinion, the tadpole formalism has two practical drawbacks: i) The classification of tadpole diagrams is much more involved than the classification of vacuum diagrams; ii) To obtain the effective potential the tadpole has to be integrated, which can be a non-trivial operation since it depends on the solution of the gap equation. However, at the end, both methods should yield the same result.

In our approximation of eqs. (6.11), (6.15) and (6.17) we have been neglecting all logarithmic terms, which amounted to not dressing non-zero modes. Including them would amount to write the previous equations as

$$\frac{1}{2}\ \bigcirc\ = \frac{1}{24}T^2m^2(\phi) - \frac{m^4(\phi)}{64\pi^2}\log\frac{Q^2}{c_BT^2} + \cdots \tag{6.49}$$

where Q is the renormalization scale in the $\overline{\rm MS}$ scheme and $\log(c_B) = 3.9076$,

$$\text{—}\bigcirc\text{—}\ = \frac{\lambda}{4}T^2 - \frac{3\lambda m^2(\phi)}{16\pi^2}\log\frac{Q^2}{c_BT^2} + \cdots \tag{6.50}$$

$$\text{—}\bigcirc\text{—} = \mathcal{O}(\lambda^2\phi^2) \tag{6.51}$$

In that case the gap equation should be written as

$$\text{═══} = \text{———} + \text{—}\bigcirc\!\!\bullet\text{—} + \text{—}\bigcirc\!\!\bullet\!\!\bigcirc\text{—} \tag{6.52}$$

and other diagrams should be added to those in (6.24)-(6.34). In particular small bubbles dressed by insertions of self-energies of the kind (6.18). But the latter are $\mathcal{O}(\lambda^2\phi^2)$ and depend on the external momentum. If we insist in keeping the logarithmic terms (which in principle are expected to constitute small corrections to the leading contribution) we should

give up resummation in the sense of the gap equation (6.52) since overlapping momenta should be disentangled. A possibility is making a γ expansion for the gap equation, and defining an $\mathcal{O}(\gamma^0)$ gap equation as

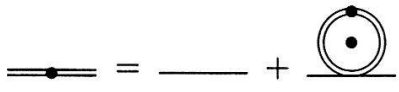

(6.53)

where the dotted double line means the solution of the truncated gap equation[21], *i.e.*

$$M^2 = m^2(\phi) + \frac{\lambda T^2}{4} - \frac{3\lambda T M}{4\pi} - \frac{3\lambda M^2}{16\pi^2}\log\frac{Q^2}{c_B T^2} + \cdots \tag{6.54}$$

However, we should pay attention to the fact that the last term in the full gap equation (6.19) is $\mathcal{O}(\alpha\beta\gamma)$ and solving it, and giving the improved effective potential to some order in β implies that we should consider the same order in γ by adding loop diagrams. In this way repeating the whole above procedure we would find that to $\mathcal{O}(\beta)$ one can write the effective potential as

$$V_{\text{eff}} = \frac{1}{2}$$ 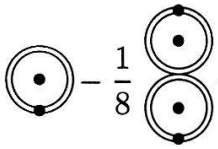 $$- \frac{1}{8}$$ $$+ \frac{1}{12}$$  $$+ \mathcal{O}(\beta^2)$$ (6.55)

where the equation (6.54) is solved to $\mathcal{O}(\beta)$. This solution coincides at $\phi = 0$ with that in ref. [48] and for all values of ϕ with that in ref. [52]. One can check that the logarithmic corrections which appear are both from the logarithms in (6.49), (6.50), (6.51), and from the overlapping momenta whose integral is explicitly considered. To higher order in β more terms should be added to (6.55) but care should be taken not to commit overcounting and non-(super)daisy diagrams should be considered.

6.3 Improved theory: functional approach

In the previous subsection we have reviewed some of the existing resummations using diagrammatic methods. Here we will see that similar results can be obtained using functional methods. Also for simplicity we will restrict ourselves to the simplest theory described by the potential (6.8). We have seen that the improved theory consists in replacing the improved propagator in (part of) the one loop effective potential. So one needs a self-consistent loop expansion of the effective potential in terms of the full propagator. This technique was developed by Cornwall, Jackiw and Tomboulis [56] and applied to the present problem by Amelino-Camelia and Pi [48].

[21] Of course the gap equation (6.53), and (6.54), is exact at the origin $\phi = 0$, where $\gamma \equiv 0$.

One considers a generalization of the effective action (3.16), $\Gamma^\beta(\phi,\mathcal{G})$, which depends not only on the classical field ϕ, but also on the propagator $\mathcal{G}(x,y)$. The physical solutions satisfy

$$\frac{\delta\Gamma^\beta[\phi,\mathcal{G}]}{\delta\phi(x)}=0 \tag{6.56}$$

and

$$\frac{\delta\Gamma^\beta[\phi,\mathcal{G}]}{\delta\mathcal{G}(x,y)}=0 \implies \mathcal{G}_0=\mathcal{G}_0(\phi) \tag{6.57}$$

while the conventional effective action is related to the new one by

$$\Gamma^\beta[\phi]\equiv\Gamma^\beta[\phi,\mathcal{G}_0(\phi)] \tag{6.58}$$

Eq. (6.57) determines the form of the propagator. It is known as the **gap** equation of the theory.

For translationally invariant field configurations, the propagator is a function of $x-y$, $\mathcal{G}=\mathcal{G}(x-y)$, and the effective potential is related to the full propagator as in (2.16)

$$\Gamma^\beta[\phi,\mathcal{G}]=-\int d^4x V^\beta_{\rm eff}(\phi,\mathcal{G}) \tag{6.59}$$

The method of ref. [56] consists in generalizing the thermal partition function (3.14) by introducing sources $k(x,y)$ on top of the usual ones $j(x)$

$$Z^\beta[j,k]=\left\langle T_C\exp\left\{i\left(\int_C d^4x j(x)\Phi(x)+\frac{1}{2}\int_C d^4x d^4y\Phi(x)k(x,y)\Phi(y)\right)\right\}\right\rangle \tag{6.60}$$

where C means here the contour used in the imaginary time formalism described in section 3.4.

The generating functional for connected Green functions is defined similarly to (3.15) as

$$Z^\beta[j,k]\equiv\exp\{iW^\beta[j,k]\} \tag{6.61}$$

The effective action $\Gamma^\beta[\phi,\mathcal{G}]$ is obtained by a double Legendre transformation of $W^\beta[j,k]$ similarly to (3.16)

$$\Gamma^\beta[\phi,\mathcal{G}]=W^\beta[j,k]-\int_C d^4x\frac{\delta W^\beta[j,k]}{\delta j(x)}j(x)-\int_C d^4x d^4y\frac{\delta W^\beta[j,k]}{\delta k(x,y)}k(x,y) \tag{6.62}$$

where the currents $j(x)$ and $k(x,y)$ are eliminated in favor of the classical fields $\phi(x)$ and propagator $\mathcal{G}(x,y)$, as in (3.17),

$$\begin{aligned}\frac{\delta W^\beta[j,k]}{\delta j(x)} &= \phi(x) \\ \frac{\delta W^\beta[j,k]}{\delta k(x,y)} &= \frac{1}{2}\left[\mathcal{G}(x,y)+\phi(x)\phi(y)\right]\end{aligned} \tag{6.63}$$

Finally eq. (3.18) generalizes to

$$\begin{aligned} \frac{\delta\Gamma^{\beta}[\phi,\mathcal{G}]}{\delta\phi(x)} &= -j(x) - \int_C d^4y k(x,y)\phi(y) \\ \frac{\delta\Gamma^{\beta}[\phi,\mathcal{G}]}{\delta\mathcal{G}(x,y)} &= -\frac{1}{2}k(x,y) \end{aligned} \tag{6.64}$$

The stationary requirements (6.56) and (6.57) are obtained from (6.64) by switching the sources $j(x)$ and $k(x,y)$ off. It is known that $\Gamma^{\beta}[\phi,\mathcal{G}]$ is the generating functional in ϕ for 2PI Green functions expressed in terms of the propagator $\mathcal{G}$.

Using the techniques of section 2.3, Cornwall, Jackiw and Tomboulis [56] find for the effective potential (6.59) the expression,

$$V^{\beta}_{\rm eff}(\phi,\mathcal{G}) = V_0(\phi) + \frac{1}{2}Tr\log\mathcal{G}^{-1} + \frac{1}{2}Tr\left[\mathcal{D}^{-1}\mathcal{G} - 1\right] + V^{\beta}_{(2)}(\phi,\mathcal{G}) \tag{6.65}$$

where $\mathcal{D}(\phi;x-y)$ is the tree level propagator in the shifted theory, as in section 2.3. $V^{\beta}_{(2)}(\phi,\mathcal{G})$ is given by all two-particle irreducible vacuum-to-vacuum graphs with two or more loops, in the shifted theory, with vertices given by the interaction part of the shifted Lagrangian ($\Phi \to \Phi + \phi$) and propagators set equal to $\mathcal{G}(x,y)$. The gap equation (6.57) can be written as,

$$\mathcal{G}^{-1}(p) = \mathcal{D}^{-1}(p) + 2\frac{\delta V^{\beta}_{(2)}}{\delta\mathcal{G}(p)} \tag{6.66}$$

where $\mathcal{G}(p)$ and $\mathcal{D}(p)$ are the Fourier transforms of $\mathcal{G}(x-y)$ and $\mathcal{D}(x-y)$, respectively.

The vertices of the shifted theory are given by the interaction Lagrangian

$$\mathcal{L}_{\rm int} = \lambda\phi\Phi^3 + \frac{\lambda}{4}\Phi^4 \tag{6.67}$$

and the two-loop diagrams contributing to $V^{\beta}_{(2)}$ are depicted in fig. 21 where each line

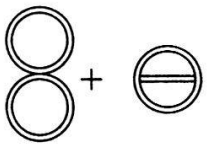

Figure 21: **One and two-loop diagrams contributing to the effective potential of (2.45)**

represents the propagator $G(x,y)$, and there are two kind of vertices, as provided by (6.67). The figure eight diagram in (21) is $\mathcal{O}(\lambda)$, while the sunset diagram is $\mathcal{O}(\lambda^2)$.

A first (naive) approximation is provided by neglecting all diagrams in fig. 21, which amounts to an $\mathcal{O}(\lambda^0)$ approximation. The gap equation gives

$$\mathcal{G}(x,y) = \mathcal{D}(x,y) \tag{6.68}$$

In that case the fourth term on the right hand side of eq. (6.65) is neglected, the third term is identically zero and the second term reproduces the one-loop correction to the tree level potential. In summary, this approximation leads to the one loop effective potential.

To be consistent with the approximation worked out in section 6.2 we will truncate $V^{\beta}_{(2)}$ to $\mathcal{O}(\lambda)$, *i.e.* we will consider only the figure eight diagram and disregard the sunset diagram [22]. In this approximation, and after making the Wick rotation (2.25), the effective potential (6.65) can be written as

$$\begin{aligned} V^{\beta}_{\rm eff}(\phi,\mathcal{G}) &= V_0(\phi) + \frac{1}{2}T\sum_n\int_k \log\mathcal{G}^{-1}(k) + \frac{1}{2}T\sum_n\int_k\left[\mathcal{D}^{-1}(\phi;k)\mathcal{G}(k) - 1\right] \\ &+ \frac{3}{4}\lambda T\sum_n\int_k \mathcal{G}(k) T\sum_m\int_p \mathcal{G}(p) \end{aligned} \tag{6.69}$$

and the gap equation (6.66) as

$$\mathcal{G}^{-1}(p) = \mathcal{D}^{-1}(p) + 3\lambda T\sum_n\int_k \mathcal{G}(k) \tag{6.70}$$

In fact the gap equation (6.70) is represented diagrammatically by eq. (6.14) when the last diagram is disregarded, as we are doing in our approximation.

We will use for Fourier transformed propagators the *Ansatz*

$$\begin{aligned} \mathcal{G}(p) &= \frac{1}{p^2+M^2} \\ \mathcal{D}(\phi;p) &= \frac{1}{p^2+3\lambda\phi^2-m^2} \end{aligned} \tag{6.71}$$

where the *effective mass* M is an unknown function of the momentum to be determined from the gap equations.

Replacing the gap equation (6.70) into the effective potential (6.69) we obtain

$$V^{\beta}_{\rm eff}(\phi,M) = V_0(\phi) + \frac{1}{2}T\sum_n\int_k \log(k^2+M^2) - \frac{3}{4}\lambda T\sum_n\int_k \mathcal{G}(k) T\sum_m\int_p \mathcal{G}(p) \tag{6.72}$$

[22] Methods leading to consider diagrams with overlapping momenta, in particular the sunset diagram of fig. 21 can be found in [49].

Notice that eq. (6.72) agrees to $\mathcal{O}(\lambda)$ with the diagrammatic equation (6.36) obtained in the section 6.2. Also the gap equation (6.70) can be written as

$$M^2 = 3\lambda\phi^2 - m^2 + 3\lambda T \sum_n \int_p \mathcal{G}(p) \tag{6.73}$$

The last term in (6.72) and (6.73) can be computed using the rules of the imaginary time formalism described in section 3.4. A high temperature expansion (in powers of M/T) of it yields

$$T\sum_n \int_p \mathcal{G}(p) = T^2\left[\frac{1}{12} - \frac{1}{4\pi}\frac{M}{T} + \mathcal{O}(\frac{M^2}{T^2})\right] \tag{6.74}$$

Using now (6.74) in (6.72) we can write the field dependent part of the effective potential as

$$\begin{aligned} V_{\rm eff}^{\beta}(\phi, M) &= V_0(\phi) + \frac{M^2T^2}{24} - \frac{M^3T}{12\pi} + \mathcal{O}\left(M^4 \log\frac{M^2}{T^2}\right) \\ &- \frac{3\lambda}{4}\left[-\frac{MT^3}{24\pi} + \frac{M^2T^2}{16\pi^2} + \mathcal{O}(M^4\log\frac{M^2}{T^2})\right] \end{aligned} \tag{6.75}$$

On the other hand, we can replace eq. (6.74) into the gap equation (6.73) as

$$M^2 = \mathcal{M}^2 - \frac{3\lambda}{4\pi}TM \tag{6.76}$$

where the Debye mass is defined in eq. (6.41). By iteratively solving eq. (6.76) we obtain,

$$M^3 = \mathcal{M}^3 - \frac{9\lambda}{8\pi}\mathcal{M}^2T \tag{6.77}$$

which, once replaced into eq. (6.75), gives for the effective potential the same result as that obtained using diagrammatic methods in eq. (6.45).

6.4 The one-loop improved Standard Model

The one-loop effective potential for the Standard Model was described in section 2.5 (at zero temperature) and in section 4.4 (at finite temperature). Higher loop corrections have also an infrared problem for the zero Matsubara modes. In fact, while the masses of the gauge bosons, eq. (2.81), vanish at $\phi = 0$, the masses of the Higgs and Goldstone bosons, eq. (2.80), vanish at $\phi^2 = m^2/3\lambda$ and $\phi^2 = m^2/\lambda$, respectively. Higher loop corrections contribute powers of

$$\begin{aligned} \alpha_{i,\rho} &= \rho\frac{T^2}{m_i^2} \\ \beta_{i,\rho} &= \rho\frac{T}{m_i} \end{aligned} \tag{6.78}$$

which generalize the parameters defined for the scalar theory, eq. (6.13). In eq. (6.78), $i = h, \chi, W, Z$ labels the different bosonic fields in the theory, and $\rho = g^2, g'^2, \lambda$ the different couplings. The first approximation consists in keeping resummation to all orders in $\alpha_{i,\rho}$ and $\mathcal{O}(\beta^0_{i,\rho})$. To this order only diagrams without overlapping momenta or the quadratically divergent part ($\mathcal{O}(T^2)$) of diagrams with overlapping momenta contribute to the polarizations in the corresponding gap equations.

Plasma effects in the leading approximation can be accounted by the one-loop effective potential improved by the daisy diagrams [16, 15, 42]. Imposing renormalization conditions preserving the tree level values of $v^2 \equiv m^2/\lambda$, as in section 2.5.5, and working in the 't Hooft-Landau gauge, the ϕ-dependent part of the effective potential can be written in the high-temperature expansion as

$$V_{\rm eff}(\phi, T) = V_{\rm tree} + \Delta V_B + \Delta V_F \tag{6.79}$$

where

$$\Delta V_B = \sum_{i=h,\chi,W_L,Z_L,\gamma_L,W_T,Z_T,\gamma_T} g_i \Delta V_i \tag{6.80}$$

$$\Delta V_i = \left\{ \frac{m_i^2(\phi)T^2}{24} - \frac{\mathcal{M}_i^3(\phi)T}{12\pi} - \frac{m_i^4(\phi)}{64\pi^2}\left[\log\frac{m_i^2(v)}{c_B T^2} - 2\frac{m_i^2(v)}{m_i^2(\phi)} + \delta_{i\chi}\log\frac{m_h^2(v)}{m_i^2(v)}\right]\right\}, \tag{6.81}$$

where the last term comes from the infinite running of the Higgs mass from $p^2 = 0$ to $p^2 = m_h^2$ and cancels the logarithmic infinity from the massless Goldstone bosons at the zero temperature minimum, and

$$\Delta V_F = g_t \left\{ \frac{m_t^2(\phi)T^2}{48} + \frac{m_t^4(\phi)}{64\pi^2}\left[\log\frac{m_t^2(v)}{c_F T^2} - 2\frac{m_t^2(v)}{m_t^2(\phi)}\right]\right\} \tag{6.82}$$

The number of degrees of freedom g_i in (6.80,6.82) are given by

$$\begin{gathered} g_h = 1,\ g_\chi = 3,\ g_t = 12 \\ \tfrac{1}{2}g_{W_L} = g_{Z_L} = g_{\gamma_L} = 1,\ \tfrac{1}{2}g_{W_T} = g_{Z_T} = g_{\gamma_T} = 2 \end{gathered} \tag{6.83}$$

while the coefficients c_B and c_F in (6.81,6.82) are defined by: $\log c_B = 3.9076$, $\log c_F = 1.1350$.

The masses $m_i^2(\phi)$ in (6.81), (6.82) are defined in (2.80), (2.81) and (2.82), and the Debye masses $\mathcal{M}_i^2$ in (6.81) for $i = h, \chi, W_L, W_T, Z_T, \gamma_T$ are

$$\mathcal{M}_i^2 = m_i^2(\phi) + \Pi_i(\phi, T) \tag{6.84}$$

where the self-energies $\Pi_i(\phi, T)$ are given by

$$\Pi_h(\phi, T) = \left(\frac{3g^2 + g'^2}{16} + \frac{\lambda}{2} + \frac{h_t^2}{4}\right)T^2 \tag{6.85}$$

$$\Pi_\chi(\phi,T)=\left(\frac{3g^2+g'^2}{16}+\frac{\lambda}{2}+\frac{h_t^2}{4}\right)T^2 \tag{6.86}$$

$$\Pi_{W_L}(\phi,T)=\frac{11}{6}g^2T^2 \tag{6.87}$$

$$\Pi_{W_T}(\phi,T)=\Pi_{Z_T}(\phi,T)=\Pi_{\gamma_T}(\phi,T)=0 \tag{6.88}$$

The Debye masses $\mathcal{M}_i^2$ for $i=Z_L,\gamma_L$ are given by

$$\begin{pmatrix}\mathcal{M}_{Z_L}^2 & 0\\ 0 & \mathcal{M}_{\gamma_L}^2\end{pmatrix}=R(\theta_W^{(1)})\begin{pmatrix}m_Z^2(\phi)+\Pi_{Z_LZ_L} & \Pi_{Z_L\gamma_L}\\ \Pi_{\gamma_LZ_L} & \Pi_{\gamma_L\gamma_L}\end{pmatrix}R^{-1}(\theta_W^{(1)}) \tag{6.89}$$

with the rotation $R(\theta_W^{(1)})$

$$R(\theta_W^{(1)})=\begin{pmatrix}\cos\theta_L^{(1)} & -\sin\theta_L^{(1)}\\ \sin\theta_L^{(1)} & \cos\theta_L^{(1)}\end{pmatrix} \tag{6.90}$$

and the self-energies

$$\begin{aligned}\Pi_{Z_LZ_L}(\phi,T) &= \left(\frac{2}{3}g^2\cos^2\theta_W+\frac{1}{6}\frac{g^2}{\cos^2\theta_W}(1-2\sin^2\theta_W\cos^2\theta_W)\right.\\ &\left.+\frac{g^2}{\cos^2\theta_W}(1-2\sin^2\theta_W+\frac{8}{3}\sin^4\theta_W)\right)T^2\end{aligned} \tag{6.91}$$

$$\Pi_{\gamma_L\gamma_L}(\phi,T)=\frac{11}{3}e^2T^2 \tag{6.92}$$

$$\Pi_{\gamma_LZ_L}(\phi,T)=\frac{11}{6}eg\frac{\cos^2\theta_W-\sin^2\theta_W}{\cos\ \theta_W}T^2 \tag{6.93}$$

The angle $\theta_L^{(1)}$ in (6.89) is the one-loop temperature dependent correction to the electroweak angle. In fact the angle $\theta_L(\phi,T)$ defined by

$$\theta_L(\phi,T)=\theta_W+\theta_L^{(1)} \tag{6.94}$$

maps (W_3,B) into (Z,γ).

Using (6.91-6.93) one obtains the eigenvalues and rotation angle in (8.6) as:

$$\mathcal{M}_{Z_L}^2=\frac{1}{2}\left[m_Z^2(\phi)+\frac{11}{6}\frac{g^2}{\cos^2\theta_W}T^2+\Delta(\phi,T)\right] \tag{6.95}$$

$$\mathcal{M}_{\gamma_L}^2=\frac{1}{2}\left[m_Z^2(\phi)+\frac{11}{6}\frac{g^2}{\cos^2\theta_W}T^2-\Delta(\phi,T)\right] \tag{6.96}$$

$$\sin\ 2\theta_L^{(1)}(\phi,T)=-\frac{2\Pi_{\gamma_LZ_L}}{\Delta} \tag{6.97}$$

$$\sin\ 2\theta_L(\phi,T) = \sin\ 2\theta_W \frac{m_Z^2(\phi)}{\Delta(\phi,T)} \tag{6.98}$$

with

$$\Delta^2(\phi,T) = m_Z^4(\phi) + \frac{11}{3}\frac{g^2\cos^2 2\theta_W}{\cos^2\theta_W}\left[m_Z^2(\phi) + \frac{11}{12}\frac{g^2}{\cos^2\theta_W}T^2\right]T^2 \tag{6.99}$$

It is clear from (6.98,6.99) that at zero temperature the electroweak angle coincides with the usual one: $\Delta(\phi,0) = m_Z^2(\phi)$, $\theta_L(\phi,0) \equiv \theta_W$.

7 Baryogenesis at phase transitions

7.1 Introduction

There are two essential problems to be understood related with the baryon number of the universe:

i) There is no evidence of antimatter in the universe. In fact, there is no antimatter in the solar system, and only $\overline{p}$ in cosmic rays. However antiprotons can be produced as secondaries in collisions ($pp \rightarrow 3p + \overline{p}$) at a rate similar to the observed one. Numerically,

$$\frac{n_{\overline{p}}}{n_p} \sim 3 \times 10^{-4}$$

and

$$\frac{n_{^4He}}{n_{^4\overline{He}}} \sim 10^{-5}$$

We can conclude that $n_B \gg n_{\overline{B}}$, so $n_{\Delta B} \equiv n_B - n_{\overline{B}} \sim n_B$.

ii) The second problem is to understand the origin of

$$\eta \equiv \frac{n_B}{n_\gamma} \sim (0.3 - 1.0) \times 10^{-9} \tag{7.1}$$

today. This parameter is essential for primordial nucleosynthesis [57].

η may not have changed since nucleosynthesis. At these energy scales ($\sim$ 1 MeV) baryon number is conserved if there are no processes which would have produced entropy to change the photon number. We can easily estimate η.

The baryon number density is,

$$n_B = \frac{\rho_B}{m_B} = \frac{\Omega_B \rho_c}{m_B} \tag{7.2}$$

where ρ_B is the baryonic energy density and $\Omega_B = \rho_B/\rho_c$. Using the critical density,

$$\rho_c = 3H_o^2 = 1.88 \times 10^{-29} h^2 gr\ cm^{-3} \tag{7.3}$$

where H_o is the Hubble parameter today and

$$h = H_o/100\ km\ Mpc^{-1} sec^{-1}$$

is

$$\frac{1}{2} \leq h \leq 1,$$

one obtains,

$$n_B = 1.1 \times 10^{-5} h^2 \Omega_B cm^{-3} \tag{7.4}$$

On the other hand, the energy density of photons is given by

$$n_\gamma = \int dn_\gamma \tag{7.5}$$

where

$$dn_\gamma = \frac{g_\gamma}{2\pi^2} \frac{1}{e^{E_\gamma/T} - 1} q^2 dq \tag{7.6}$$

with $g_\gamma = 2$ (the number of degrees of freedom of photons), and $E_\gamma = q$. Using the integral [7]

$$\int_0^\infty \frac{x^{\nu-1}}{e^{\mu x} - 1} dx = \mu^{-\nu} \Gamma(\nu) \zeta(\nu) \tag{7.7}$$

where

$$\zeta(\nu) = \sum_{n=1}^{\infty} \frac{1}{n^\nu} \tag{7.8}$$

we obtain

$$n_\gamma = \frac{2\zeta(3)}{\pi^2} T^3 \tag{7.9}$$

where [7] $\zeta(3) = 1.20$. Using now the equivalence,

$$(2.735\ K)^3 = 1.71 \times 10^3 cm^{-3}$$

we can write

$$n_\gamma = 415 \left[\frac{T_o}{2.735}\right]^3 cm^{-3} \tag{7.10}$$

where T_o is the present temperature of the background radiation.

Putting (7.4) and (7.10) together we obtain

$$\eta = 2.65 \times 10^{-8} \Omega_B h^2 \left[\frac{2.735}{T_o}\right]^3 \tag{7.11}$$

However, the range of η consistent with D and ^3He primordial abundances is [57]

$$4(3) \leq 10^{10}\eta \leq 7(10) \tag{7.12}$$

where the most conservatives bounds are given in parenthesis. From (7.11) we obtain Ω_B as a function of η

$$\Omega_B = 3.77 \times 10^7 \eta h^2 \left[\frac{T_o}{2.735}\right]^3 \tag{7.13}$$

Now, using the range (7.12) for η and for h we obtain,

$$\begin{aligned} 0.015(0.011) \leq \quad \Omega_B h^2 \quad &\leq 0.026(0.038) \\ 0.015(0.011) \leq \quad \Omega_B \quad &\leq 0.16(0.21) \end{aligned} \tag{7.14}$$

where, as in (7.12) the most conservatives bounds are in parenthesis [23].

Sometimes it is useful to describe baryon asymmetry in terms of n_B/s instead of n_B/n_γ. Let us give the relationship between s and n_γ. From (7.9),

$$s = \frac{2\pi^2}{45} g_{\text{eff}}(T) T^3 = \frac{\pi^4}{45\zeta(3)} g_{\text{eff}}(T) n_\gamma \tag{7.15}$$

$$g_{\text{eff}} = g_{\text{eff}\gamma} + \left[\frac{T_\nu}{T_\gamma}\right]^3 g_{\text{eff}\nu} = 2 + \frac{4}{11} \times \frac{7}{4} \times 3 = 3.91 \tag{7.16}$$

In this way,

$$s = \frac{\pi^4}{45\zeta(3)} 3.91 \; n_\gamma = 7.04 \; n_\gamma \tag{7.17}$$

and the range (7.12) translates into

$$5.7(4.3) \leq \frac{n_B}{s} 10^{11} \leq 9.9(14) \tag{7.18}$$

Can we explain the value of η, eq. (7.12), in the standard cosmological model? Suppose that initially $n_{\Delta B} = 0$ exactly, so $\eta = 0$, and we can compute the final number density of nucleons left over after annihilations have frozen out. For $T < 1 \; GeV$ the equilibrium abundance of nucleons and antinucleons is [57]

$$\frac{n_B}{n_\gamma} \simeq \frac{n_{\overline{B}}}{n_\gamma} \simeq \left[\frac{m_B}{T}\right]^{3/2} e^{-\frac{m_B}{T}} \tag{7.19}$$

where $m_B \sim 1 \; GeV$.

[23] If the idea of inflation is correct, then $\Omega = 1$ and other form of matter has to exist in large quantities to close the universe. This matter (neutrinos, photinos, sneutrinos, axions, MACHOS,...) is called *dark matter*.

When the universe cooled, the number of nucleons and antinucleons decreased as long as the annihilation rate $\Gamma_{\rm ann}$ was larger than H. At

$$T_f \simeq 20\ MeV$$

$\Gamma_{\rm ann} \simeq H$ and annihilations freeze out, nucleons and antinucleons being so rare that they can no longer annihilate. Therefore, from (7.19) we obtain,

$$\frac{n_B}{n_\gamma} \sim \frac{n_{\overline{B}}}{n_\gamma} \sim 10^{-18} \tag{7.20}$$

which is much smaller than the value (7.12) required for nucleosynthesis, as well as one obtains $n_B \simeq n_{\overline{B}}$.

In conclusion, in the standard cosmological model there is no explanation for the smallness of the ratio (7.12) if we start from $n_{\Delta B} = 0$. An initial asymmetry has to be imposed by hand as an initial condition (which violates any naturalness principle) or dynamically generated at phase transitions, which is the way we will explore all along this section.

7.2 Conditions for baryogenesis

As we have seen in the previous subsection the universe was initially baryon symmetric ($n_B \simeq n_{\overline{B}}$) although the matter-antimatter asymmetry appears to be large today ($n_{\Delta B} \simeq n_B \gg n_{\overline{B}}$). In the standard cosmological model there is no explanation for the value of η consistent with nucleosynthesis, eq. (7.12), and it has to be imposed by hand as an initial condition. However, it was suggested by Sakharov long ago [58] that a tiny $n_{\Delta B}$ might have been produced in the early universe leading, after $p\overline{p}$ annihilations, to (7.12). The three ingredients necessary for baryogenesis are:

7.2.1 B-nonconserving interactions

This condition is obvious since we want to start with a baryon symmetric universe ($\Delta B = 0$) and evolve it to a universe where $\Delta B \neq 0$. B-nonconserving interactions might mediate proton decay; in that case the phenomenological constraints are provided by the proton lifetime measurements [59] $\tau_p \gtrsim 10^{32} yr$.

7.2.2 C and CP violation

The action of C (charge conjugation) and CP (combined action of charge conjugation and parity) interchange particles with antiparticles, changing therefore the sign of B. For instance if we describe spin-$\frac{1}{2}$ fermions by two-component fields of definite chirality (left-handed fields ψ_L and right-handed fields ψ_R) the action of C and CP over them is given by

$$\begin{aligned} P &: \psi_L \longrightarrow \psi_R, \quad \psi_R \longrightarrow \psi_L \\ C &: \psi_L \longrightarrow \psi_L^C \equiv \sigma_2 \psi_R^*, \quad \psi_R \longrightarrow \psi_R^C \equiv -\sigma_2 \psi_L^* \\ CP &: \psi_L \longrightarrow \psi_R^C, \quad \psi_R \longrightarrow \psi_L^C \end{aligned} \tag{7.21}$$

If the universe is initially matter-antimatter symmetric, and without a preferred direction of time as in the standard cosmological model, it is represented by a C and CP invariant state, $|\phi_o\rangle$, with $B = 0$. If C and CP were conserved, *i.e.*

$$[C, H] = [CP, H] = 0 \tag{7.22}$$

H being the hamiltonian, then the state of the universe at a later time t,

$$|\phi(t)\rangle = e^{iHt}|\phi_o\rangle \tag{7.23}$$

would be C and CP invariant and, therefore, baryon number conserving, $\Delta B = 0$. The only way to generate a net $\Delta B \neq 0$ is to have C and CP violating interactions.

7.2.3 Departure from thermal equilibrium

If all particles in the universe remained in thermal equilibrium, then no direction for time would be defined and CPT invariance would prevent the appearance of any baryon excess, rendering CP violating interactions irrelevant [60].

A particle species is in thermal equilibrium if all its reaction rates, Γ, are much faster than the expansion rate of the universe, H. On the other hand a departure from thermal equilibrium is expected whenever a rate crucial for maintaining it is less than the expansion rate ($\Gamma < H$). Deviation from thermal equilibrium cannot occur in a homogeneous isotropic universe containing only massless species: massive species are needed in general for such deviations to occur.

The number density of a particle species p in thermal equilibrium, for $T \gg m_p$, is given by,

$$n_p \simeq g_{\text{eff}} \left(m_p T\right)^{3/2} e^{-\frac{m_p}{T} + \frac{\mu_p}{T}} \tag{7.24}$$

where μ_p is the chemical potential. In general, if the species A, B, C, D are in chemical equilibrium through the reaction

$$A + B \longleftrightarrow C + D,$$

we have

$$\mu_A + \mu_B = \mu_C + \mu_D.$$

In this way the number density in thermal equilibrium of the antiparticle $\overline{p}$ ($m_{\overline{p}} = m_p$) is

$$n_{\overline{p}} \simeq g_{\rm eff} \left(m_p T\right)^{3/2} e^{-\frac{m_p}{T} - \frac{\mu_p}{T}} \tag{7.25}$$

where we have used that $\mu_{\overline{p}} = -\mu_p$ by the presence of processes as

$$p\overline{p} \longleftrightarrow \gamma\gamma$$

and $\mu_\gamma = 0$. If p carries a baryon number B, then from (7.24) and (7.25),

$$n_{\Delta B} = B(n_p - n_{\overline{p}}) = 2B g_{\rm eff} \left(m_p T\right)^{3/2} e^{-\frac{m_p}{T}} \sinh\left[\frac{\mu_p}{T}\right] \tag{7.26}$$

If $p, \overline{p}$ undergo the B-violating reactions

$$pp \longleftrightarrow \overline{p}\overline{p}$$

then $\mu_p = 0$ and $n_{\Delta B} = 0$. Only a departure from chemical equilibrium, *i.e.* from distributions (7.24) and (7.25) can allow for a finite baryon excess, $n_{\Delta B} \neq 0$.

7.3 The standard out-of-equilibrium decay scenario

The so-called standard scenario [61] is the out-of-equilibrium decay mechanism, which incorporates the three above requirements and that will be described in what follows.

Let X_1 be a superheavy boson (vector or scalar) coupled to light fermions with strength $\alpha^{1/2}$ (where $\alpha^{1/2}$ is either a gauge or a Yukawa coupling). Then from dimensional analysis its decay rate is given by,

$$\Gamma_1 \sim \alpha M_1 \tag{7.27}$$

where M_1 is the mass of X_1. Notice that here we are assuming that X_1 is coupled by renormalizable interactions (gauge or Yukawa interactions). However, it is also interesting to study the case of a gauge singlet scalar boson X_2, coupled to light matter only through

gravitational interactions. This is the case of a singlet in the hidden sector of supergravity models [62]. In this case, the decay rate of X_2 is, from dimensional analysis,

$$\Gamma_2 \sim M_2^3/M_{P\ell}^2 \tag{7.28}$$

where M_2 is the mass of X_2. We will study in parallel both cases, just considering X_i, Γ_i and M_i, for i=1,2.

At the Planck time ($T \sim M_{P\ell}$) we assume all particle species are in thermal equilibrium, *i.e.* $n_{X_i} = n_{\overline{X}_i} \simeq n_\gamma$ (up to statistical factors), and $n_{\Delta B} = 0$. Since we are assuming $M_i < M_{P\ell}$, nothing interesting happens until $T \simeq M_i$.

At $T \lesssim M_i$ the equilibrium abundance of X_i and $\overline{X}_i$ relative to photons is, see eq. (7.19),

$$\frac{n_{X_i}}{n_\gamma} \simeq \frac{n_{\overline{X}_i}}{n_\gamma} \simeq \left[\frac{M_i}{T}\right]^{3/2} e^{-\frac{M_i}{T}} \tag{7.29}$$

where we have neglected the chemical potential μ_i. Then for X_i and $\overline{X}_i$ to maintain their equilibrium abundances, they must be able to diminish their number rapidly (with respect to $H(T)$). The most efficient way of doing it is by decay, their decay rates Γ_i in (7.27) and (7.28) being the keystone for thermal equilibrium.

♠ First, if the decay rate is

$$\Gamma_i \gg H(M_i), \tag{7.30}$$

then X_i and $\overline{X}_i$ will adjust their abundances by decay to their equilibrium abundance and no baryogenesis can be induced by X_i and $\overline{X}_i$ decays. In that case, using (7.27) and (7.28) and

$$H(T) \sim g_{\text{eff}}^{1/2} \frac{T^2}{M_{P\ell}}$$

condition (7.30) is equivalent, for the strongly coupled X_1 and $\overline{X}_1$, to

$$M_1 \ll g_{\text{eff}}^{-1/2} \alpha M_{P\ell} \tag{7.31}$$

and for gravitationally (weakly) coupled X_2 and $\overline{X}_2$, to

$$M_2 \gg g_{\text{eff}}^{1/2} M_{P\ell} \tag{7.32}$$

Obviously, condition (7.32) will never be satisfied for $M_2 \lesssim M_{P\ell}$.

♢ Second, if the decay rate

$$\Gamma_i < H(M_i) \tag{7.33}$$

then, X_i and $\overline{X}_i$ cannot decay on the expansion timescale H and **so remain as abundant as photons for** $T \lesssim M_i$. This **overabundance** (with respect to their equilibrium abundance) is the **departure from the thermal equilibrium.** In that case, condition (7.33) is equivalent, for strongly coupled X_1 and $\overline{X}_1$, to

$$M_1 > g_{\rm eff}^{-1/2} \alpha M_{P\ell} \tag{7.34}$$

and, for gravitationally coupled X_2 and $\overline{X}_2$, to

$$M_2 < g_{\rm eff}^{1/2} M_{P\ell} \tag{7.35}$$

It is clear that condition (7.35) is always satisfied, while condition (7.34) is based on the smallness of $g_{\rm eff}^{-1/2}\alpha$. In particular, if X_1 is a gauge boson, α can be in the range between 10^{-1} and 2.5×10^{-2}, while $g_{\rm eff}$ can be in the range between 3×10^2 and 10^2. In this way we obtain, from (7.34) that condition (7.33) can be satisfied for

$$M_1 > (10^{-3} - 10^{-4}) M_{P\ell} \sim (10^{16} - 10^{15})\ GeV \tag{7.36}$$

If X_1 is a scalar, its coupling α_Y is proportional to the squared mass of a fermion,

$$\alpha_Y \sim \left(\frac{m_f}{m_W}\right)^2 \alpha,$$

typically in the range $(10^{-2} - 10^{-7})$, from where

$$M_1 > (10^{-3} - 10^{-8})\ M_{P\ell} \sim (10^{16} - 10^{10})\ GeV \tag{7.37}$$

Obviously, condition (7.37) is more easily satisfied than condition (7.36). In general, baryogenesis is more easily produced by scalars than by bosons. On the other hand, as we have said above, condition (7.35) for gravitationally interacting particles is automatically satisfied for any mass M_2 below the Planck scale.

Later on, at T_D, when

$$\Gamma_i \simeq H(T_D) \tag{7.38}$$

i.e. at

$$T_D \sim g_{\rm eff}^{-1/4} \alpha^{1/2} (M_1 M_{P\ell})^{1/2} < M_1 \tag{7.39}$$

the last inequality coming from (7.34), or,

$$T_D \sim g_{\rm eff}^{-1/4} M_2 \left(\frac{M_2}{M_{P\ell}}\right)^{1/2} < M_2, \tag{7.40}$$

the last inequality coming from (7.35), X_i and $\overline{X}_i$ will start to decay and decrease their number. If their decay violate baryon number, as we are assuming, they will generate a net baryon number per decay.

Suppose, to fix the ideas, that X has two decay channels a and b, with baryon numbers B_a and B_b, respectively. Correspondingly, the decay channels of $\overline{X}$, $\overline{a}$ and $\overline{b}$, have baryon numbers $-B_a$ and $-B_b$, respectively. Let $r(\overline{r})$ be the branching ratio of $X(\overline{X})$ in channel $a(\overline{a})$, and $1-r(1-\overline{r})$ the branching ratio of $X(\overline{X})$ in channel $b(\overline{b})$,

$$\begin{aligned} r &= \frac{\Gamma(X \longrightarrow a)}{\Gamma_X} \\ \overline{r} &= \frac{\Gamma(\overline{X} \longrightarrow \overline{a})}{\Gamma_X} \\ 1-r &= \frac{\Gamma(X \longrightarrow b)}{\Gamma_X} \\ 1-\overline{r} &= \frac{\Gamma(\overline{X} \longrightarrow \overline{b})}{\Gamma_X} \end{aligned} \tag{7.41}$$

where we are using equality between the total decay rates of X and $\overline{X}$ (CPT+unitarity). The mean net baryon number produced in X-decays is

$$rB_a + (1-r)B_b$$

and that produced in $\overline{X}$-decays is

$$-\overline{r}B_a - (1-\overline{r})B_b.$$

Finally, the mean net baryon number produced in X and $\overline{X}$-decays is

$$\Delta B = (r-\overline{r})B_a + [(1-r)-(1-\overline{r})]\,B_b = (r-\overline{r})(B_a - B_b) \tag{7.42}$$

Equation (7.42) can be generalized to the case when $X(\overline{X})$ can decay to a set of final states $f_n(\overline{f}_n)$ with baryon number $B_n(-B_n)$. In that case, the net baryon number per decay is

$$\Delta B = \frac{1}{\Gamma_X}\sum_n B_n \left[\Gamma(X \longrightarrow f_n) - \Gamma(\overline{X} \longrightarrow \overline{f}_n)\right] \tag{7.43}$$

At the decay temperature $T_D < M_i$ the inverse decay processes are greatly suppressed with respect to the direct decay,

$$\Gamma(f_n \longrightarrow X_i) \simeq e^{-\frac{M_i}{T_D}}\Gamma(X_i \longrightarrow f_n) \tag{7.44}$$

and thus the net baryon number produced per decay ΔB is not destroyed by the net baryon number produced per inverse decay $-\Delta B$. At T_D,

$$n_{X_i} = n_{\overline{X}_i} \simeq n_\gamma$$

and therefore the net baryon number density produced is

$$n_{\Delta B} = \Delta B \; n_{X_i} \tag{7.45}$$

from where we see that ΔB coincides with the parameter η defined in (7.1) if $n_{X_i} \simeq n_\gamma$.

The three ingredients of baryogenesis can be easily traced back here:

- If B is not violated, then $B_n = 0$ and $\Delta B = 0$.
- If C and CP are not violated, then $\Gamma(X \longrightarrow f_n) = \Gamma(\overline{X} \longrightarrow \overline{f}_n)$, and also $\Delta B = 0$.
- In thermal equilibrium, the inverse decay processes are not suppressed and the net baryon number generated per decay is cancelled by inverse decays.

We have assumed to obtain (7.45) that $n_{X_i} \simeq n_\gamma$ at the decay temperature T_D. However, the entropy release in X_i-decays can be very important (especially if the X_i decay very late, $T_D \ll M_i$) and has to be taken into account. In that case, neglecting the initial entropy and assuming that the energy density at T_D,

$$\rho_{X_i} \simeq M_i n_{X_i}$$

is converted into radiation at the reheating temperature T_{RH}

$$\rho = \frac{\pi^2}{30} g_{\text{eff}} T_{RH}^4$$

we obtain,

$$n_{X_i} \simeq \frac{\pi^2}{30} g_{\text{eff}} \frac{T_{RH}^4}{M_i} \tag{7.46}$$

and, using (7.9), (7.15) and (7.45) we can write the baryon-to-entropy ratio as,

$$\frac{n_{\Delta B}}{s} \simeq \frac{3}{4} \frac{T_{RH}}{M_i} \Delta B \tag{7.47}$$

We can now relate T_{RH} with the decay rate Γ_i using the decay condition

$$\Gamma_i^2 \simeq H^2(T_D) \simeq \frac{\rho_{X_i}}{3 M_{P\ell}^2}$$

and so write (7.47) as

$$\frac{n_{\Delta B}}{s} = \beta \left(\frac{g_{\text{eff}}^{-1/2} \Gamma_i M_{P\ell}}{M_i^2} \right)^{1/2} \Delta B \tag{7.48}$$

where the coefficient β is

$$\beta = \left(\frac{90}{\pi^2}\right)^{1/4} \sim 1.7 \tag{7.49}$$

Now we can replace the values of Γ_i (i=1,2). For the case of strongly decaying (through renormalizable interactions) bosons X_1, eq. (7.27) leads to

$$\frac{n_{\Delta B}}{s} = \beta \left[\frac{g_{\rm eff}^{-1/2}\alpha M_{P\ell}}{M_1}\right]^{1/2} \Delta B \tag{7.50}$$

and for the case of weakly decaying (through gravitational interactions) bosons X_2, eq. (7.28) leads to

$$\frac{n_{\Delta B}}{s} = \beta \left[\frac{M_2}{g_{\rm eff}^{1/2} M_{P\ell}}\right]^{1/2} \Delta B \tag{7.51}$$

In both cases, eqs. (7.50) and (7.51), the conditions (7.34) and (7.35), respectively, guarantee that the numerical coefficients in front of ΔB are smaller (even much smaller) than unity and the net baryon number per decay has to be larger than that initially thought to be necessary to explain the condition (7.18).

The quantitative analysis of the out-of-equilibrium decay scenario, including the Boltzmann equations for the evolution of η, has been performed in ref. [60, 63, 64]. The numerical analysis essentially confirms the qualitative picture we have described, the only difference being that the asymmetry does not fall off that rapidly with $K = \Gamma_i/H(M_i)$ until $K \gg 1$.

7.4 Baryogenesis at the electroweak phase transitions

Baryogenesis can be generated at the GUT phase transition. This possibility suffers, however, from two serious drawbacks:

- If there is a period of cosmological inflation of the universe, any pre-existing baryon asymmetry would be washed out by the exponential expansion of the universe. In many cases, the reheating temperature after inflation is not as high as the unification scale (poor reheating) and so baryon asymmetry cannot be regenerated by the GUT phase transition.

- There is no experimental evidence of any GUT, and so baryon asymmetry generation at the GUT phase transition rely on parameters which cannot be experimentally tested.

It has been recently realized [65, 66] that the three Sakharov's conditions for baryogenesis, sections 7.2.1, 7.2.2 and 7.2.3, can be fulfilled at the electroweak phase transition:

- Baryonic charge non-conservation was discovered by 't Hooft [67]. In fact baryon and lepton number are conserved anomalous global symmetries in the Standard Model. They are violated by non-perturbative effects.
- CP violation can be generated in the Standard Model from phases in the fermion mass matrix, Cabibbo, Kobayashi, Maskawa (CKM) phases [68]. This effect is much too small to explain the observed baryon to entropy ratio. However, in extensions of the Standard Model, as the singlet majoron model or the minimal supersymmetric standard model (MSSM), a sizeable CP violation can happen through an extended Higgs sector.
- The out of equilibrium condition can be achieved, if the phase transition is strong enough first order, in the bubble walls. In that case the B-violating interactions are out of equilibrium in the bubble walls and a net B-number can be generated during the phase transition.

7.4.1 Baryon and lepton number violation in the electroweak theory

Violation of baryon and lepton number in the electroweak theory is a very striking phenomenon. Classically, baryonic and leptonic currents are conserved in the electroweak theory. However, that conservation is spoiled by quantum corrections through the chiral anomaly associated with triangle fermionic loop in external gauge fields. The calculation gives,

$$\partial_\mu j^\mu_B = \partial_\mu j^\mu_L = N_f \left(\frac{g^2}{32\pi^2} W\tilde{W} - \frac{g'^2}{32\pi^2} Y\tilde{Y} \right) \tag{7.52}$$

where N_f is the number of fermion generations, $W_{\mu\nu}$ and $Y_{\mu\nu}$ are the gauge field strength tensors for $SU(2)$ and $U(1)_Y$, respectively, and the tilde means the dual tensor,

$$\tilde{W}^{\mu\nu} = \frac{1}{2}\epsilon^{\mu\nu\alpha\beta} W_{\alpha\beta}.$$

A very important feature of (7.52) is that the difference $B - L$ is strictly conserved, and so only the sum $B + L$ is anomalous and can be violated. Another feature is that fluctuations of the gauge field strengths can lead to fluctuations of the corresponding value of $B + L$. The product of gauge field strengths on the right hand side of eq. (7.52) can be written as

four-divergences,

$$\begin{aligned} W\tilde{W} &= \partial_\mu k_W^\mu \\ Y\tilde{Y} &= \partial_\mu k_Y^\mu \end{aligned} \tag{7.53}$$

where

$$\begin{aligned} k_Y^\mu &= \epsilon^{\mu\nu\alpha\beta} Y_{\nu\alpha} Y_\beta \\ k_W^\mu &= \epsilon^{\mu\nu\alpha\beta} \left(W_{\nu\alpha}^a W_\beta^a - \frac{g}{3} \epsilon_{abc} W_\nu^a W_\alpha^b W_\beta^c \right) \end{aligned} \tag{7.54}$$

and W_μ, Y_μ are the gauge fields of $SU(2)$ and $U(1)_Y$, respectively. In general total derivatives are unobservable because they can be integrated by parts and drop from the integrals. This is true for the terms in the four-vectors (7.54) proportional to the field strengths $W_{\mu\nu}$ and $Y_{\mu\nu}$ [24]. This means that for the abelian subgroup $U(1)_Y$ the current non conservation induced by quantum effects becomes non observable. However this is not mandatory for gauge fields, for which the integral can be nonzero. Hence only for non-abelian groups can the current non conservation induced by quantum effects become observable. In particular one can write,

$$\Delta B = \Delta L = N_f \Delta N_{CS} \tag{7.55}$$

where N_{CS} is the so-called Chern-Simons number characterizing the topology of the gauge field configuration,

$$N_{CS} = \frac{g^2}{32\pi^2} \int d^3x \epsilon^{ijk} \left(W_{ij}^a W_k^a - \frac{g}{3} \epsilon_{abc} W_i^a W_j^b W_k^c \right) \tag{7.56}$$

Note that though N_{CS} is not gauge invariant, its variation ΔN_{CS} is.

We want to compute now ΔB between an initial and a final configuration of gauge fields. As we have said we are considering (vacuum) field strength tensors $W_{\mu\nu}$ which vanish. The corresponding potentials are not necessarily zero but can be represented by purely gauge fields,

$$W_\mu = -\frac{i}{g} U(x) \partial_\mu U^{-1}(x) \tag{7.57}$$

There are two classes of gauge transformations keeping $W_{\mu\nu} = 0$:

- Continuous transformations of the potentials yielding $\Delta N_{CS} = 0$.
- If one tries to generate $\Delta N_{CS} \neq 0$ by a continuous variation of the potentials, then one has to enter a region where $W_{\mu\nu} \neq 0$. This means that vacuum states with different topological charges are separated by potential barriers.

[24] We are generically interested in cases where initial and final average values of field strengths are zero.

The probability of barrier penetration can be calculated using the quasi-classical approximation as in previous sections. In euclidean space time, the trajectory in field space configuration which connects two vacua differing by a unit of topological charge is called instanton. The euclidean action evaluated at this trajectory gives the probability for barrier penetration as,

$$\Gamma \sim \exp\left(-\frac{4\pi}{\alpha_W}\right) \sim 10^{-162} \tag{7.58}$$

where $\alpha_W = g^2/4\pi$. The number in (7.58) is so small that the calculation of the pre-exponential is unnecessary and the probability for barrier penetration is essentially zero.

7.4.2 Baryon violation at finite temperature: sphalerons

Expression (7.58) gives the probability for barrier penetration at zero temperature. However, in a system with non zero temperature a particle may classically go over the barrier with a probability determined by the Boltzmann exponent, as we have seen in section 5.

What we have is a potential which depend on the gauge field configurations W_μ. This potential has an infinite number of degenerate minima, labeled as Ω_n. These minima are characterized by different values of the Chern-Simons number. The minimum Ω_0 corresponds to the configuration $W_\mu = 0$ and we can take conventionally the value of the potential at this point to be zero. Other minima have gauge fields given by (7.57). In the temporal gauge $W_0 = 0$, the gauge transformation U must be time independent (since we are considering gauge configurations with $W_{\mu\nu} = 0$), *i.e.* $U = U(\vec{x})$, and so functions U define maps,

$$U : S^3 \longrightarrow SU(2)$$

All the minima with $W_{\mu\nu} = 0$ have equally zero potential energy, but those defined by a map $U(\vec{x})$ with nonzero Chern-Simons number

$$n[U] = \frac{1}{24\pi^2}\int d^3x \epsilon^{ijk} Tr(U\partial_i U^{-1} U\partial_j U^{-1} U\partial_k U^{-1}) \tag{7.59}$$

correspond to degenerate minima in the configuration space with non-zero baryon and lepton number.

Degenerate minima are separated by a potential barrier. The field configuration at the top of the barrier is called **sphaleron**, which is a *static unstable* solution to the classic equations of motion [69]. The sphaleron solution has been explicitly computed in ref. [69] for the case of zero Weinberg angle, (*i.e.* neglecting terms $\mathcal{O}(g')$), and for an arbitrary value of $\sin^2\theta_W$ in ref. [70].

An ansatz for the sphaleron solution for the case of zero Weinberg angle was given (for the zero temperature potential) in ref. [69], for the Standard Model with a single Higgs doublet, as,

$$W_i^a \sigma^a dx^i = -\frac{2i}{g} f(\xi) dU\ U^{-1} \tag{7.60}$$

for the gauge field, and

$$\Phi = \frac{v}{\sqrt{2}} h(\xi) U \begin{pmatrix} 0 \\ 1 \end{pmatrix} \tag{7.61}$$

for the Higgs field, where the gauge transformation U is taken to be,

$$U = \frac{1}{r} \begin{pmatrix} z & x+iy \\ -x+iy & z \end{pmatrix} \tag{7.62}$$

and we have introduced the dimensionless radial distance $\xi = gvr$.

Using the ansatz (7.60), (7.61) and (7.62) the field equations reduce to,

$$\begin{aligned} \xi^2 \frac{d^2 f}{d\xi^2} &= 2f(1-f)(1-2f) - \frac{\xi^2}{4} h^2 (1-f) \\ \frac{d}{d\xi}\left(\xi^2 \frac{dh}{d\xi}\right) &= 2h(1-f)^2 + \frac{\lambda}{g^2} \xi^2 (h^2-1)h \end{aligned} \tag{7.63}$$

with the boundary conditions, $f(0) = h(0) = 0$ and $f(\infty) = h(\infty) = 1$. The energy functional becomes then,

$$\begin{aligned} E &= \frac{4\pi v}{g} \int_0^\infty \left\{ 4\left(\frac{df}{d\xi}\right)^2 + \frac{8}{\xi^2}[f(1-f)]^2 + \frac{1}{2}\xi^2 \left(\frac{dh}{d\xi}\right)^2 \right. \\ &+ \left. [h(1-f)]^2 + \frac{1}{4}\left(\frac{\lambda}{g^2}\right) \xi^2 (h^2-1)^2 \right\} d\xi \end{aligned} \tag{7.64}$$

The solution to eqs. (7.63) has to be found numerically. The solutions depend on the gauge and quartic couplings, g and λ. Once replaced into the energy functional (7.64) they give the sphaleron energy which is the height of the barrier between different degenerate minima. It is customary to write the solution as,

$$E_{\rm sph} = \frac{2m_W}{\alpha_W} B(\lambda/g^2) \tag{7.65}$$

where B is the constant which requires numerical evaluation. For the standard model with a single Higgs doublet this parameter ranges from $B(0) = 1.5$ to $B(\infty) = 2.7$. A fit valid for values of the Higgs mass,

$$25\ GeV \leq m_h \leq 250\ GeV$$

can be written as,

$$B(x) = 1.58 + 0.32x - 0.05x^2 \tag{7.66}$$

where $x = m_h/m_W$.

The previous calculation of the sphaleron energy was performed at zero temperature. The sphaleron at finite temperature was computed in ref. [71]. Its energy follows the approximate scaling law,

$$E_{\rm sph}(T) = E_{\rm sph}\frac{\langle\phi(T)\rangle}{\langle\phi(0)\rangle} \tag{7.67}$$

which, using (7.65), can be written as,

$$E_{\rm sph}(T) = \frac{2m_W(T)}{\alpha_W}B(\lambda/g^2) \tag{7.68}$$

where $m_W(T) = \frac{1}{2}g\langle\phi(T)\rangle$

7.4.3 Baryon violation rate at $T > T_c$

The calculation of the baryon violation rate at $T > T_c$, *i.e.* in the symmetric phase, is very different from that in the broken phase, that will be reviewed in the next section. In the symmetric phase, at $\phi = 0$, the perturbation theory is spoiled by infrared divergences, as we saw in section 6, and so we cannot rely upon perturbative calculations to compute the baryon violation rate in this phase. In fact, the infrared divergences are cut off by the non-perturbative generation of a **magnetic mass**,

$$m_M \sim \alpha_W T \tag{7.69}$$

i.e. a **magnetic screening length**, $\xi_M \sim (\alpha_W T)^{-1}$. The rate of baryon violation per unit time and unit volume Γ does not contain any exponential Boltzmann factor [25]. The pre-exponential can be computed from dimensional grounds, [72] as

$$\Gamma = k(\alpha_W T)^4 \tag{7.70}$$

where the coefficient k has been evaluated numerically in ref. [73] with the result

$$0.1 \lesssim k \lesssim 1.0$$

Now the rate of baryon number non-conserving processes $V_B(t)$ is related to the rate Γ per unit time and unit volume of fluctuations with changing of the topological number by

[25] It would disappear from (5.71) in the limit $T \to \infty$

[74]

$$V_B(t) = \frac{13}{2} N_f \frac{\Gamma}{T^3} \tag{7.71}$$

We have to compare now the rate (7.71) with the expansion rate of the universe, given by,

$$H(t) = \frac{\dot{a}(t)}{a(t)} = \frac{1}{2} t^{-1} \tag{7.72}$$

where the last equality holds in the radiation dominated era. Using now eq. (5.100) and (7.72) we can write the Hubble constant as,

$$H(t) = 17.2 \frac{T^2}{M_{P\ell}} \tag{7.73}$$

and the condition for baryon number violation,

$$V_B(t) > H(t) \tag{7.74}$$

translates into the condition,

$$T < 0.377 \; N_f k \alpha_W^4 M_{P\ell} \sim 10^{12} \; GeV \tag{7.75}$$

where we have taken the most conservative value for k, $k = 0.1$, and

$$\alpha_W = 0.0336 \tag{7.76}$$

7.4.4 Baryon violation rate at $T < T_c$

After the phase transition, the calculation of baryon violation rate can be done using the semiclassical approximations of section 5, as given by eq. (5.71). The rate per unit time and unit volume for fluctuations between neighboring minima contains a Boltzmann suppression factor $\exp\left(-E_{\rm sph}(T)/T\right)$, where $E_{\rm sph}(T)$ is given by (7.68), and a pre-factor containing the determinant of all zero and non-zero modes, eq. (5.70). The prefactor was computed in ref. [75] as

$$\Gamma \sim 2.8 \times 10^5 T^4 \left(\frac{\alpha_W}{4\pi}\right)^4 \kappa \frac{\zeta^7}{B^7} e^{-\zeta} \tag{7.77}$$

where we have defined

$$\zeta(T) = \frac{E_{\rm sph}(T)}{T}, \tag{7.78}$$

the coefficient B is the function of λ/g^2 defined in (7.66) and κ is the functional determinant associated with fluctuations about the sphaleron. It has been estimated [76] to be in the range,

$$10^{-4} \lesssim \kappa \lesssim 10^{-1} \tag{7.79}$$

The equation describing the dilution of the baryon asymmetry in the anomalous electroweak processes reads [74]

$$\frac{\partial(B+L)}{\partial t} = -V_B(t)(B+L) \tag{7.80}$$

where $V_B(t)$ is the rate (7.71) of the baryon number non-conserving processes. Assuming T is constant during the phase transition [26] the integration of (7.80) yields

$$\frac{(B+L)_{\text{final}}}{(B+L)_{\text{initial}}} = S \tag{7.81}$$

where the suppression factor is given by

$$S = e^{-X} \tag{7.82}$$

and

$$X = \frac{13}{2} N_f \frac{\Gamma}{T^3} t \tag{7.83}$$

Using now (7.77) and (5.100)

$$t = 0.029 \frac{M_{P\ell}}{T^2} \tag{7.84}$$

we can write the exponent X as,

$$X \sim 10^{10} \kappa \zeta^7 e^{-\zeta} \tag{7.85}$$

where we have taken the values of the parameters, $B = 1.87$, $\alpha_W = 0.0336$, $N_f = 3$, $T_c \sim 10^2\ GeV$. Imposing now the condition

$$S \gtrsim 10^{-5} \tag{7.86}$$

or

$$X \lesssim 10 \tag{7.87}$$

leads to the condition on $\zeta(T_c)$,

$$\zeta(T_c) \gtrsim 7 \log \zeta(T_c) + 9 \log 10 + \log \kappa \tag{7.88}$$

Now, taking κ at its upper bound in (7.79), $\kappa = 10^{-1}$, we obtain from (7.88) the bound [77]

$$\frac{E_{\text{sph}}(T_c)}{T_c} \gtrsim 45, \tag{7.89}$$

[26] Actually this is a very good approximation since phase transition happens very fast at almost a constant temperature.

and using the lower bound of (7.79), $\kappa = 10^{-4}$ we obtain,

$$\frac{E_{\rm sph}(T_c)}{T_c} \gtrsim 37, \tag{7.90}$$

Eq. (7.89) is the usual bound used to test different theories while eq. (7.90) gives an idea on how much can one move away from the bound (7.89), *i.e.* the uncertainty on the bound (7.89).

The bounds (7.89) and (7.90) can be translated into bounds on $\phi(T_c)/T_c$ using the relation (7.68) and

$$m_W(T_c) = \frac{1}{2} g \phi(T_c) \tag{7.91}$$

we can write

$$\frac{\phi(T_c)}{T_c} = \frac{g}{4\pi B} \frac{E_{\rm sph}(T_c)}{T_c} \sim \frac{1}{36} \frac{E_{\rm sph}(T_c)}{T_c} \tag{7.92}$$

where we have used the previous values of the parameters. The bound (7.89) translates into

$$\frac{\phi(T_c)}{T_c} \gtrsim 1.3 \tag{7.93}$$

while the bound (7.90) translates into,

$$\frac{\phi(T_c)}{T_c} \gtrsim 1.0 \tag{7.94}$$

These bounds, eqs. (7.93) and (7.89), require that the phase transition is strong enough first order. In fact for a second order phase transition, $\phi(T_c) \simeq 0$ and any previously generated baryon asymmetry would be washed out during the phase transition. For the case of the Standard Model, sections 2.5 and 4.4, the previous bounds translate into a bound on the Higgs mass, as we will see in the next section.

7.4.5 Bounds on the Higgs mass in the Standard Model

The effective potential for the Standard Model was analyzed in sections 2.5 and 4.4 in the one-loop approximation, and in section 6.4 including leading order plasma effects (see eqs. (6.79-6.99)). In this approximation, the longitudinal components of the gauge bosons are screened by plasma effects while the transverse components remain unscreened. In this way a good approximation to the effective potential including these plasma effects is provided by eqs. (4.53-4.59), where the coefficient E in (4.56) is replaced by

$$E = \frac{2}{3} \frac{2m_W^3 + m_Z^3}{4\pi v^3} \sim 9.5 \times 10^{-3} \tag{7.95}$$

Now we can use eq. (5.14) and $m_h^2 = 2\lambda v^2$ to write,

$$\frac{\phi(T_c)}{T_c} \sim \frac{4Ev^2}{m_h^2} \tag{7.96}$$

In this way the bound (7.93) translates into the bound on the Higgs mass,

$$m_h \lesssim \sqrt{\frac{4E}{1.3}} \sim 42\ GeV \tag{7.97}$$

while the bound (7.94) would translate into the bound

$$m_h \lesssim \sqrt{4E}v \sim 48\ GeV. \tag{7.98}$$

The bound (7.98) is excluded by LEP measurements [59], and so the Standard Model is unable to keep any previously generated baryon asymmetry. Is it possible, in extensions of the Standard Model, to overcome this difficulty? We will see in the next sections two typical examples where the Standard Model is extended: one is the well motivated supersymmetric extension of the Standard Model (MSSM) and the other is the simplest extension of the Standard Model with a complex singlet which does not acquire any vacuum expectation value.

8 Electroweak Phase Transitions in Extensions of the Standard Model

The condition that the baryon excess generated at the electroweak phase transition is not washed out requires a strong enough first-order phase transition, as we have seen in the previous section, which translates into an upper bound on the Higgs boson mass, see eq. (7.98). Recent analyses of the minimal Standard Model (MSM) at one-loop [12], and including plasma effects [15, 16, 27, 40, 42] in various approximations [43]-[53], show that the above upper bound is inconsistent with the present experimental lower bound [59], *i.e.* that the phase transition is not strongly enough first order. Though, in our opinion, this issue is not yet fully settled it is interesting to study extensions of the MSM where the phase transition can be made consistent with present experimental lower bounds on the Higgs boson mass.

8.1 Standard Model with a singlet

In this section we study the phase transition in the simplest of these extensions, which consists in adding to the MSM a complex gauge singlet with zero vacuum expectation value.

This extension was proposed in refs. [12, 76, 78] as the simplest way of overcoming the problems encountered in the MSM. In fact the added boson generates a cubic term in the one-loop effective potential, which can trigger a strong first-order phase transition if it is not shielded by a heavy $SU(2) \times U(1)$ invariant mass [27]. However, as noticed in ref. [80], the extra boson behaves as the longitudinal components of W and Z gauge bosons and the corresponding cubic term can also be shielded by plasma effects. Fortunately we will see this is not always the case and find the region in parameter space where the phase transition is strong enough first order for values of the Higgs boson mass beyond the experimental bounds.

The lagrangian of the model is defined as:

$$\mathcal{L} = \mathcal{L}_{MSM} + \partial^\mu S^* \partial_\mu S - M^2 S^* S - \lambda_S (S^* S)^2 - 2\zeta^2 S^* S H^* H \tag{8.1}$$

where H is the MSM doublet with $\langle H \rangle = \phi/\sqrt{2}$, ϕ is the classical field, and $M^2, \lambda_S, \zeta^2 \geq 0$, to guarantee that $\langle S \rangle = 0$ at all temperatures [28].

The tree-level potential is that of the MSM (2.79), and the fields contributing to the effective potential are those of the MSM, *i.e.* the Higgs field h, the Goldstone bosons $\vec{\chi}$, the gauge bosons $W^\pm, Z, \gamma$ and the top quark t, with masses given by (2.80), (2.81), and (2.82), and the S boson, with a mass

$$m_S^2(\phi) = M^2 + \zeta^2 \phi^2 \ . \tag{8.2}$$

The temperature dependent effective potential can be calculated using standard techniques. Plasma effects in the leading approximation can be accounted by the one-loop effective potential improved by the daisy diagrams. Imposing renormalization conditions preserving the tree level values of $v^2 \equiv \mu^2/\lambda$, and working in the 't Hooft-Landau gauge, the ϕ-dependent part of the effective potential can be written in the high-temperature expansion as

$$V_{\text{eff}}(\phi, T) = V_{\text{tree}} + \Delta V_B + \Delta V_F \tag{8.3}$$

where

$$\Delta V_B = \sum_{i=h,\chi,W_L,Z_L,\gamma_L,W_T,Z_T,\gamma_T,S} g_i \Delta V_i \tag{8.4}$$

(ΔV_i being defined in (6.81) and ΔV_F given by (6.82)). The number of degrees of freedom g_i in (8.4) is given by (6.83) and

$$g_S = 2 \tag{8.5}$$

[27] This result also holds when the gauge singlet acquires a vacuum expectation value. This case has been recently analyzed at the one-loop level in ref. [79], where plasma effects are not considered.

[28] A cubic term in (8.1) would destabilize the potential along some direction in the S plane for $\lambda_S = 0$. We assume a global $U(1)$ symmetry $S \to e^{i\alpha} S$ which prevents the appearance of such cubic term.

The Debye masses $\mathcal{M}_i^2$ in (6.81) for $i = h, \chi, S, W_L, W_T, Z_T, \gamma_T$ are (see eq. (6.84))

$$\mathcal{M}_i^2 = m_i^2(\phi) + \Pi_i(\phi, T) \tag{8.6}$$

where the self-energies $\Pi_i(\phi, T)$ are given by

$$\Pi_h(\phi, T) = \left(\frac{3g^2 + g'^2}{16} + \frac{\lambda}{2} + \frac{h_t^2}{4} + \frac{\zeta^2}{6}\right) T^2 \tag{8.7}$$

$$\Pi_\chi(\phi, T) = \left(\frac{3g^2 + g'^2}{16} + \frac{\lambda}{2} + \frac{h_t^2}{4} + \frac{\zeta^2}{6}\right) T^2 \tag{8.8}$$

$$\Pi_S(\phi, T) = \frac{\lambda_S + \zeta^2}{3} T^2 \tag{8.9}$$

while $\Pi_{W_L}(\phi, T)$, $\Pi_{W_T}(\phi, T)$, $\Pi_{Z_T}(\phi, T)$, and $\Pi_{\gamma_T}(\phi, T)$ are given by (6.87) and (6.88). The Debye masses $\mathcal{M}_i^2$ for $i = Z_L, \gamma_L$ are given through (6.89) to (6.99).

An analytic treatment of the one-loop effective potential was given in ref. [12]. In the presence of plasma effects a similar treatment of the potential can be done [81] assuming that the bosonic contribution (8.4) to the effective potential (8.3) is dominated by one field, namely the S field, and neglecting the contribution from the other bosons. The ϕ dependent part of the effective potential (8.3) can be written as

$$V(\phi) = A(T)\phi^2 + B(T)\phi^4 + C(T)\left(\phi^2 + K^2(T)\right)^{3/2} \tag{8.10}$$

where

$$A(T) = -\frac{1}{2}\mu_T^2 + \frac{1}{4}\left(\frac{\zeta^2}{3} + \frac{h_t^2}{2}\right) T^2 \tag{8.11}$$

$$B(T) = \frac{1}{4}\lambda_T \tag{8.12}$$

$$C(T) = -\frac{\zeta^3 T}{6\pi} \tag{8.13}$$

$$K^2(T) = \frac{(\zeta^2 + \lambda_S)T^2 + 3M^2}{3\zeta^2} \tag{8.14}$$

and

$$\mu_T^2 = \mu^2 - \frac{\zeta^2}{8\pi^2}\left\{m_S^2(v) + M^2 \log\frac{c_B T^2}{m_S^2(v)}\right\} + \frac{3}{8\pi^2} h_t^2 m_t^2(v) \log\frac{m_t^2(v)}{c_F T^2} \tag{8.15}$$

$$\lambda_T = \lambda + \frac{\zeta^4}{8\pi^2}\log\frac{c_B T^2}{m_S^2(v)} + \frac{3}{16\pi^2} h_t^4 \log\frac{m_t^2(v)}{c_F T^2} \tag{8.16}$$

The temperature T_2 is defined by the condition $V''(0) = 0$, or

$$4A^2 - 9C^2K^2 = 0 \tag{8.17}$$

For $T < T_2$ the origin is a maximum, and there is a global minimum at $\phi \neq 0$ that evolves towards the zero temperature minimum. For $T > T_2$ the origin is a minimum and there is a maximum at $\phi_-(T)$ and a minimum at $\phi_+(T)$ given by

$$\phi_\pm^2(T) = \frac{1}{32B^2}\left\{9C^2 - 16AB \pm 3|C|\sqrt{9C^2 + 32(2B^2K^2 - AB)}\right\} \tag{8.18}$$

At the temperature T_1 defined by the condition

$$9C^2 + 32(2B^2K^2 - AB) = 0 \tag{8.19}$$

the maximum and minimum collapse $\phi_-(T_1) = \phi_+(T_1)$. For $T > T_1$ the origin is the only minimum.

Using (8.11-8.14) the temperatures T_1 and T_2 can be written as

$$\zeta^2 T_1^2 = \frac{2\lambda_{T_1}(\zeta^2\mu_{T_1}^2 + \lambda_{T_1}M^2)}{(\frac{\zeta^2}{3} + \frac{h_t^2}{2})\lambda_{T_1} - \frac{\zeta^6}{8\pi^2} - \frac{2\lambda_{T_1}^2}{3\zeta^2}(\zeta^2 + \lambda_S)} \tag{8.20}$$

$$T_2^2 = \frac{1}{2\alpha}\left\{\Lambda^2(T_2) + \sqrt{\Lambda^4(T_2) - 16\alpha\mu_{T_2}^4}\right\} \tag{8.21}$$

where

$$\alpha = \left(\frac{\zeta^2}{3} + \frac{h_t^2}{2}\right)^2 - \frac{1}{3\pi^2}\zeta^4\left(\zeta^2 + \lambda_S\right) \tag{8.22}$$

$$\Lambda^2(T) = \frac{1}{\pi^2}\zeta^4 M^2 + 4\left(\frac{\zeta^2}{3} + \frac{h_t^2}{2}\right)\mu_T^2 \tag{8.23}$$

The nature of the phase transition depends on the relation between T_1 and T_2. For values of the parameters (ζ^2, λ_S, M) such that $T_1 > T_2$ the phase transition is first order and the plasma screening is not very effective. When $T_1 = T_2$ the phase transition becomes second order because the screening became more effective. In fact, the condition $T_1 = T_2$ gives the turn-over from first to second order. It provides a surface in the space (ζ, λ_S, M) which separates first-order from second-order regions. An analytic approximation can be given, if one neglects loop corrections in (8.15,8.16), as

$$\frac{\zeta^8}{8\pi^2} - \frac{2}{3}\lambda^2(\zeta^2 + \lambda_S) \geq \left[\lambda\left(\frac{\zeta^2}{3} + \frac{h_t^2}{2}\right) - \frac{\zeta^6}{4\pi^2}\right]\left(\frac{M}{v}\right)^2 \tag{8.24}$$

where the strict inequality corresponds to the subregion of the space (ζ, λ_S, M) for which the phase transition is first-order, and the equality corresponds to the turn-over to a second order phase transition. Since the right-hand side of eq. (8.24) is positive-definite [29], we can

[29] It is easy to see that the necessary and sufficient condition for this turn-over to exist is that the right-hand-side of eq. (8.24) is positive-definite. It is not a priori excluded that an isolated region exists in the space (ζ, λ_S, M) where the phase transition is second order. However we have checked that for phenomenological values of the parameters (λ, h_t) this region does not exist.

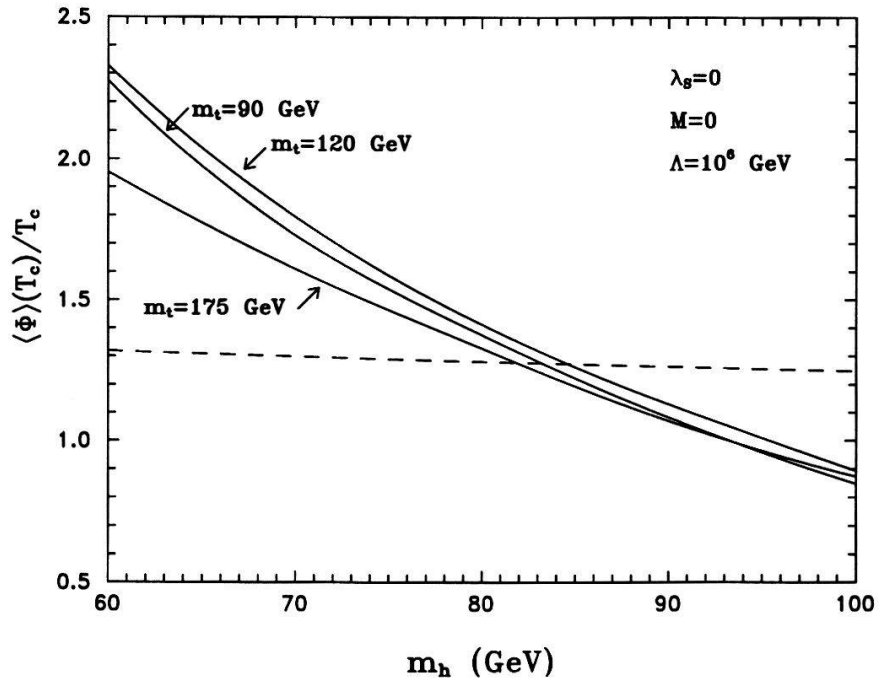

Figure 22: **Plot of $\phi_+(T_c)/T_c$ versus m_h for $m_t = 90,\ 150$ and $175\ GeV$, $\Lambda = 10^6\ GeV$ and $\zeta_{\max}$ taken from the Table.**

see from (8.24) how the parameters M^2 and $\zeta^2 + \lambda_S$ in (4) and (5) influence the shielding of the first order phase transition. First, the larger the value of M is, the easier one saturates the inequality in (8.24) and the easier one reaches a second-order phase transition. The same can be stated on λ_S, though its effect is damped by λ^2 and would become important only for a very heavy Higgs. For the same reason the effect of ζ is opposite, unless the Higgs is very heavy.

The complete numerical analysis has been performed in ref. [81]. If we want to establish an absolute upper bound on the mass of the Higgs boson we need to optimize the phase transition with respect to the new parameters (ζ, λ_S, M). As can be seen from eq. (8.24) this is accomplished for $M = 0$ [30] and $\lambda_S = 0$. As for ζ, a quick glance at eq. (8.24) shows that we should put it to its maximum value $\zeta_{\max}$. The usual requirement for $\zeta_{\max}$ is that the theory remains perturbative in all its domain of validity, from the electroweak scale to a high scale Λ. For that we have to study the renormalization group equations (RGE) of the minimal extension of the MSM provided by the lagrangian (8.1). At one-loop the only β-function of the MSM modified by the interactions of S is β_λ while there appear new

[30] We are aware that values $M \ll v$ would require much more fine tuning than that required for the Higgs sector of the MSM. However we are taking $M = 0$ only to establish an absolute upper limit on the Higgs mass.

β-functions for the new couplings λ_S and ζ, as [82]

$$\Delta\beta_\lambda = 8\zeta^4 \tag{8.25}$$

$$\beta_{\lambda_S} = 20\lambda_S^2 + 8\zeta^4 \tag{8.26}$$

$$\beta_{\zeta^2} = \zeta^2\left[6\lambda + 6h_t^2 + 8\lambda_S + 8\zeta^2 - \frac{3}{2}(3g^3 + g'^2)\right] \tag{8.27}$$

where we are using the convention

$$16\pi^2\frac{dx}{dt} = \beta_x \tag{8.28}$$

for all couplings $x = \zeta^2, \lambda_S, \lambda, ...$ From eqs.(8.26,8.27) we see that imposing $\lambda_S(m_W) = 0$ as boundary condition, consistent with our previous requirement, we can reach the maximum value of $\zeta(m_W)$, $\zeta_{\max}$, that will depend on m_h, m_t and Λ. We have solved the system of RGE corresponding to the lagrangian (8.1) between m_W and Λ and obtained $\zeta_{\max}$ for different values of m_h and m_t. The dependence of $\zeta_{\max}$ on m_h is negligible for 60 $GeV \leq m_h \leq$ 100 GeV. In the Table we show $\zeta^2_{\max}$ for different values of Λ and $m_t = 90,\ 120,\ 175\ GeV$.

	$m_t\ (GeV)$		
$\Lambda\ (GeV)$	90	120	175
10^4	1.774	1.742	1.667
10^6	1.095	1.067	1.011
10^8	0.793	0.770	0.728
10^{10}	0.624	0.604	0.573
10^{12}	0.515	0.498	0.473
10^{14}	0.439	0.424	0.405
10^{16}	0.384	0.370	0.356

Table

To exhibit the dependence on m_t we plot in fig. 22 $\phi_+(T_c)/T_c$ versus m_h for $\lambda_S = 0$, $M = 0$, $m_t = 90,\ 120$ and $175\ GeV$, and $\zeta = \zeta_{\max}$, corresponding to $\Lambda = 10^6\ GeV$. In that case we see from fig. 22 that avoiding baryon asymmetry washout imposes on the Higgs mass an upper bound of order 80 GeV.

8.2 The Minimal Supersymmetric Standard Model

Among the extensions of the MSM, the physically most motivated and phenomenologically most acceptable one is the Minimal Supersymmetric Standard Model (MSSM). This model

allows for extra CP-violating phases besides the Kobayashi-Maskawa one, which could help in generating the observed baryon asymmetry [84]. It is then interesting to study whether in the MSSM the nature of the phase transition can be significantly modified with respect to the MSM.

In this section (see refs. [85, 86]), we extend the considerations of the previous section to the full parameter space, characterizing the Higgs sector of the MSSM. We will include a full discussion of the top/stop sector and resum the leading plasma corrections to gauge bosons and stop masses, improving over previous studies [87]. Even barring the interesting possibility of spontaneous CP-violation at finite temperature [88], as well as the possibility of charge- and colour-breaking minima, we have to deal with a complicated two-variable potential, which requires a numerical analysis. After including the most important experimental constraints, we find that there is very little room for the MSSM to improve over the MSM.

The main tool for our study is the one-loop, daisy-improved finite-temperature effective potential of the MSSM, $V_{\rm eff}(\phi,T)$. We are actually interested in the dependence of the potential on $\phi_1 \equiv \mathrm{Re}\, H_1^0$ and $\phi_2 \equiv \mathrm{Re}\, H_2^0$ only, where H_1^0 and H_2^0 are the neutral components of the Higgs doublets H_1 and H_2, thus ϕ will stand for (ϕ_1,ϕ_2). Working in the 't Hooft-Landau gauge and in the $\overline{DR}$-scheme, we can write

$$V_{\rm eff}(\phi,T) = V_0(\phi) + V_1(\phi,0) + \Delta V_1(\phi,T) + \Delta V_{\rm daisy}(\phi,T)\,, \tag{8.29}$$

where

$$V_0(\phi) = m_1^2\phi_1^2 + m_2^2\phi_2^2 + 2m_3^2\phi_1\phi_2 + \frac{g^2+g'^2}{8}(\phi_1^2-\phi_2^2)^2\,, \tag{8.30}$$

$$V_1(\phi,0) = \sum_i \frac{n_i}{64\pi^2} m_i^4(\phi)\left[\log\frac{m_i^2(\phi)}{Q^2} - \frac{3}{2}\right]\,, \tag{8.31}$$

$$\Delta V_1(\phi,T) = \frac{T^4}{2\pi^2}\left\{\sum_i n_i\, J_i\left[\frac{m_i^2(\phi)}{T^2}\right]\right\}\,, \tag{8.32}$$

$$\Delta V_{\rm daisy}(\phi,T) = -\frac{T}{12\pi}\sum_i n_i\left[\mathcal{M}_i^3(\phi,T) - m_i^3(\phi)\right]\,. \tag{8.33}$$

The four contributions (8.30–8.33) to the effective potential (8.29) have the following meaning. The first term, eq. (8.30), is the tree-level potential. The second term, eq. (8.31), is the one-loop contribution at $T = 0$: Q is the renormalization scale, where we choose for definiteness $Q^2 = m_Z^2$, $m_i^2(\phi)$ is the field-dependent mass of the i^{th} particle, and n_i is the corresponding number of degrees of freedom, taken negative for fermions. Since $V_1(\phi,0)$ is dominated by top (t) and stop ($\tilde{t}_1,\tilde{t}_2$) contributions, only these will be included in the following. The third term, eq. (8.32), is the additional one-loop contribution due to temperature

effects. Here $J_i = J_+(J_-)$ if the i^{th} particle is a boson (fermion), and (see eqs. (4.15) and (4.40))

$$J_\pm(y^2) \equiv \int_0^\infty dx\, x^2 \log\left(1 \mp e^{-\sqrt{x^2+y^2}}\right) . \tag{8.34}$$

Since the relevant contributions to $\Delta V_1(\phi, T)$ are due to top (t), stops ($\tilde{t}_1, \tilde{t}_2$) and gauge bosons (W, Z), only these will be considered in the following. Finally, the last term, eq. (8.33), is a correction coming from the resummation of the leading infrared-dominated higher-loop contributions, associated with the so-called daisy diagrams. The sum runs over bosons only. The masses $\mathcal{M}_i^2(\phi, T)$ are obtained from the $m_i^2(\phi)$ by adding the leading T-dependent self-energy contributions, which are proportional to T^2. We recall that, in the gauge boson sector, only the longitudinal components (W_L, Z_L, γ_L) receive such contributions.

The relevant degrees of freedom for our calculation are:

$$n_t = -12\,,\ \ n_{\tilde{t}_1} = n_{\tilde{t}_2} = 6\,,\ \ n_W = 6\,,\ \ n_Z = 3\,,\ \ n_{W_L} = 2\,,\ \ n_{Z_L} = n_{\gamma_L} = 1\,. \tag{8.35}$$

The field-dependent top mass is

$$m_t^2(\phi) = h_t^2 \phi_2^2\,. \tag{8.36}$$

The entries of the field-dependent stop mass matrix are

$$m_{\tilde{t}_L}^2(\phi) = m_{Q_3}^2 + m_t^2(\phi) + D_{\tilde{t}_L}^2(\phi)\,, \tag{8.37}$$

$$m_{\tilde{t}_R}^2(\phi) = m_{U_3}^2 + m_t^2(\phi) + D_{\tilde{t}_R}^2(\phi)\,, \tag{8.38}$$

$$m_X^2(\phi) = h_t(A_t\phi_2 + \mu\phi_1)\,, \tag{8.39}$$

where m_{Q_3}, m_{U_3} and A_t are soft supersymmetry-breaking mass parameters, μ is a superpotential Higgs mass term, and

$$D_{\tilde{t}_L}^2(\phi) = \left(\frac{1}{2} - \frac{2}{3}\sin^2\theta_W\right)\frac{g^2 + g'^2}{2}(\phi_1^2 - \phi_2^2), \tag{8.40}$$

$$D_{\tilde{t}_R}^2(\phi) = \left(\frac{2}{3}\sin^2\theta_W\right)\frac{g^2 + g'^2}{2}(\phi_1^2 - \phi_2^2) \tag{8.41}$$

are the D-term contributions. The field-dependent stop masses are then

$$m_{\tilde{t}_{1,2}}^2(\phi) = \frac{m_{\tilde{t}_L}^2(\phi) + m_{\tilde{t}_R}^2(\phi)}{2} \pm \sqrt{\left[\frac{m_{\tilde{t}_L}^2(\phi) - m_{\tilde{t}_R}^2(\phi)}{2}\right]^2 + [m_X^2(\phi)]^2}\,. \tag{8.42}$$

The corresponding effective T-dependent masses, $\mathcal{M}_{\tilde{t}_{1,2}}^2(\phi, T)$, are given by expressions identical to (8.42), apart from the replacement

$$m_{\tilde{t}_{L,R}}^2(\phi) \to \mathcal{M}_{\tilde{t}_{L,R}}^2(\phi, T) \equiv m_{\tilde{t}_{L,R}}^2(\phi) + \Pi_{\tilde{t}_{L,R}}(T)\,. \tag{8.43}$$

The $\Pi_{\tilde{t}_{L,R}}(T)$ are the leading parts of the T-dependent self-energies of $\tilde{t}_{L,R}$,

$$\Pi_{\tilde{t}_L}(T) = \frac{4}{9}g_s^2T^2 + \frac{1}{4}g^2T^2 + \frac{1}{108}g'^2T^2 + \frac{1}{6}h_t^2T^2\,, \tag{8.44}$$

$$\Pi_{\tilde{t}_R}(T) = \frac{4}{9}g_s^2T^2 + \frac{4}{27}g'^2T^2 + \frac{1}{3}h_t^2T^2\,, \tag{8.45}$$

where g_s is the strong gauge coupling constant. Only loops of gauge bosons, Higgs bosons and third generation squarks have been included, implicitly assuming that all remaining supersymmetric particles are heavy and decouple. If some of these are also light, the plasma masses for the stops will be even larger, further suppressing the effects of the associated cubic terms, and therefore weakening the first-order nature of the phase transition. Finally, the field-dependent gauge boson masses are

$$m_W^2(\phi) = \frac{g^2}{2}(\phi_1^2+\phi_2^2)\,, \qquad m_Z^2(\phi) = \frac{g^2+g'^2}{2}(\phi_1^2+\phi_2^2)\,, \tag{8.46}$$

and the effective T-dependent masses of the longitudinal gauge bosons are

$$\mathcal{M}_{W_L}^2(\phi,T) = m_W^2(\phi) + \Pi_{W_L}(T)\,, \tag{8.47}$$

$$\mathcal{M}_{Z_L,\gamma_L}^2(\phi,T) = \frac{1}{2}\left[m_Z^2(\phi) + \Pi_{W_L}(T) + \Pi_{B_L}(T)\right] \pm \sqrt{\frac{1}{4}\left[\frac{g^2-g'^2}{2}(\phi_1^2+\phi_2^2) + \Pi_{W_L}(T) - \Pi_{B_L}(T)\right]^2 + \left[\frac{gg'}{2}(\phi_1^2+\phi_2^2)\right]^2}\,. \tag{8.48}$$

In eqs. (8.47) and (8.48), $\Pi_{W_L}(T)$ and $\Pi_{B_L}(T)$ are the leading parts of the T-dependent self-energies of W_L and B_L, given by

$$\Pi_{W_L}(T) = \frac{5}{2}g^2T^2\,, \qquad \Pi_{B_L}(T) = \frac{47}{18}g'^2T^2\,, \tag{8.49}$$

where only loops of Higgs bosons, gauge bosons, Standard Model fermions and third-generation squarks have been included.

We shall now analyse the effective potential (8.29) as a function of ϕ and T. Before doing this, however, we trade the parameters m_1^2, m_2^2, m_3^2 appearing in the tree-level potential (8.30) for more convenient parameters. To this purpose, we first minimize the zero-temperature effective potential, i.e. we impose the vanishing of the first derivatives of $V_0(\phi)+V_1(\phi,0)$ at $(\phi_1,\phi_2)=(v_1,v_2)$, where (v_1,v_2) are the one-loop vacuum expectation values at $T=0$. This allows us to eliminate m_1^2 and m_2^2 in favour of m_Z^2 and $\tan\beta \equiv v_2/v_1$:

$$m_1^2 = -m_3^2\tan\beta - \frac{m_Z^2}{2}\cos 2\beta - \sum_i \frac{n_i}{64\pi^2}\left[\frac{\partial m_i^2}{\partial\phi_1}\frac{m_i^2}{\phi_1}\left(\log\frac{m_i^2}{Q^2}-1\right)\right]_{\phi_{1,2}=v_{1,2}}\,, \tag{8.50}$$

$$m_2^2 = -m_3^2\cot\beta + \frac{m_Z^2}{2}\cos 2\beta - \sum_i \frac{n_i}{64\pi^2}\left[\frac{\partial m_i^2}{\partial\phi_2}\frac{m_i^2}{\phi_2}\left(\log\frac{m_i^2}{Q^2}-1\right)\right]_{\phi_{1,2}=v_{1,2}}\,. \tag{8.51}$$

Moreover, m_3^2 can be traded for the one-loop-corrected mass m_A^2 of the CP-odd neutral Higgs boson. In our approximation [89]

$$m_3^2 = -m_A^2 \sin\beta\cos\beta - \frac{3g^2 m_t^2 \mu A_t}{32\pi^2 m_W^2 \sin^2\beta} \frac{m_{\tilde{t}_1}^2\left(\log\frac{m_{\tilde{t}_1}^2}{Q^2}-1\right) - m_{\tilde{t}_2}^2\left(\log\frac{m_{\tilde{t}_2}^2}{Q^2}-1\right)}{m_{\tilde{t}_1}^2 - m_{\tilde{t}_2}^2}\,. \tag{8.52}$$

Therefore the whole effective potential (8.29) is completely determined, in our approximation, by the parameters $(m_A, \tan\beta)$ of the Higgs sector, and by the parameters (m_t, m_{Q_3}, m_{U_3}, μ, A_t) of the top/stop sector. The same set of parameters also determines the one-loop-corrected masses and couplings of the MSSM Higgs bosons.

The next steps are the computation of the critical temperature and of the location of the minimum of the effective potential at the critical temperature. We define here T_0 as the temperature at which the determinant of the second derivatives of $V_{\rm eff}(\phi, T)$ at $\phi = 0$ vanishes:

$$\det\left[\frac{\partial^2 V_{\rm eff}(\phi, T_0)}{\partial\phi_i \partial\phi_j}\right]_{\phi_{1,2}=0} = 0\,. \tag{8.53}$$

It is straightforward to compute the derivatives in eq. (8.53) from the previous formulae; the explicit expressions are

$$\begin{aligned}
\frac{1}{2}\left[\frac{\partial^2 V_{\rm eff}}{\partial\phi_i^2}\right]_0 &= m_i^2 + \frac{1}{64\pi^2}\left[6a_{ii}m_{Q_3}^2\left(\log\frac{m_{Q_3}^2}{Q^2}-1\right) + 6b_{ii}m_{U_3}^2\left(\log\frac{m_{U_3}^2}{Q^2}-1\right)\right] \\
&+ \frac{T^2}{4\pi^2}\left[\frac{\pi^2}{12}(9g^2 + 3g'^2 + \delta_{i2}\cdot 12h_t^2) + 6a_{ii}J'_+\left(\frac{m_{Q_3}^2}{T^2}\right) + 6b_{ii}J'_+\left(\frac{m_{U_3}^2}{T^2}\right)\right] \\
&- \frac{T}{16\pi}\left\{3g^2\left[\Pi_{W_L}(T)\right]^{\frac{1}{2}} + g'^2\left[\Pi_{B_L}(T)\right]^{\frac{1}{2}}\right. \\
&+ 6\left[\overline{a}_{ii}\left(m_{Q_3}^2 + \Pi_{\tilde{t}_L}(T)\right)^{\frac{1}{2}} - a_{ii}\left(m_{Q_3}^2\right)^{\frac{1}{2}}\right] \\
&+ \left. 6\left[\overline{b}_{ii}\left(m_{U_3}^2 + \Pi_{\tilde{t}_R}(T)\right)^{\frac{1}{2}} - b_{ii}\left(m_{U_3}^2\right)^{\frac{1}{2}}\right]\right\}, \\
\frac{1}{2}\left[\frac{\partial^2 V_{\rm eff}}{\partial\phi_1\partial\phi_2}\right]_0 &= m_3^2 + \frac{1}{64\pi^2}6a_{12}\left[m_{Q_3}^2\left(\log\frac{m_{Q_3}^2}{Q^2}-1\right) - m_{U_3}^2\left(\log\frac{m_{U_3}^2}{Q^2}-1\right)\right] \\
&+ \frac{T^2}{4\pi^2}6a_{12}\left[J'_+\left(\frac{m_{Q_3}^2}{T^2}\right) - J'_+\left(\frac{m_{U_3}^2}{T^2}\right)\right] \\
&- \frac{T}{16\pi}\left\{6\overline{a}_{12}\left[\left(m_{Q_3}^2 + \Pi_{\tilde{t}_L}(T)\right)^{\frac{1}{2}} - \left(m_{U_3}^2 + \Pi_{\tilde{t}_R}(T)\right)^{\frac{1}{2}}\right]\right. \\
&- \left. 6a_{12}\left[\left(m_{Q_3}^2\right)^{\frac{1}{2}} - \left(m_{U_3}^2\right)^{\frac{1}{2}}\right]\right\}.
\end{aligned} \tag{8.54}$$

The coefficients a_{ij}, b_{ij} are given by

$$a_{11} \equiv \left(\frac{1}{2} - \frac{2}{3}\sin^2\theta_W\right)(g^2 + g'^2) + \frac{2h_t^2\mu^2}{m_{Q_3}^2 - m_{U_3}^2}\,,$$

$$
\begin{aligned}
b_{11} &\equiv \left(\frac{2}{3}\sin^2\theta_W\right)(g^2+g'^2) - \frac{2h_t^2\mu^2}{m_{Q_3}^2 - m_{U_3}^2}\,, \\
a_{22} &\equiv 2h_t^2 - \left(\frac{1}{2} - \frac{2}{3}\sin^2\theta_W\right)(g^2+g'^2) + \frac{2h_t^2 A_t^2}{m_{Q_3}^2 - m_{U_3}^2} \\
b_{22} &\equiv 2h_t^2 - \left(\frac{2}{3}\sin^2\theta_W\right)(g^2+g'^2) - \frac{2h_t^2 A_t^2}{m_{Q_3}^2 - m_{U_3}^2}\,, \\
a_{12} &\equiv \frac{2h_t^2\mu A_t}{m_{Q_3}^2 - m_{U_3}^2}\,,
\end{aligned}
\tag{8.55}
$$

and the coefficients $\overline{a}_{ij}, \overline{b}_{ij}$ are given by identical expressions, apart from the replacement

$$
m_{Q_3}^2 - m_{U_3}^2 \;\to\; m_{Q_3}^2 - m_{U_3}^2 + \Pi_{\tilde{t}_L}(T) - \Pi_{\tilde{t}_R}(T)\,. \tag{8.56}
$$

Once eq. (8.53) is solved (numerically) and T_0 is found, one can minimize (numerically) the potential $V_{\rm eff}(\phi, T_0)$ and find the minimum $[v_1(T_0), v_2(T_0)]$. The quantity of interest is indeed, as will be discussed later, the ratio $v(T_0)/T_0$, where $v(T_0) \equiv \sqrt{v_1^2(T_0) + v_2^2(T_0)}$.

We now discuss the particle physics constraints on the parameters of the top/stop sector and of the Higgs sector. To be as general as possible, we treat m_{Q_3}, m_{U_3} and the other soft mass terms as independent parameters, even if they can be related in specific supergravity models.

The constraints on the top/stop sector will be briefly discussed. Direct and indirect searches at LEP [59] imply that $m_{\tilde{b}_L} \gtrsim 45$ GeV, which in turn translates into a bound in the $(m_{Q_3}, \tan\beta)$ plane. Electroweak precision measurements [90] put stringent constraints on a light stop-sbottom sector: in first approximation, and taking into account possible effects [91] of other light particles of the MSSM, we conservatively summarize the constraints by $\Delta\rho(t,b) + \Delta\rho(\tilde{t},\tilde{b}) < 0.01$, where the explicit expression for $\Delta\rho(\tilde{t},\tilde{b})$ can be found in [92].

We finally need to consider the constraints coming from LEP searches for supersymmetric Higgs bosons [59]. Experimentalists put limits on the processes $Z \to hZ^*$ and $Z \to hA$, where h is the lighter neutral CP-even boson. We need to translate these limits into exclusion contours in the $(m_A, \tan\beta)$ plane, for given values of the top/stop parameters. In order to do this, we identify the value of $BR(Z \to hZ^*)$, which corresponds to the limit $m_\phi > 63.5$ GeV on the SM Higgs, and the value of $BR(Z \to hA)$, which best fits the published limits for the representative parameter choice $m_t = 140$ GeV, $m_{Q_3} = m_{U_3} \equiv \tilde{m} = 1$ TeV, $A_t = \mu = 0$. We then compare those values of $BR(Z \to hZ^*)$ and $BR(Z \to hA)$ with the theoretical predictions of the MSSM, for any desired parameter choice and after including the radiative corrections associated to top/stop loops [93],[89]. Of course, this procedure is not entirely

correct, since it ignores the variations of the efficiencies with the Higgs masses and branching ratios, as well as the possible presence of candidate events at some mass values, but it is adequate for our purposes.

According to eq. (7.89), the condition to avoid erasing any previously generated baryon asymmetry via sphaleron transitions is

$$\frac{E_{sph}(T_c)}{T_c} > 45\,, \tag{8.57}$$

Particularizing to the MSSM the studies of sphalerons in general two-Higgs models [94], we obtain that

$$E_{sph}^{MSSM}(T) \leq E_{sph}^{SM}(T)\,, \tag{8.58}$$

where, in our conventions,

$$\frac{E_{sph}^{SM}(T)}{T} = \frac{4\sqrt{2}\pi}{g} B\left\{\frac{\lambda_{\rm eff}[\theta(T)]}{4g^2}\right\}\frac{v(T)}{T}\,, \tag{8.59}$$

and B is a smoothly varying function whose values can be found in (7.66). Finally, the corrections in E_{sph}^{SM} due to $g' \neq 0$ have been estimated and shown to be small [70]. Therefore, a conservative bound to be imposed is

$$R \equiv \frac{v(T_0)}{T_0}\frac{4\sqrt{2}\pi B\left\{\frac{\lambda_{\rm eff}[\theta(T_0)]}{4g^2}\right\}}{45g} > 1\,. \tag{8.60}$$

The last point to be discussed is the determination of the value of $\lambda_{\rm eff}[\theta(T_0)]$ to be plugged into eq. (8.60). The B-function we use is taken from ref. [69], where the sphaleron energy was computed using the zero-temperature 'Mexican-hat' potential, $V = \frac{\lambda}{4}(\phi^2 - v^2)^2$. The sphaleron energy at finite temperature was computed in ref. [95], where it was proven that it scales like $v(T)$, i.e. as in (7.67), with great accuracy. Therefore, to determine the value of $\lambda_{\rm eff}[\theta(T_0)]$ we have fitted $V_{\rm eff}(\phi, T_0)$, as given by eq. (8.29), to the appropriate approximate expression,

$$V_{\rm eff}(\phi, T_0) \simeq \frac{1}{4}\lambda_{\rm eff}[\theta(T_0)][\phi^2 - v^2(T_0)]^2 + \text{field–independent terms}\,, \tag{8.61}$$

where the field-independent terms are just to take care of the different normalizations of the left- and right-hand sides. The value of $\lambda_{\rm eff}$ obtained from (8.61),

$$\lambda_{\rm eff}[\theta(T_0)] = 4\,\frac{V_{\rm eff}(0, T_0) - V_{\rm eff}[v(T_0), T_0]}{v^4(T_0)}\,, \tag{8.62}$$

where all quantities on the right-hand side are calculated numerically from the potential of eq. (8.29), is then plugged into eq. (8.60) to obtain our bounds. We have explicitly checked

the quality of the fit in eq. (8.61), finding an agreement that is more than adequate for our purposes.

The numerical results are summarized in fig. 23, in the $(m_A, \tan\beta)$ plane and for the value of the top quark mass $m_t = 170$ GeV. The values of the remaining free parameters have

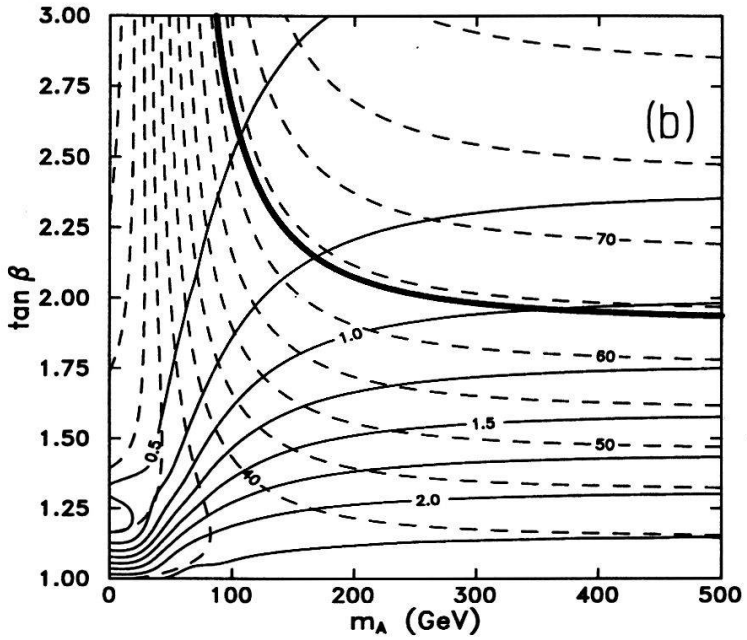

Figure 23: **Contours of R in the $(m_A, \tan\beta)$ plane, for the parameter choice $m_t = 170$ GeV, $m_{Q_3} = 280$ GeV, $m_{U_3} = 0$ ($m_{\tilde{t}_L} \sim 330$ GeV, $m_{\tilde{t}_R} \sim 170$ GeV, $m_{\tilde{b}_L} \sim 280$ GeV), $A_t = \mu = 0$. The region excluded by Higgs searches at LEP is delimited by the thick solid line. For reference, contours of constant m_h (in GeV) are also represented as dashed lines.**

been chosen in order to maximize the strength of the phase transition, given the experimental constraints on the top-stop sector. Notice that arbitrarily small values of m_{U_3} cannot be excluded on general grounds, even if they are disfavored by model calculations. Also, we have explicitly checked that, as in ref. [85], mixing effects in the stop mass matrix always worsen the case. In fig. 23, solid lines correspond to contours of constant R: one can see that the requirement of large values of R favours small $\tan\beta$ and $m_A \gg m_Z$. The thick solid line corresponds to the limits coming from Higgs searches at LEP: for our parameter choices, the allowed regions correspond to large $\tan\beta$ and/or $m_A \gg m_Z$. For reference, contours of constant m_h (in GeV) have also been plotted as dashed lines. One can see that, even for third-generation squarks as light as allowed by all phenomenological constraints, only a very small globally allowed region can exist in the $(m_A, \tan\beta)$ plane, and that the most

favourable situation is the one already discussed in ref. [85]. More precisely, the region that is still marginally allowed corresponds to $m_A \gg m_Z$, $\tan\beta \sim 2$, stop and sbottom sectors as light as otherwise allowed, a heavy top, and a light Higgs boson with SM-like properties and mass $m_h \sim 65$ GeV, just above the present experimental limit. A less conservative interpretation of the limits from precision measurements, the inclusion of some theoretically motivated constraints on the model parameters, or a few GeV improvement in the SM Higgs mass limit, would each be enough to fully exclude electroweak baryogenesis in the MSSM.

Some final comments on possible ways out are in order. First, one could think of relaxing the constraint $\tan\beta \geq 1$ (and the corresponding LEP bounds), which is usually motivated by the theoretical assumption of universal soft Higgs masses at the SUSY-GUT scale, $M_U \sim 10^{16}$ GeV. The possibility of $\tan\beta < 1$, however, is incompatible with a heavy top quark, since, for $m_t \gtrsim 130$ GeV and supersymmetric particle masses of order m_Z, the running top Yukawa coupling would become non-perturbative at scales smaller than M_U: such a possibility is strongly disfavored by the successful predictions of the low-energy gauge couplings in SUSY GUTs.

A second possibility is that large non-perturbative effects, neglected by conventional calculational techniques, modify the predicted values of the sphaleron energy and/or of $v(T_0)/T_0$ (for recent suggestions along this line, see [96]). We do not see strong physical arguments to favour this, but we admit that it cannot be rigorously excluded. Perhaps alternative approaches to the electroweak phase transition [97] could help clarify this point in the future.

A third possibility is that including unconsidered effects the baryon violation rate be suppressed with respect to the value used throughout these notes (eq. (7.77)). This possibility has been recently considered in ref. [98] where one-loop contributions of bosonic and fermionic fluctuations have been showed to suppress the sphaleron transition, thus shifting the upper bound on the Standard Model Higgs mass beyond its present experimental limit ($\sim 66\ GeV$). However the authors of ref. [98] have to make the technical (but not very realistic!) assumption that the top-bottom Standard Model doublet is degenerate in mass. Since treating the non-degeneracy as a perturbation is not a good approximation the results of this paper should not be trusted till a more realistic case can be considered.

Barring the above-mentioned possibilities, one could still try to rescue electroweak baryogenesis by further enlarging the MSSM Higgs sector, for example by introducing an extra singlet. Supersymmetric models with singlets and non-supersymmetric models, however, develop dangerous instabilities if coupled to the superheavy sector of an underlying unified

theory. It might well be that baryogenesis has to be described by physics at a scale larger than the electroweak one.

Acknowledgements

I would like to thank Prof. J.-P. Derendinger and the *Troisième Cycle de Physique de la Suisse Romande* for the kind invitation to give this course. My warmest thanks go to Philippe Page for his invaluable assistance in the preparation of the manuscript and figures. I am grateful to all the participants, in particular Cliff Burgess, Jean Pierre Derendinger, Olivier Piguet and Fernando Quevedo, who greatly improved with their questions and comments the final version of these notes. Finally, I want to express my deepest gratitude to all my collaborators in the considered topics, in particular Andrea Brignole, Alberto Casas, José Ramón Espinosa, Jesús Moreno, Antonio Riotto and Fabio Zwirner, for many hours devoted to understand so many difficult questions.

References

[1] W. Heisenberg and H. Euler, *Z. Phys.* **98** (1936) 714; J. Schwinger, *Phys. Rev.* **82** (1951) 664.

[2] J. Goldstone, A. Salam and S. Weinberg, *Phys. Rev.* **127** (1962) 965; G. Jona-Lasinio, *Nuovo Cimento* **34** (1964) 1790.

[3] S. Coleman and E. Weinberg, *Phys. Rev.* **D7** (1973) 1888.

[4] R. Jackiw, *Phys. Rev.* **D9** (1974) 1686.

[5] J. Iliopoulos, C. Itzykson and A. Martin, *Rev. Mod. Phys.* **47** (1975) 165.

[6] J.D. Bjorken and S.D. Drell, *Relativistic Quantum Mechanics* (McGraw-Hill, 1964); *Relativistic Quantum Fields* (McGraw-Hill, 1965).

[7] I.S. Gradshteyn and I.M. Ryzhik, *Table of Integrals Series and Products* (Academic Press, 1965).

[8] G. t'Hooft and M. Veltman, *Nucl. Phys.* **B44** (1972) 189; C.G. Bollini and J.J. Giambiagi, *Phys. Lett.* **B40** (1972) 366; J.F. Ashmore, *Nuovo Cimento Letters* **4** (1972) 289.

[9] W Siegel, *Phys. Lett.* **B84** (1979) 193.

[10] G. t'Hooft and M. Veltman, *Nucl. Phys.* **B61** (1973) 455; W.A. Bardeen, A.J. Buras, D.W. Duke and T. Muta, *Phys. Rev.* **D18** (1978) 3998.

[11] See, *e.g.*: J. Collins, *Renormalization* (Cambridge University Press, 1984).

[12] G.W. Anderson and L.J. Hall, *Phys. Rev.* **D45** (1992) 2685.

[13] B. Kastening, *Phys. Lett.* **B283** (1992) 287; M. Bando, T. Kugo, N. Maekawa and H. Nakano, *Phys. Lett.* **B301** (1993) 83; C. Ford, D.R.T. Jones, P.W. Stephenson and M.B. Einhorn, *Nucl. Phys.* **B395** (1993) 17.

[14] A. Casas, J.R. Espinosa, M. Quirós and A. Riotto, preprint CERN-TH.7334/94 (July 1994).

[15] L. Dolan and R. Jackiw, *Phys. Rev.* **D9** (1974) 3320.

[16] S. Weinberg, *Phys. Rev.* **D9** (1974) 3357.

[17] R.H. Brandenberger, *Rev. Mod. Phys.* **57** (1985) 1.

[18] N.P. Landsman and Ch.G. van Weert, *Phys. Rep.* **145** (1987) 141.

[19] J.I. Kapusta, *Finite-temperature field theory* (Cambridge University Press, 1989).

[20] R. Kubo, *J. Phys. Soc. Japan* **12** (1957) 570; P.C. Martin and J. Schwinger, *Phys. Rev.* **115** (1959) 1342.

[21] T. Matsubara, *Prog. Theor. Phys.* **14** (1955) 351.

[22] H. Matsumoto, Y. Nakano, H. Umezawa, F. Mancini and M. Marinaro, *Prog. Theor. Phys.* **70** (1983) 599; H. Matsumoto, Y. Nakano and H. Umezawa, *J. Math. Phys.* **25** (1984) 3076.

[23] L.V. Keldish, *Sov. Phys. JETP* **20** (1964) 1018.

[24] T.S. Evans, *Phys. Rev.* **D47** (1993) R4196; T. Altherr, CERN preprint, CERN-TH.6942/93.

[25] R. Kobes, *Phys. Rev.* **D42** (1990) 562 and *Phys. Rev. Lett.* **67** (1991) 1384; T.S. Evans, *Phys. Lett.* **B249** (1990) 286, *Phys. Lett.* **B252** (1990) 108, *Nucl. Phys.* **B371** (1992) 340; P. Aurenche and T. Becherrawy, *Nucl. Phys.* **B379** (1992) 259; M.A. van Eijck and Ch. G. van Weert, *Phys. Lett.* **B278** (1992) 305.

[26] D.A. Kirzhnits, *JETP Lett.* **15** (1972) 529.

[27] D.A. Kirzhnits and A.D. Linde, *Phys. Lett.* **42B** (1972) 471; D.A. Kirzhnits and A.D. Linde, *JETP* **40** (1974) 628; D.A. Kirzhnits and A.D. Linde, *Ann. Phys.* **101** (1976) 195.

[28] A.D. Linde, *Rep. Prog. Phys.* **42** (1979) 389; A.D. Linde, *Phys. Lett.* **99B** (1981) 391; A.D. Linde, *Phys. Lett.* **99B** (1981) 391; A.D. Linde, *Particle Physics and Inflationary Cosmology* (Harwood, Chur, Switzerland, 1990).

[29] A.D. Linde, *Phys. Lett.* **B108** (1982) 389; A. Albrecht and P.J. Steinhardt, *Phys. Rev. Lett.* **48** (1082) 1226.

[30] M. Dine, R.G. Leigh, P. Huet, A. Linde and D. Linde, *Phys. Lett.* **B283** (1992) 319; *Phys. Rev.* **D46** (1992) 550.

[31] S. Coleman, *Phys. Rev.* **D15** (1977) 2929.

[32] C.G. Callan and S. Coleman, *Phys. Rev.* **D16** (1977) 1762.

[33] S. Coleman and F. De Luccia, *Phys. Rev.* **D21** (1980) 3305.

[34] T. Banks, C. Bender and T.T. Wu, *Phys. Rev.* **D8** (1973) 3346 and 3366.

[35] S. Coleman, V. Glaiser and A. Martin, *Comm. Math. Phys.* **58** (1978) 211.

[36] A.D. Linde, *Phys. Lett.* **70B** (1977) 306; **100B** (1981) 37; *Nucl. Phys.* **B216** (1983) 421.

[37] L. McLerran, M. Shaposhnikov, N. Turok and M. Voloshin, *Phys. Lett.* **B256** (1991) 451.

[38] M. Dine, P. Huet and R. Singleton, *Nucl. Phys.* **B375** (1992) 625.

[39] A.H. Guth and E. Weinberg, *Phys. Rev.* **D23** (1981) 876.

[40] P. Fendley, *Phys. Lett.* **B196** (1987) 175.

[41] J.R. Espinosa, M. Quirós and F. Zwirner, *Phys. Lett.* **B291** (1992) 115.

[42] D.J. Gross, R.D. Pisarski and L.G. Yaffe, Rev. Mod. Phys. **53** (1981) 43.

[43] M.E. Carrington, Phys. Rev. **D45** (1992) 2933.

[44] M.E. Shaposhnikov, Phys. Lett. **B277** (1992) 324 and (E) **B282** (1992) 483.

[45] M. Dine, R.G. Leigh, P. Huet, A. Linde and D. Linde, Phys. Lett. **B283** (1992) 319 and Phys. Rev. **D46** (1992) 550.

[46] P. Arnold, Phys. Rev. D46 (1992) 2628.

[47] C.G. Boyd, D.E. Brahm and S.D. Hsu, *Phys. Rev.* **D48** (1993) 4963.

[48] G. Amelino-Camelia and S.-Y. Pi, *Phys. Rev.* **D47** (1993) 2356.

[49] G. Amelino-Camelia, *Phys. Rev.* **D49** (1994) 2740.

[50] J.R. Espinosa, M. Quirós and F. Zwirner, *Phys. Lett.* **B314** (1993) 206.

[51] W. Buchmüller, T. Helbig and D. Walliser, *Nucl. Phys.* **B407** (1993) 387; W. Buchmüller, Z. Fodor, T. Helbig and D. Walliser, preprint DESY 93-021 (Feb. 1993).

[52] P. Arnold and O. Espinosa, *Phys. Rev.* **D47** (1993) 3546.

[53] J.E. Bagnasco and M. Dine, *Phys. Lett.* **B303** (1993) 308.

[54] R.R. Parwani, Phys. Rev. **D45** (1992) 4695.

[55] M. Quirós, *On daisy and superdaisy resummation of the effective potential at finite temperature*, preprint IEM-FT-71/93, to appear at the proceedings of the *4th Hellenic School on Elementary Particle Physics*, Corfu (Greece), September 1992.

[56] J.M. Cornwall, R. Jackiw and E. Tomboulis, Phys. Rev. **D10** (1974) 2428.

[57] E.W. Kolb and M.S. Turner, *The Early Universe* (Addison-Wesley, 1990).

[58] A.D. Sakharov, *Zh. Eksp. Teor. Fiz. Pis'ma* **5** (1967) 32; *JETP Lett.* **91B** (1967) 24.

[59] Particle Data Group, Review of Particle Properties, *Phys. Rev.* **D45** (1992) 1.

[60] E.W. Kolb and S. Wolfram, *Nucl. Phys.* **B172** (1980) 224; *Phys. Lett.* **B91** (1980) 217.

[61] D. Toussaint, S.B. Treiman, F. Wilczek and A. Zee, *Phys. Rev.* **D19** (1979) 1036; S. Weinberg, *Phys. Rev. Lett.* **42** (1979) 850.

[62] See, *e.g.*: H.P. Nilles, *Phys. Rep.* **110C** (1984) 1.

[63] J.N. Fry, K.A. Olive and M.S. Turner, *Phys. Rev.* **D22** (1980) 2953; *Phys. Rev.* **D22** (1980) 2977; *Phys. Rev. Lett.* **45** (1980) 2074; J.A. Harvey, E.W. Kolb, D.B. Reiss and S. Wolfram, *Nucl. Phys.* **B201** (1982) 16.

[64] E. Kolb and M. Turner, *Ann. Rev. Nucl. Part. Sci.* **33** (1983) 645.

[65] V.A. Kuzmin, V.A. Rubakov and M.E. Shaposhnikov, *Phys. Lett.* **B155** (1985) 36; *Phys. Lett.* **B191** (1987) 171.

[66] A.G. Cohen, D.B. Kaplan and A.E. Nelson, *Annu. Rev. Nucl. Part. Sci.* **43** (1993) 27.

[67] G. t' Hooft, *Phys. Rev. Lett.* **37** (1976) 8; *Phys. Rev.* **D14** (1976) 3432.

[68] M. Kobayashi and M. Maskawa, *Prog. Theor. Phys.* **49** (1973) 652.

[69] N.S. Manton, *Phys. Rev.* **D28** (1983) 2019; F.R. Klinkhamer and N.S. Manton, *Phys. Rev.* **D30** (1984) 2212.

[70] J. Kunz, B. Kleihaus and Y. Brihaye, *Phys. Rev.* **D46** (1992) 3587.

[71] Y. Brihaye and J. Kunz, *Phys. Rev.* **D48** (1993) 3884.

[72] P. Arnold and L. McLerran, *Phys. Rev.* **D36** (1987) 581; S.Yu. Khlebnikov and M.E. Shaposhnikov, *Nucl. Phys.* **B308** (1988) 885.

[73] J. Ambjorn, M. Laursen and M. Shaposhnikov, *Phys. Lett.* **B197** (1989)49; J. Ambjorn, T. Askaard, H. Porter and M. Shaposhnikov, *Phys. Lett.* **B244** (1990) 479; *Nucl. Phys.* **B353** (1991) 346; J. Ambjorn and K. Farakos, *Phys. Lett.* **B294** (1992) 248.

[74] M.E. Shaposhnikov, *Nucl. Phys.* **B287** (1987) 757; *Nucl. Phys.* **B299** (1988) 797; A.I. Bochkarev and M.E. Shaposhnikov, *Mod. Phys. Lett* **A2** (1987) 417.

[75] L. Carson, Xu Li, L. McLerran and R.-T. Wang, *Phys. Rev.* **D42** (1990) 2127.

[76] M. Dine, P. Huet and R. Singleton Jr., *Nucl. Phys.* **B375** (1992) 625.

[77] A.I. Bochkarev, S.V. Kuzmin and M.E. Shaposhnikov, *Phys. Rev.* **D43** (1991) 369.

[78] M. Dine, P. Huet, R. Singleton Jr. and L. Susskind, *Phys. Lett.* **B257** (1991) 351.

[79] K. Enqvist, K. Kainulainen and I. Vilja, *Phys. Rev.* **D45** (1992) 3415; N. Sei, I. Umemura and K. Yamamoto, *Phys. Lett.* **B299** (1993) 286.

[80] V. Jain and A. Papadopoulos, *Phys. Lett.* **B303** (1993) 315.

[81] J.R. Espinosa and M. Quirós, *Phys. Lett.* **B305** (1993) 98.

[82] T.P. Cheng, E. Eichten and L.-F. Li, *Phys. Rev.* **D9** (1974) 2259.

[83] B. Kastening and X. Zhang, *Phys. Rev.* **D45** (1992) 3884.

[84] A.G. Cohen and A.E. Nelson, *Phys. Lett.* **B297 (1992)** 111.

[85] J.R. Espinosa, M. Quirós and F. Zwirner, *Phys. Lett.* bf B307 (1993) 106.

[86] A. Brignole, J.R. Espinosa, M. Quirós and F. Zwirner, *Phys. Lett.* bf B324 (1994) 181.

[87] G.F. Giudice, *Phys. Rev.* **D45** (1992) 3177; S. Myint, *Phys. Lett.* **B287** (1992) 325.

[88] D. Comelli and M. Pietroni, *Phys. Lett.* **B306** (1993) 67; J.R. Espinosa, J.M. Moreno and M. Quirós, *Phys. Lett.* **B319** (1993) 505.

[89] J. Ellis, G. Ridolfi and F. Zwirner, *Phys. Lett.* **B262** (1991) 477.

[90] See, e.g.: G. Altarelli, Proceedings of the *International Europhysics Conference on High Energy Physics*, Marseille, 22–28 July 1993, (Ed. Frontieres, 1994), page 689.

[91] R. Barbieri, M. Frigeni and F. Caravaglios, *Phys. Lett.* **B279** (1992) 169; G. Altarelli, R. Barbieri and F. Caravaglios, *Nucl. Phys.* **B405** (1993) 3, preprint CERN-TH.6859/93 and *Phys. Lett.* **B314** (1993) 357; J. Ellis, G.L. Fogli and E. Lisi, *Phys. Lett.* **B285** (1992) 238, **B286** (1992) 85 and *Nucl. Phys.* **B393** (1993) 3.

[92] L. Alvarez-Gaumé, J. Polchinski and M. Wise, *Nucl. Phys.* **B221** (1983) 495; R. Barbieri and L. Maiani, *Nucl. Phys.* **B224** (1983) 32; C.S. Lim, T. Inami and N. Sakai, *Phys. Rev.* **D29** (1984) 1488.

[93] Y. Okada, M. Yamaguchi and T. Yanagida, *Prog. Theor. Phys.* **85** (1991) 1 and *Phys. Lett.* **B262** (1991) 54; J. Ellis, G. Ridolfi and F. Zwirner, *Phys. Lett.* **B257** (1991) 83; H.E. Haber and R. Hempfling, *Phys. Rev. Lett.* **66** (1991) 1815; R. Barbieri and M. Frigeni, *Phys. Lett.* **B258** (1991) 395.

[94] A. Bochkarev, S. Kuzmin and M. Shaposhnikov, *Phys. Rev.* **D43** (1991) 369 and *Phys. Lett.* **B244** (1990) 275; B. Kastening, R.D. Peccei and X. Zhang, *Phys. Lett.* **B266** (1991) 413.

[95] S. Braibant, Y. Brihaye and J. Kunz, *Int. J. Mod. Phys.* **A8** (1993) 5563.

[96] K. Kajantie, K. Rummukainen and M. Shaposhnikov, *Nucl. Phys.* **B407** (1993) 356; M. Shaposhnikov, *Phys. Lett.* **B316** (1993) 112; K Farakos, K. Kajantie, K. Rummukainen and M. Shaposhnikov, CERN preprint, CERN-TH.7244/94 (May 1994).

[97] B. Bunk, E.M. Ilgenfritz, J. Kripfganz and A. Schiller, *Phys. Lett.* **B284** (1992) 371 and *Nucl. Phys.* **B403** (1993) 453; J. March-Russell, *Phys. Lett.* **B296** (1992) 364; H. Meyer-Ortmanns and A. Patkós, *Phys. Lett.* **B297** (1993) 331; A. Jakovác and A. Patkós, *Z. Physik, Particles and Fields* **C60** (1993) 361; N. Tetradis and C. Wetterich, *Nucl. Phys.* **B398** (1993) 659 and preprint DESY-93-128; P. Arnold and L.G. Yaffe, *Phys. Rev.* **D49** (1994) 3003.

[98] D. Diakonov, M. Polyakov, P. Pobylitsa, P. Sieber, J. Schaldach and K. Goeke, preprint RUB-TPII-05/94 and hep-ph/9407238 (July 1994).